A New Approach to Establish Tactility in Minimally Invasive Robotic Surgery

Development, Design, and First Evaluation of a Haptic-Tactile Feedback System for Improved Localization of Arteries During Surgery such as Closed-Chest Revascularization

Von der Fakultät Energie-, Verfahrens- und Biotechnik der Universität Stuttgart zur Erlangung der Würde eines Doktor-Ingenieurs (Dr.-Ing.) genehmigte Abhandlung

Vorgelegt von
Bernhard Kübler
aus Heilbronn

Hauptberichter:	Univ.-Prof. Dr. rer. nat. Joachim H. Nagel
Mitberichter:	Hon.-Prof. Dr.-Ing. Gerhard Hirzinger

Tag der mündlichen Prüfung: 07. Juli 2010

Institut und Lehrstuhl für Biomedizinische Technik der Universität Stuttgart
2010

Preface

The perception of haptic and tactile information is a basic human ability. Especially in classical open surgery physicians are used to relying on these capabilities, e. g. for palpation, for reliably tightened knots or for intraoperative tissue differentiation, and for intraoperative recognition of unusual or abnormal tissue locations.

In minimally invasive surgery (MIS), however, the patient's skin forms a highly effective barrier between operating field and surgeon, confining the transmission of haptic and tactile information to the tools being used. Even worse, in minimally invasive robotic surgery (MIRS) – the advancement of MIS – the surgeon is actually totally mechanically decoupled from the patient. This leads to a complete loss of haptic and tactile feedback. The establishment of pure *kinesthetic* impressions in robot assisted MIS has already been realized in a promising manner. One of the biggest challenges in teleoperated minimally invasive surgery for the near future is the establishment of *tactile* impressions.

A number of attempts with miniaturized tactile sensors and tactile man-machine interfaces (MMI) were undertaken but did not prevail. In this dissertation a different approach is presented to solve one of the main problems: the recognition and localization of optically undetectable arteries beneath covering tissue. In open surgery the surgeon can feel a hidden artery as a soft pulsation, preventing him from injuring the vessel and causing arterial bleeding which is difficult to control. In minimally invasive (robotic) surgery the tissue of interest cannot be touched by the surgeon's finger, and to stem any bleeding is even harder than in open surgery. Blood may contaminate the endoscopic optics and severely obstruct the view of the operating site which may lead to a forced conversion to open surgery.

Based on Doppler's principle an ultrasound sensor was developed to recognize optically undetectable arteries beneath covering tissue in the operating field. By appropriate signal processing and analysis the information provided by the sensor can be converted into an intuitive representation using standardized, commercially available force feedback devices, visual displays, or acoustic signals. A system was realized and used to provide widely intuitive feedback and to reliably detect arteries of relevant size.

The system is thought to be one step towards providing tactile feedback on a variant route. It uses a non-tactile sensor to generate haptic expressions for expected tactile information – and this as intuitively as possible, meaning substantial improvement of patient safety and reduction of required training time. The system does not provide full tactile sensation and feedback but presents a useful and relatively simple solution to a serious problem in MIS and MIRS caused by the loss of tactile feedback. Furthermore, with the aid of pulse recognition and robot position determination, the path of an invisible but superficial artery (e. g. coronary arteries during heart surgeries) can be mapped. Thereby, planned bypass anastomoses positions can be located more easily.

This modality substitution with false haptic signals is the quintessence of the presented dissertation and has been granted a patent.

Abstract

In conventional minimally invasive robotic surgery (MIRS) the physician is no longer in direct mechanical contact with the patient and the surgical instruments. The establishment of kinesthetic impressions shows promising results technically but tactile feedback is still a problem. Various attempts with full remote perception of tactile impressions did not prevail for a number of reasons. Above all, the tactile feedback actor commonly is a secondary device which hinders simultaneous perception of feedback signals and guidance of instruments. Human perception of tactile impressions, however, often is a result of active palpation which is hard to emulate in two separate devices; so far, interpretation of feedback signals was not sufficiently clear and intuitive.

One of the most serious problems resulting from the absence of tactile feedback in minimally invasive (robotic) surgery is the augmented risk of an unintended blunt artery dissection causing bleeding which would be difficult to control. In open surgery, tissue can be palpated and a pulsating perception indicates a hidden artery. In open cardiac surgery preoperatively planned bypass anastomoses positions can be found by palpation. Using optical examination only, a dissection of the arteries, which is very time consuming, may become necessary to locate the correct positions.

The solution presented in this dissertation does not provide full remote tactile perception, but focuses on the quasi-tactile detection of special structures under covering tissue using ultrasound. The acquired signals are subjected to a modality substitution and presented to the user as an intuitive haptic or multi channel signal. For this purpose, an ultrasound transducer embedded in a minimally invasive surgical instrument is used to acquire Doppler frequency shifts of blood flow in the vessels to be detected. The acquired signals are analyzed and transferred to a haptic feedback device. Here, the detection and characteristics of a covered vessel is presented in an intuitive way. A slight twitch of the feedback device accompanied by the characteristic Doppler shift sound are, based on the results of first experiments, expected to be very reliable and intuitive and effectively replace palpation. Further investigations to prove the validity and deepen the understanding of this hypothesis are pending.

It is highly questionable whether full feedback of all possible tactile impressions in MIRS is worth striving for – the medical benefit does not appear to justify the efforts and cost. Therefore, the substitution of only selected components of full tactility, comparable to the human perception, such as carried out in this dissertation promises to be a better solution. In contrast to realizations described in literature that have not prevailed in practical application the system described here has passed first tests and demonstrated its superior performance. A patent was granted on April 5th, 2007.

Keywords

medical robotics, minimally invasive surgery, tactility, haptic feedback, telesurgery, modality substitution, telemanipulation, telepresence.

Kurzzusammenfassung

In der konventionellen robotergestützten, minimal invasiven Chirurgie (MIC) besteht eine vollständige mechanische Entkopplung zwischen Chirurg und Patient. Die Entwicklung kinästhetischer Rückkopplungssysteme ist fortgeschritten, die Rückkopplung taktiler Eindrücke ist jedoch nach wie vor problematisch. Es wurden viele Versuche unternommen, vollständige teletaktile Eindrücke zu vermitteln, die jedoch aus unterschiedlichen Gründen scheiterten. Als hauptsächlicher Grund hierfür ist anzusehen, dass die Ausgabeschnittstelle üblicherweise ein eigenständiges Gerät ist, was die gleichzeitige Wahrnehmung von Eindrücken und Steuerung des Instruments erschwert. Die menschliche Wahrnehmung taktiler Eindrücke beruht weitgehend auf dem Betasten des Objekts mit Bewegen des "Sensors", was mit zwei verschiedenen Geräten schwer nachzubilden ist. Außerdem war die Interpretation des rückgekoppelten Signals nicht eindeutig und intuitiv genug.

Eine der größten Schwierigkeiten in der (robotergestützten) minimal invasiven Chirurgie ist die große, durch die fehlende taktile Rückkopplung begründete Gefahr einer unbeabsichtigten Arterienverletzung mit der Folge schwer kontrollierbarer Blutungen. In der offenen Chirurgie kann Gewebe betastet werden, und ein Pulsieren deutet auf eine im Gewebe liegende Arterie hin. Eine Substitution des Tastsinns wäre aber auch aus anderen Gründen wünschenswert. So können in der offenen Herzchirurgie die präoperativ geplanten Anastomosestellen durch Betasten aufgefunden werden. Stehen jedoch nur optische Untersuchungsmethoden zur Verfügung, kann ein sehr zeitaufwendiges Freipräparieren der Arterien notwendig werden, um die präoperativ geplanten Anastomosestellen aufzufinden.

Die in dieser Arbeit vorgeschlagene Lösung bietet keine umfassende taktile Rückkopplung, sondern konzentriert sich auf das ultraschallgestützte, quasi taktile Lokalisieren besonderer Strukturen unter verdeckendem Gewebe. Mit den erfassten Daten erfolgt eine Modalitätssubstitution, dem Nutzer werden intuitive haptische bzw. Mehrkanalinformationen zurückgegeben. Um die Doppler-Frequenzverschiebung des in den betreffenden Arterien fließenden Blutes zu erkennen, wird ein Ultraschalltransducer verwendet, der in ein minimal invasives Instrument integriert ist. Die gemessenen Signale werden analysiert und an ein haptisches Eingabegerät weitergeleitet, mit dem die Erkennung und die Eigenschaften der verdeckten Gefäße intuitiv erfassbar dargestellt werden. Erste Versuche zeigten, dass ein leichtes Zucken des Eingabegerätes in Verbindung mit dem typischen Doppler-Geräusch das direkte Betasten sehr zuverlässig und intuitiv ersetzen. Weiterführende Untersuchungen, die die Verlässlichkeit bestätigen und zu einem tieferen Verständnis dieser Ergebnisse führen sollen, stehen noch aus.

Es ist sehr fraglich, ob eine vollständige Rückkopplung aller möglichen taktilen Eindrücke in der robotergestützten MIC erstrebenswert ist – der medizinische Nutzen scheint die Anstrengungen und Kosten nicht zu rechtfertigen. Deshalb verspricht, wie in dieser Arbeit, der Ersatz nur von Teilen der Taktilität, der mit der menschlichen Wahrnehmung vergleichbar ist, eine bessere Lösung zu sein. Im Gegensatz zu in der Literatur beschriebenen Realisierungen, die sich im praktischen Einsatz nicht durchgesetzt haben, hat das hier beschriebene System erste Tests bestanden und seine überlegene Leistungsfähigkeit bewiesen. Ein Patent hierzu wurde bereits erteilt.

Schlüsselworte

Medizinische Robotik; minimal invasive Chirurgie; Taktilität; haptische Rückkopplung; Telechirurgie; Modalitätssubstitution; Telemanipulation; Telepräsenz.

Acknowledgements

This dissertation was developed during my work at the German Aerospace Center (DLR), Oberpfaffenhofen near Munich, Institute of Robotics and Mechatronics, and supervised by the Director of the Department of Biomedical Engineering, University of Stuttgart.

First, I would like to thank my PhD advisor, Prof. Dr. rer. nat. Joachim H. Nagel, Director of the Department of Biomedical Engineering, University of Stuttgart. Though I was working as an external PhD student he supported me and the result of my work. He always made time to answer my questions and gave me a lot of freedom to develop my ideas and perform my work and provided invaluable advice.

Second but just as sincerely I would like to thank my employer and second PhD advisor, Prof. Dr.-Ing. Gerd Hirzinger, Director of the Institute of Robotics and Mechatronics, German Aerospace Center (DLR) where this dissertation was developed. He provided me the opportunity to work in one of the most prolific surroundings, visit congresses to discuss my work, and even to get paid for my efforts. I really hope that my work is also beneficial for him and the institute.

Then I would like to thank all my colleagues in the Institute of Robotics and Mechatronics as well as in the Department of Biomedical Engineering who supported me in my work. Exemplarily I would like to name Dipl.-Ing. Robin Gruber, Dr.-Ing. Georg Passig, Prof. Dr.-Ing. Tobias Ortmaier, Dr.-Ing. Holger Weiß, Dipl.-Ing. Ulrich Seibold, Dipl.-Ing. Ulrich Hagn, Dr.-Ing. Johannes Port and Dipl.-Ing. (FH) Christoph Joppek who all contributed to the success of this thesis.

Last but not least I would like to thank my parents without whom I would not be what and where I am.

The work of this thesis was financially supported by the German Research Association (DFG) within the Collaborative Research Center (SFB) 453. In the letter of approval to the President of the Technische Universität München the DFG wrote, based on the results of the examining board evaluating the application for this subproject: ”Die Arbeitsgruppe hat Potenzial, auf einem relevanten Forschungsfeld der Medizintechnik noch einen wesentlichen Schritt weiter zu kommen. Dies gilt nicht nur bezogen auf die grundlagenwissenschaftlich ausgerichteten Fragestellungen, sondern auch bezogen auf die Umsetzung der Ergebnisse in die konkrete Anwendung.” which can be translated as: ”The research group has the capability to make essential progress in a relevant field of research in medical engineering. This is not only related to problems of basic research but also to the implementation of the results in the specific application.”

Contents

1 Introduction

A LOT OF PROBLEMS in minimally invasive robotic surgery (MIRS) are still unsolved. Nonetheless, surgical interventions with the help of robots and telemanipulators are performed daily in a number of university hospitals and specialized clinics. Since 1999 more than 1.200[1] installations of the only minimally invasive robotic surgery system presently commercially available, the daVinci Surgical System from Intuitive Surgical, Inc., have been sold [1]. During that time the number of different procedures which can be performed with the daVinci Surgical System has steadily increased [2].

The advantages of minimally invasive surgery (MIS) in general (see Cha. 2.1 for a more detailed description) are widely accepted today, especially considering the reduction of trauma to healthy tissue. However, many types of surgery require a high amount of manipulability, making conventional minimally invasive methods, characterized by limited dexterity, more difficult. Systems to overcome the drawbacks of conventional MIS (cf. Cha. 2.2) can and will considerably widen the field of possible applications.

With the introduction of MIRS systems, a lot of efforts have been made to improve the immersion of the surgeon into the operation site, by e. g. the reestablishment of intuitive hand-eye coordination, elimination of variable leverage perception, as well as tremor filtering. All of these improvements have found their way into commercial availability. Force (*kinesthetic*) feedback (see Cha. 2.3), which is thought to be the next step to better immersion, is still not commercially available, but is being intensely investigated and prototyped with promising results.

In this dissertation yet another step towards better immersion was studied: the goal-oriented implementation of *tactile* feedback. A surgeon usually relies on his tactile perception during manipulations. For instance

- unusual hardening of tissue may indicate (malignant) tumors; the perception of other abnormalities gained by palpation adds important diagnostic information;
- the sensation of a slight pulsation might indicate an artery beneath the visible

[1] As of June 30th, 2009; 916 systems have been sold in the United States of America, 221 in Europe and 105 in the rest of the world [1].

tissue surface, implying the risk of uncontrolled bleeding in case of a blunt dissection;

- the localization of known anatomical structures to orientate himself.

Hence, a lot of research has already been performed in order to establish tactile feedback in MIS and, even more importantly, in MIRS. Many different approaches have been followed (cf. Cha. 2.4), unfortunately, applicable and convincing solutions for routine use and commercial systems could not yet be found. Therefore, a new, specific approach was developed, successfully tested, and is presented within this dissertation.

1.1 Objectives

Pure kinesthetic feedback in MIS and MIRS systems has been investigated and realized by many research groups and can thus be considered a solved problem. Obviously, the next step to expand the capabilities of minimally invasive surgery should be the realization of tactile feedback, which is the feature mostly desired by the user, i. e. the surgeon.

A thorough literature search, summarized in Sec. 2.4, revealed that there have actually been numerous previous approaches to restoring tactile feedback in MIS and MIRS, surprisingly however, none of them achieved clinically satisfying results. A tactile feedback system consists of the two essential components, a sensor to acquire tactile surface data and an actor to transmit and present those data to the surgeon. These two components are completely different systems, they are not realized using the same technology and, therefore, their development demands different knowledge, abilities, and expertise. Rarely are these different prerequisites found in one single research group, making the challenge of developing an adequate tactile sensor/actor feedback system very hard to accomplish. This may explain that so far none of the proposed approaches showed convincing solutions for both components. In addition, most of the previous approaches were overambitious in the sense that they aimed at achieving full tactile feedback comparable to that of the human fingertip and thus the reestablishment of the entire range of tactile perceptions that a physician would have performing open surgery, a currently unrealistic endeavor.

Limitation to the substitution of one single type of tactility relevant in MIS and MIRS appears to be a more reasonable approach to achieving a clinically beneficial advancement of feedback, which is the highest objective of this dissertation. First step towards the definition of the individual tasks of this project, i. e. the development of sensor and actor as well as their integration into an MIRS system, was to decide on which aspect of the missing tactile feedback to restore. In other words, which is the most urgent problem the surgeon faces in MIS and MIRS due to missing tactile perception?

The worst adverse event during surgery is to cause harm. The converse argument is that avoiding harm has the highest priority. The highest risk of causing harm during MIS and MIRS is to cut into arteries hidden by some covering tissue which can be critical. In open surgery, this risk is low because the surgeon can palpate the hidden artery. Feeling a slight pulsation within tissue with the finger tip always indicates a pressurized vessel. Thus, before performing a blunt dissection into any unknown tissue a surgeon will first palpate the tissue and avoid the risk of uncontrolled bleeding [3, 4]. In MIS with no direct manual contact with the affected tissue and even more severely in MIRS with total mechanical separation of patient and surgeon this is impossible. There is the inherent risk of injuring an artery. Stopping the unintended bleeding in MIS (and MIRS) is more time-consuming since it is more intricate and cumbersome compared to open surgery. Additionally, blood can contaminate the endoscope, possibly leading to a complete loss of sight and forcing the surgeon to convert intraoperatively to open surgery, resulting in time delay and, possibly, danger to the patient's life. The following three examples demonstrate the relevance of the problem:

- In laparoscopic hernioplasty (repair of inguinal hernia) a known, severe complication is the laceration of epigastric arteries which can cause severe bleeding[2] [5–7]. Since specifically the iliac and femoral vessels are affected [7] the patient will possibly lose a leg. This is of particular relevance since inguinal hernia surgery is one of the most often performed procedures, at least in Germany and the USA [8].

- Cholecystectomy (gall bladder removal) is another example for a frequently performed procedure. In modern health care, more than 80% are carried out minimally invasively [9, p. 877]. Common complications are bleeding of the cystic and/or proper hepatic arteries due to anatomical variants as well as lesions of vascular structures within the hepato-duodenal ligament. Especially the latter are hard to appraise [9, p. 879]. In this case, complications can make intraoperative conversion to open surgery necessary as well.

- In coronary artery revascularization the path of the coronary arteries is usually known from the patient specific coronary arteriogram. Nevertheless, coronary arteries are largely covered by the subepicardial tissue, also known as Tela subepicardiaca (cf. Sec. 3.2.1), and, therefore, cannot be seen intraoperatively[3]; in minimally invasive surgery they cannot even be palpated. Finding the exact location of anastomoses is often difficult and time consuming [10, p. 20], [11, p. 33], [12, p. 125], [13, 14].

There does not yet exist a method to find invisible arteries in minimally invasive surgery. Their forces are too low for the detection by force feedback and covering

[2] Generally two laparoscopic procedures are differentiated: the transabdominal preperitoneal hernioplasty (TAPP) and the total extraperitoneal hernioplasty (TEP). Both of them pose the mentioned risk.

[3] The registration of imaging data and the real situs is particularly problematic.

tissue is preventing optical discovery. This does not only lead to a major inconvenience for the surgeon, the possibility of damage to a hidden artery poses a serious potential danger to the patient. Even in standard procedures patient safety and the quality of surgery can be increased due to a possible check for hidden arteries before any dissection.

Therefore, the objective of this dissertation is to concentrate on the replacement of one single type of tactile perception concerning MIRS: palpation of pulsating vessels, i. e. the detection and display of pulsating vessels. The tactile feedback replaces palpation. The ability to detect hidden arteries before each surgical incision will greatly enhance the quality of MIS and MIRS and, at the same time, has the potential to significantly increase patient safety.

1.2 Outline of the Proposed Solutions to the Problem – the Tasks

In accordance to the problem described above, it is neither the aim of this thesis to provide fully realistic, unaltered tactile feedback comparable to the human tactile perception nor is the system meant to be able to deal with a complex branching of vessels as it is present e. g. in the liver.

In this first step the system ought to have abilities comparable to the human fingertip, regarding the perception of pulsation within tissue: vessels too deep under the tissue surface cannot be perceived by the human fingertip and can not be detected by the system. Very superficial vessels are visible and, therefore, do not have to (and cannot) be detected by the system. Consequently, the aim is not to strive for fully realistic feedback comparable to the human tactile perception with an unavoidably unsatisfying result but rather to provide simply one single but highly important aspect of tactile information in a satisfying manner, i. e. the detection of vessels hidden under covering tissue within the operating field, thus preventing unintended, uncontrolled intraoperative injury and bleeding.

To meet these requirements, known technologies were expanded and used in a new combination:

Ultrasound Doppler technology was used for the detection of vessels. For this purpose, an multidirectional sensor suitable in size for MIS/MIRS was developed in close cooperation with the Fraunhofer Institute for Biomedical Engineering (IBMT) since the rotary motion with conventional Doppler transducers for reliable detection of arteries is very cumbersome (to the point of being impossible) in MIS/MIRS[4]. The new sensor (cf. Sec. 3, p. 43 et seqq.) just has to be positioned on the intracorporeal tissue surface and is able to reliably detect vessels in their physiological course and in axial sensor direction within the cutting depth (comparable to the human fingertip).

[4]This multidirectional Doppler sensor with circularly arranged single ultrasound transducers (cf. Cha. 3.4, p. 53 et seqq.) was summarized in the unexamined and first publication of patent application No. DE 10 2008 005 041 A1, disclosure July 30th, 2009 (patent pending) [15] .

Therefore, the transducer is mounted on an existing, distortable MIRS instrument, an in-house development of the Institute of Robotics and Mechatronics, German Aerospace Center (DLR). This instrument also allows the measurement of interaction forces/torques when the integrated transducer is placed on tissue (cf. following Sec. 1.3, Fig. 1.4 and Sec. 3.4). The entire ”tactile sensation instrument” is guided by a surgical robot also an in-house development of the DLR (cf. following Sec. 1.3, Fig. 1.1), thereby forming a complete minimally invasive, tactile slave system.

Transducer control and data acquisition as well as the transfer to a customary computer are performed by an in-house developed electronics adjusted to the new transducer. Measurement results are then analyzed for blood flow signals by a specially developed MATLAB (RT Lab) programme.

The entire system's master station (input system) consists, among others, of a force reflecting input device for the left and right hand to control the MIRS instruments (cf. Sec. 1.3). The interaction forces captured by force/torque sensors integrated in the instruments are processed and displayed to the user. In this way, the surgeon regains kinesthetic feedback from the operation site.

To display the acquired ”tactile” data to the surgeon a modality transformation is performed: The surgeon guides the sensor instrument with a special input device (cf. following Sec. 1.3, Fig. 1.2) and expects tactile information. As soon as a vessel is detected under the multidirectional Doppler sensor the information is transformed into an intuitive, soft twitch of the input device's open/close-input-master (index finger, cf. Fig. 1.2, right). Thus, an expected tactile information is captured non-tactically (i. e. with the aid of Doppler ultrasound) and displayed kinesthetically. This is intended to help the operator to guide the sensor instrument and perceive best possible (”tactile”) feedback simultaneously[5].

Softly twitching movements of the input device's entire handpiece were considered, intuitively being identifiable as ”pulsation”, but there are two main reasons to reject this approach: Firstly, it is assumed to be more realistic to perceive the ”pulsation” on the finger as in open surgery. Secondly, an input device's position modification caused by a detected artery will be misinterpreted by the system as a simultaneous modification of the instrument's requested position. An unwanted oscillation of the system might be the consequence. Furthermore, force feedback due to instrument contact with the tissue surface might be misinterpreted by the surgeon as a pulsation feedback. These reasons led to the decision to separate pulsation feedback as well as position input commands and kinesthetic feedback respectively.

Additionally, further perceptive channels can be addressed by synchronous or separate presentation of the characteristic Doppler sound or a flashlight signal on the operator's screen. The most intuitive presentation or combination of presentations is to be suggested by occupational psychological tests (see Cha. 5.2).

[5]For this data transformation the expression ”modality substitution” was chosen. The way of transmission, consequently, is called here a ”false haptic representation” (cf. Sec. A.2).

Fig. 1.1: DLR surgery scenario. *Left:* remote surgeon with force feedback input devices and 3D display. *Right:* DLR slave system consisting of three MIRO robot arms; one carrying the endoscope (semitransparent), two more carrying MIRS instruments for two handed manipulation (photos: DLR).

Moreover, displaying detected vessels on the input device of the surgical instruments by a soft twitch of the open/close-input-master allows the surgeon to keep his hands on the input device and look at the operation site while simultaneously perceiving the transformed pulsation signal. This should simplify handling on the one hand and increase immersion on the other hand.

1.3 Integration into the DLR Robotic Surgery Scenario

The sensor system described in this thesis is intended to expand the functionality of an already existing, in-house developed surgery system introduced by the DLR. The basic functionality of telerobotic surgery systems in general is explained in Sec. 2.2. Therefore, this section is limited to a short presentation of the DLR surgery system and the integration of the tactile sensor device into it.

The DLR surgery system is designed as a versatile telerobotic system, suitable e. g. for MIRS, pedicle screwing on the spinal column [16], or brain biopsy [17]. MIRS, thereby, is a further basic application of the system. In this case, the system basically consists of a slave system (executing unit) usually comprising three robot arms – one carrying an endoscope, the two others carrying special MIRS instruments guided by the left and the right hand of the surgeon (see Fig. 1.1, right) – and a master station (input system, cf. Fig. 1.1, left) from which the surgeon operates the slave system.

The *master station* basically consists of a 3D video screen, foot pedals, and a special force reflecting input device for the left and right hand of the user (surgeon, cf. Fig. 1.1, left, and Fig. 1.2). To control the MIRS instruments the input device's handpiece is gripped and moved within the six degrees of freedom (DoF) workspace (three rotational and three translational DoF). An additional functional DoF can be controlled with the index finger (e. g. to open/close a gripper by degrees). The used haptic input devices (omega.7 devices from Force Dimension,

Fig. 1.2: Omega.7 seven DoF input device with 4DoF feedback (photo courtesy of Force Dimension, Inc., 2009).

Inc., Lausanne, Switzerland, Fig. 1.2) are limited to displaying forces in translational direction and gripping forces only. Rotational movements are passive – although input movements are recorded and transmitted to the slave system, torques cannot be displayed to the user. The omega.7, therefore, is a seven DoF (three rotational DoF, three translational DoF, one functional DoF) input and a four DoF (three translational DoF, one functional DoF) force reflecting input device. The delta-based kinematics of the omega.7's translational part yields a cylindrical workspace of about 160 mm in diameter and 110 mm in length at achievable continuous forces of ± 8 N. The rotational extension offers a workspace of about $240^\circ \times 140^\circ \times 180^\circ$, and the length of the gripper's traverse path is about 25 mm [18].

By means of the foot pedals two functionalities are possible: Firstly, the control of one instrument can be switched over to the endoscope during the operation to modify the intracorporeal perspective. Secondly, indexing is possible: when reaching the workspace limits of the input devices or working in an uncomfortable arm posture the robot connection can be temporarily intermitted to reorient the input devices. Thereafter, telemanipulation can be continued in the middle of the input device's workspace and in a comfortable posture respectively.

An auto-stereoscopic display (from SeeFront, Inc., Hamburg, Germany) provides three dimensional vision without the need of head-mounted displays or special shutter glasses and enables free movement of the viewer in front of the screen: Initially, the user's eye position is tracked in real-time by a pair of cameras integrated in the monitor and with a special algorithm developed in-house at the DLR [19]. The pixels displayed on screen are then moved accordingly to the tracked eye position behind a lenticular screen directly mounted in front of an LCD display. Thus, an appropriately interlaced stereo image pair is separated into two images for the user's left and right eye [20]. The resulting three-dimensional impression is comparable to the one gained with shutter glasses and well suited for

Fig. 1.3: Previous version of the DLR MIRS instrument. The gripper branches are developed in a basic form. In the instrument presented in this thesis the end-effector (gripper) is replaced by the ultrasound transducer, cf. Fig. 1.4 (photos: DLR).

MIS/MIRS.

Basic component of the *slave system* is a versatile robot arm ("MIRO") for surgical interventions, an in-house development of the DLR (cf. Fig. 1.1, right). Its dimensions are comparable to those of the human arm (maximum arm length: 1.1 m), the design follows a light-weight strategy (total weight: 10 kg; payload: 30 N at maximum extended arm position), it is kinematically redundant (7 DoF), and all joints are fully torque-controlled avoiding unintended collisions and allowing sensitive robot movements induced by the surgeon in direct cooperation with the robot next to the patient. In general the MIRO robot arm was designed as a sophisticated carrier for specialized instruments in a very wide spread range of medical applications. In Hagn et al. more details about the development and characteristics of the MIRO robot arm are given [19, 21].

The first generations of specialized instruments applicable with the MIRO robot arm were intended for MIRS including kinesthetic feedback [19]. These instruments (see Fig. 1.3) allow 2 DoF distal bending to reestablish full dexterity inside the patient (cf. Sec. 2.1 et seqq. and Fig. 2.2), provide one functional DoF, and measure manipulation forces/torques in six DoF by a Stewart-Gough platform based hexapod sensor as well as the functional end's load in one DoF. The hexapod sensor is based on a parallel manipulator kinematics using an octahedral assembly of six elastic struts linked with flexural hinges and, therefore, has a roughly cylindrical shape with a hollow section (cf. heightened picture detail in Fig. 1.3). Strain gauges are adhesively bonded to the struts measuring elongation caused by external loads. By means of a corresponding transformation matrix the six measured elongation values can then be transformed into forces/torques referring to an arbitrary coordinate system. The geometry of the instrument's functional DoF can e. g. be adapted to the commonly used instruments in MIS/MIRS. Development of the actuated and sensor integrated DLR MIRS instruments as well as their basic characteristics are described in [22, 23].

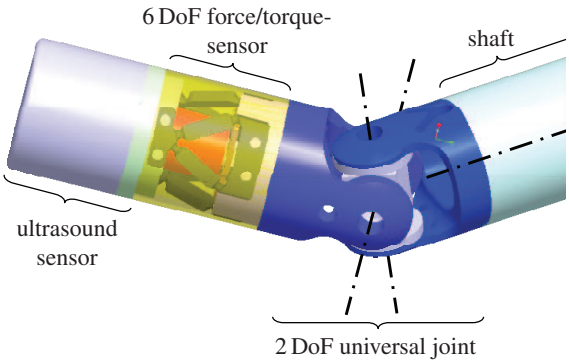

Fig. 1.4: Ultrasound transducer mounted on the tip of the DLR MIRS instrument in rendered CAD depiction: indicated transducer on the instrument tip (light violet on the left), force/torque sensor (yellow), universal joint for instrument distortion (blue), and partial view of instrument shaft (on the right). Outer diameter of the instrument is 10 mm.

The ”tactile” ultrasound sensor presented in this thesis is designed to replace the functional DoF of the previous DLR MIRS instruments and fits through the hollow section of the 6-DoF force/torque sensor. Thus, the contact forces of ultrasound sensor and tissue can be measured and estimated by the surgeon. Nevertheless, for initiation and tests the ultrasound sensor can also be used without the hexapod sensor which then has to be replaced by a simple carrier. Fig. 1.4 shows the setup with the force/torque sensor. As described in Sec. 1.2 the measured data of the ultrasound sensor can be displayed acoustically as well, e. g. with the characteristic Doppler ultrasound noise, in the auto-stereoscopic display, e. g. with a flash signal, or with the omega.7 devices, e. g. as an intuitive, soft twitch of the index finger's open/close-input-master.

To subdivide the performed work the thesis is structured into five chapters: After this introduction the state of technology and related work is described (Cha. 2) followed by the delineation of the ultrasound sensor developed collaboratively with the Fraunhofer Institute for Biomedical Engineering (FhG IBMT, Cha. 3). Chapter 4 summarizes the completion of the entire system consisting of patient sided sensor/robot system, processing unit, and user sided input system. Cha. 5 concludes the thesis with a summary of findings and an outlook on future work on this matter.

The appendix rounds off the thesis, including a glossary for better understanding and best possible precision of word definition, compiling the most important expressions and technical terms in Sec. A.2, p. 82 et seqq.

2 State of Technology

THIS CHAPTER AIMS TO GIVE a brief overview of the state of the art in technologically enhanced surgery, particularly with regard to the reasons for the development of haptic and tactile feedback. Explaining all technological devices for modern surgery in detail, however, would go far beyond the scope of this chapter.

This section is structured as follows: first, advantages and disadvantages of minimally invasive surgery are pointed out (Sec. 2.1). To compensate for its drawbacks telemanipulated minimally invasive surgery (Sec. 2.2) was developed to the present standards, and the shortcomings of this technology led to attempts to establish haptic feedback in minimally invasive robotic surgery (Sec. 2.3).

Extensive research on and prototyping of haptic, specifically kinesthetic feedback have been described in the literature (cf. Sec. 2.3). The work presented in this thesis goes one step beyond simple kinesthesia and focuses on tactile feedback. Hence, in Sec. 2.4 a compilation of publications concerning tactile feedback particularly related to this thesis is presented and discussed, thereby revealing the reasons for the proposed approach.

The chapter closes with a brief description of the ultrasound technology's fundamental principles on which the developments in this thesis are based (Sec. 2.5). The detailed technical realization of the sensor is then described in Cha. 3.

2.1 Minimally Invasive Surgery

Minimally invasive surgery (MIS) is a well established operation technique in modern health care, especially for standard procedures like cholecystectomies (gall bladder removals). Long, slender instruments providing only a *functional* degree of freedom (DoF) are used through small incisions in the patient's body wall to access the intracorporeal operating field (cf. Fig. 2.1). Thereby, the epidermis forms an effective barrier preventing direct view and manual contact. In addition, dexterity is heavily constricted due to the so called *chopstick-effect*[1] (inversion of moving direction) and two missing DoF inside the patient caused by the invariant point

[1]The name derives from the expression for Chinese eating sticks, called *chopsticks*.

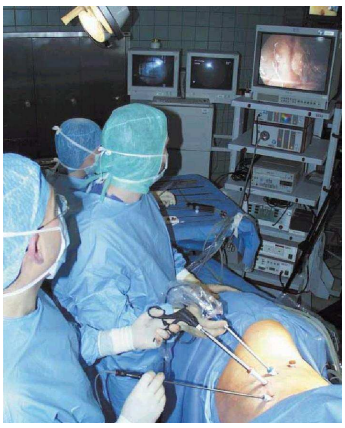

(a) View into operating room during laparoscopic surgery.

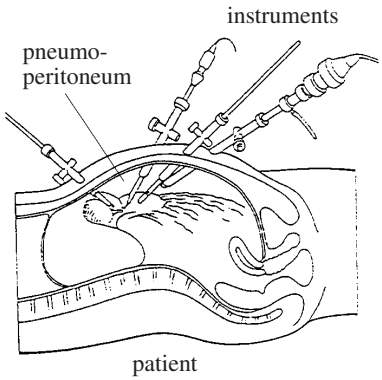

(b) Principle of laparoscopic surgery, example: cholecystectomy.

Fig. 2.1: Minimally invasive operation technique.

of incision (*fulcrum point*, cf. below and Fig. 2.2) [24]. Therefore, acquiring the necessary skills for MIS is very time consuming, one main reason being the unavoidable distortion of the kinesthetic and tactile feedback.

Kinematically, the fulcrum point must be regarded as a combination of an elastic, gimballed, and prismatic bearing. Therefore, the endoscopic instrument shaft can only be rotated around its longitudinal axis as well as in two planes around the fulcrum point and be moved translationally in axial direction (cf. Fig. 2.2). Consequently, there are only four DoF available to reach any point in the workspace, an arbitrary orientation of the instrument tip is impossible. Additionally, the depth of instrument insertion has an influence on the motion: According to the leverage, instruments inserted far into the patient generate big movements at the distal end with relatively small movements outside the patient, whereas the effort of manipulation is comparably large. Vice versa, if the instruments are inserted only a little, vast movements outside the patient are necessary to achieve relatively small movements at the instrument tip, but, correspondingly, the achievable forces at the distal end are larger. Executing large movements outside the patient may also cause collisions with neighboring instruments, thus constricting the workspace. The combination of all these influences – chopstick effect, the loss of two DoF, and the leverage effect – crucially disturbs the hand-eye-coordination of the surgeon which leads to an increased demand for training and familiarization.

The lack of dexterity inside the patient significantly complicates manipulation and, therefore, prevents a vast variety of operation types, especially those that require a high amount of manipulability like the viscerosynthesis[2]. Particularly for highly manipulable tasks at least two additional DoF inside the patient are desirable: arbitrary orientation of the instrument and reaching around obstacles to a

[2] *Viscerosynthesis:* joining of two (or more) tissue parts (e. g. by suturing, clipping).

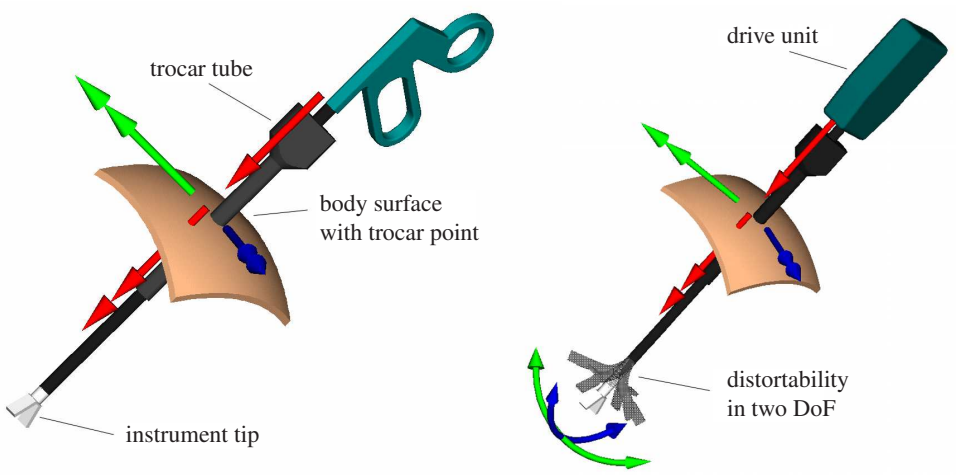

Fig. 2.2: *Left:* Diagram of the four available degrees of freedom (DoF) in conventional minimally invasive surgery (MIS); the instruments are under constraint by the fulcrum point. Double-headed arrows indicate rotational DoF, single-headed translational DoF. *Right:* Diagram of two additional DoF at the distal end of the instrument e. g. in teleoperated MIS. Actuation effects on the proximal end of the instrument, outside the patient [25].

limited degree are then possible. Direct manual guidance of these extra DoF by the surgeon is only feasible with additional mechanisms, which potentially complicate the handling of the instruments and thereby extend the demand for training. A robotic transmission system for simplified instrument actuation has shown to ease these effects [24].

Of course, conventional minimally invasive surgery provides some obvious and fundamental advantages, too. However, it has to be emphasized that almost all of these advantages are in favor of the patient and almost all disadvantages affect the surgeon. Tab. 2.1 gives a compilation of the main advantages and disadvantages of conventional minimally invasive surgery.

2.2 Minimally Invasive Robotic Surgery

One approach to overcome the drawbacks of conventional minimally invasive surgery is telemanipulated minimally invasive robotic surgery[3] (MIRS). Especially the missing dexterity inside the patient and the chopstick effect can be compensated for [26, 27]. Almost all of the previous system approaches follow a telemanipulated, ”master-slave” design with a division into an input unit for the surgeon and a patient sided execution unit [28]. The surgeon comfortably works in front of a master console (operator) separated from the patient and remotely commands an executing slave-robot (teleoperator) with surgical instruments in direct patient

[3] In the strict terminological sense the systems presented in the following are no robots but telemanipulators (cf. Appendix A.2 ’medical robotics’, p. 84).

Tab. 2.1: Major advantages and disadvantages of minimally invasive surgery.

reduced tissue traumatization	**no direct access to the operating field**
+ less post-operative pain	– lost hand-eye coordination (chopstick effect)
+ minor loss of blood	– constricted dexterity (four intracorporeal DoF)
+ less wound healing disorders	– limited perspective, 2-D sight, falsification of color representation
+ reduced risk of infected wounds/general infections	– movement/applied forces depend on instrument insertion way (lever)
+ less risk of deep-vein thrombosis	– heavily diminished kinesthetic/ tactile feedback
+ shorter hospitalization and rehabilitation time (less risk of hospital-acquired infections)	– delayed emergency access
+ faster social reintegration (lower health care cost)	– significantly longer operating time
+ favorable cosmetic results	– complex reorientation after instrument changes
	– necessity of expensive and sophisticated equipment (e. g. endoscope, light/gas insufflation, trocars)
	– higher maintenance cost (sterilization, preparation)
	– extended learning curve, high training needs
advantages (for patient)	*disadvantages (for surgeon)*

contact – preferably with low time delay. This makes it possible to endoscopically perform surgery that requires a relatively high amount of manipulability. However, the entire mechanically decoupled arrangement of surgeon and patient leads to a total absence of kinesthetic and tactile feedback.

The biggest patient benefit can be achieved using MIRS in cardiac surgery since the very traumatizing median sternotomy[4] becomes unnecessary. Many of the developed systems are primarily intended for this purpose. Nevertheless, more and more other surgical disciplines increasingly apply these medical robots effectively, too. New robot supported operation techniques are being invented to perform traditional open surgeries now in a minimally invasive way [2, 29].

Until 2003 over 35 surgical robotic systems have been developed [30]. At the university clinic of Mannheim a research group compiles an online list of all known medical robots which, up to now, even itemizes over 200 systems[5] [31]. For minimally invasive robotic surgery at least three systems have found their way

[4] Operational transsection of the breastbone (*lat.:* sternum).

[5] As of November 2006. The figure refers to all medical disciplines.

Fig. 2.3: DaVinci Surgical System from Intuitive Surgical, Inc. In the front left the master console of the system; in the center the slave-robot (photo courtesy of Intuitive Surgical, Inc., 2009).

into commercial use: the ZEUS-system from Computer Motion, Inc. [28, 32–34], Laprotek from endoVia Medical, Inc. [26,35,36], and the daVinci Surgical System from Intuitive Surgical, Inc. [28, 32, 37]. After the insolvency of endoVia Medical and the merger of Intuitive Surgical/Computer Motion presently only one system is commercially available: the daVinci Surgical System from Intuitive Surgical, Inc. (see Fig. 2.3 – 2.5).

The daVinci Surgical System consists of two main components, a master console and a slave-robot (cf. Fig. 2.4). The posture of the surgeon in front of the console is quite comfortable (cf. Fig. 2.3); he looks towards his hands which are represented by the console as the video picture of the surgical instruments (cf. Fig. 2.5). The instruments offer two plus one[6] additional intracorporeal DoF which allows for full dexterity inside the patient's body. Endoscopic viscerosynthesis is feasible but a feedback e. g. of how tight knots are tied is possible only visually. Extensive operating fields (e. g. for the mobilization of the intestine after cancer resection) can not be handled without multiple reconfigurations and/or additional ports since the workspace of the instruments in one configuration is limited.

Regarding setup and shut-down time as well as overall operating time, robotic surgery takes significantly longer than open surgery. For example an experienced surgeon needs at least a few seconds to tie a knot in robotic surgery whereas in open surgery the same procedure can be performed in less than a second.

Compared to conventional minimally invasive surgery, the daVinci system can

[6]The two branches of the functional end are bound by one single joint but are actuated independently (cf. Fig. 2.5).

(a) Master console.

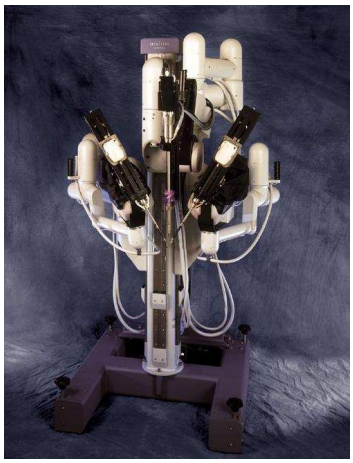

(b) Slave-robot.

Fig. 2.4: Main components of the daVinci Surgical System (photo courtesy of Intuitive Surgical, Inc., 2009).

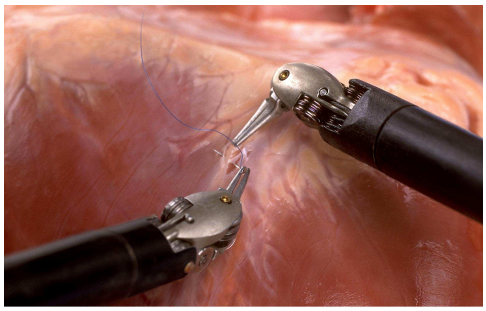

Fig. 2.5: Reestablishment of hand eye coordination in the daVinci Surgical System (photo courtesy of Intuitive Surgical, Inc., 2009).

Tab. 2.2: Major advantages and disadvantages of present minimally invasive robotic surgery.

Separation of surgeon/patient, suitable surgical input console	**Necessity of additional technical equipment**
+ reestablishment of hand-eye coordination	– high purchase cost
+ intuitive use, relatively short learning curve	– high maintenance cost (regular instrument attendance obligatory)
+ comfortable posture for the surgeon (plus indexing)	– limited number of standardized operation types
+ less fatigue, prolonged concentrated work	– considerable setup time
+ 3D vision	– cumbersome instrument change
+ tremor filtering	– longer operating time (vs. MIS)
+ motion scaling	– self-contained system setup
	– no haptic/tactile feedback
	– necessity of specially trained/ educated back staff
advantages	*disadvantages*

support the surgeon in a number of ways, e. g. by reestablishing usual hand-eye coordination or by tremor filtering [26,27,30,38]. However, the self-contained system is applicable only as a whole: Single functional elements like the automated camera guidance with manual MIS can not be taken out. There is prevailing consensus that the high acquisition and maintenance cost, the limited number of performable surgeries, the operating time that is usually longer than in open surgery, and the conservative wait-and-see attitude of many chief physicians are the main reasons preventing that even more systems are being sold.

On account of the described drawbacks, conventional MIS (Sec. 2.1) did not become much more widespread as it was expected after its implementation in the 1980s [32]. A lot of surgical interventions are not appropriately feasible in a minimally invasive way due to the lack of dexterity of the surgical instruments. As presented, the shortcomings can be overcome by minimally invasive robotic surgery. However, this technology holds a variety of drawbacks, too. A summary of the main advantages and disadvantages is given in Tab. 2.2. One of the main problems during use is believed to be the lack of haptic feedback as described in the following section.

2.3 Kinesthetic Feedback in Minimally Invasive (Robotic) Surgery

As described in Sec. 2.2 minimally invasive robotic surgery entails the total absence of haptic feedback due to the complete mechanical decoupling of patient

and surgeon. However, its reestablishment, and even the necessity of kinesthetic feedback in minimally invasive (robotic) surgery was seriously discussed by surgeons and ergonomics scientists, though without doubt haptic feedback is helpful in open surgery. A short compilation of the most important approaches on kinesthetic feedback in MIRS and a detailed description of the ones developed by the DLR are presented in [22, 39]. Recently, quite a number of publications have indicated a noteworthy benefit in reestablishing haptic feedback, however, MIRS systems including kinesthetic feedback are still not commercially available.

In the following, the contents of some of these publications are summarized exemplarily and the positive effects of force feedback are shown with the additional intention to justify the background of this dissertation.

The work of Deml et al. suggests that haptic feedback lets surgeons proceed more gently and cautiously in MIRS as shown in an empirical comparison of an artificial artery preparation using a prototypic MIRS setup with activated and inactivated haptic feedback [40, 41].

Comparable results were presented by the group around Robert D. Howe. Their studies show that the existence of force feedback reduces the extent of unwanted penetrations and enhances performance [42]. Average force and peak force magnitude as well as unwanted tissue damage can be reduced [43, 44]. Additionally, the group points out that the sense of touch is one of the surgeon's most important tools [45].

Allison Okamura's team also performed teleoperation tasks with and without three DoF force feedback, among others blunt dissection tests with phantom tissue. They could show that force feedback is a statistically significant improvement over teleoperation without force feedback [46].

In a test run with 20 test persons and an in-house developed laparoscopic grasper, Tholey et al. documented that providing both vision and force feedback leads to better tissue characterization than vision feedback only [47].

Rassweiler et al. strongly believe that MIRS will entirely change the future of laparoscopic surgery due to the compensation of conventional laparoscopic surgery's drawbacks. Moreover, they point out that amongst others, especially haptic feedback can shorten the learning curve of MI(R)S [27, 38, 48]. Additionally, Russel Taylor and Dan Stoianovici are convinced that force and haptic feedback is often important for telesurgical applications [30].

The group around Knoll and Bauernschmitt were able to present an experimental MIRS system with kinesthetic feedback using customary instruments (Intuitive Surgical, Inc., see Fig. 2.5, top) with strain gauges adhesively bonded to the instrument shaft. The instruments were guided by industrial robots (Melfa RV-6SL, Mitsubishi robots, Inc.), force feedback was provided by customary input devices (Phantom 1.5, SensAble Technologies, Inc.). After evaluation tests they strongly believe that kinesthetic feedback is crucial in MIRS [49, 50].

Intracorporeal knot tying is considered to be a task where haptic feedback is particularly favorable. If knots are not tightened enough they tend to loosen. On the other hand, if the suture threads are pulled too strongly, one side may tear off

and the force still applied to the other side at that moment may rupture the lesion. Bethea et al., Kitagawa et al., and Akinbiyi et al. (Department of Mechanical Engineering and Division of Cardiac Surgery, Johns Hopkins University, Baltimore, USA) presented a system with visual feedback: Three blips comparable to traffic lights, representing force feedback of the left- and right-hand instruments, are superimposed on the top corners of the endoscopic image. "Green" means low forces, "yellow" means ideal forces for knot tying, and "red" means excessive forces. Sensory information is gained by a prototype with strain gauges adhesively bonded to the instrument shaft providing evidence for the benefit of haptic feedback by comparative tests. Each of the cited publications emphasizes the demand for haptic feedback [51–54].

Moreover, Tavakoli et al. investigated two different contact feedback modalities: kinesthetic and visual feedback. They could show that the localization accuracies between both modalities are comparable, but kinesthetic feedback enhances performance significantly in comparison to visual force feedback [55]. In their book Tavakoli et al. give an overview of haptic feedback and its favorable influence in MIRS [56, p. 16 et seqq.].

Srinivasan and LaMotte have shown in direct manipulation experiments that pure kinesthetic (force-position) sensing alone is not sufficient if stiffness is the focus. In absence of the distributed skin sensation of surface deformation their subjects were actually unable to determine the difference between even the hardest and softest rubber samples. They suggest that even the most accurately relayed force feedback is inadequate for compliance discrimination [57] implying the necessity of further feedback modalities.

Concerning the question whether the endeavors to reestablish haptic feedback are worthwhile, two further arguments should be mentioned: First, to evaluate the benefit of kinesthetic feedback compared to its absence it is sensible to implement full kinesthetic feedback. Reliable conclusions then can be drawn by testing and prospective randomized trials. Second, surgeons performing minimally invasive robotic surgery would at least welcome reliable information on how tight knots are tied in viscerosynthesis. However, it is not a large step from implementing the necessary sensors for acquiring thread tension forces in a commercially acceptable manner to realizing sensors for full haptic feedback.

In conclusion, kinesthetic feedback in general is not necessary, however, it seems to be important for single, particular tasks. Therefore, it is assumed that full tactile feedback is not necessary either in most cases since the efforts need to be in proportion to the derived benefit. However, single substitutions of full tactility comparable to the human perception, like detecting pulsations of sub-surficial vessels with the aid of ultrasound, seem appropriate.

As mentioned in Sec. 1 et seqq. the next logical step after achieving satisfying kinesthetic feedback is tactile feedback. As Brouwer et al. point out, the reduction of tactile perception in MIS can even counteract MIS advantages and tactile sensing is of crucial importance [58]. Related work on tactile feedback and publications referring to this dissertation are summarized in the following Sec. 2.4 .

2.4 Related Work

According to literature quite a number of different approaches were followed by various research groups with the objective of achieving full intuitive remote tactile perception. Regrettably, none of them prevailed or found their way to application, most probably due to the fact that tactile sensing is a very complex task and difficult to emulate: not only the development of a sensor/actor-system is problematic but also the generation of an intuitive perception and usage for the surgeon.

In the following the most relevant previous research approaches are introduced and briefly discussed. The underlying principles of the solution proposed in this dissertation against that background shall be presented at the end of the section.

The PhD-thesis of Harald Fischer [59], also published in condensed form [60], describes a miniaturized sensor-actuator system for teletactility. The sensor system is integrated into an endoscopic gripper and contains 8×8 pressure points on 0.64 cm^2. Each pressure point is made up of a partially fixed hollow silicon cylinder which is illuminated by a flexible electro-luminescent sheet at the front end. Applied forces to the silicon cylinders narrow the hollow section and thereby dilute the irradiation guided to a light-sensitive CCD chip by fiber optics. The CCD chip's measurement results can also be displayed graphically through pressure mountains. The actor system comprises an 8×8 array of shape memory alloy brads activated by electric current heating in a one-way effect achieving deflections of up to 3.5 mm at a force of 2.5 N, and a spring readjustment.

However, for higher actuation frequencies the cooling of the shape memory alloy brads remained problematic. Additionally, the size of the presented actuator system does not allow for integration in a customary input device. The basic problem is the finger, resting on the display not allowing for adequate perception (see above and [61]).

An earlier publication of Fischer et al. presents a less sophisticated technical approach for a tactile feedback system [62]: The foil sensor fixed on the branch of a laparoscopic grasper is built of two piezo-resistive conductive polymer layers in lamellar arrangement staggered by 90° and yielding 64 measuring points (12×15 mm). The actor consists of three electromagnetically driven 24 needle printing-heads arranged under the user's fingertip. Since the needles have only two stages, the applied pressure is transformed into corresponding actuation frequencies (limited to 600 Hz). Test results are not reported. However, according to the publication, sensors with higher resolution ought to be developed.

Several research groups[7] cooperated within the TAMIC-Project (*Ta*ktiles *Mi*krosystem für die *M*inimal *I*nvasive *C*hirurgie, tactile microsystem for minimally invasive surgery) to develop three different types of palpation sensors[8] for intraop-

[7] Adolf Bausch GmbH, Medizintechnik, Munich; Daimler-Benz AG, Forschung und Technik, Munich; Daum GmbH, Schwerin; Fraunhofer-Institut für Biomedizinische Technik (FhG IBMT), St. Ingbert; ViewPoint Bildverarbeitung GmbH, Gilching; German Aerospace Center (DLR), Institute of Robotics and Mechatronics, Oberpfaffenhofen; all Germany.

[8] Man-machine interfaces (MMI) were not investigated.

erative result analysis [63, 64]: a pulsatile sensor measuring pressure variations, a vibro-tactile sensor measuring compression as well as shear modulus, and a pressure sensor line measuring forces.

The pulsatile sensor was designed to detect arteries by means of the perfusing, pulsing bloodstream. Therefore, a piezo polymer layer was attached to the tip of a sensor bar measuring pressure fluctuations in longitudinal direction. An impedance converter and evaluation electronics were fitted into the instrument shaft. The evaluation electronics detects signal switches and displays them as a beep [65]. The detection of a pulse on the wrist and carotid arteries on humans showed promising results, endoscopic detection of the hepatic and mesenteric arteries (2.5 mm in diameter under 1 mm of overlay) could be shown in four animal experiments on pigs. However, the piezo polymer layer was prone to damage and the feedback was insufficient. Most troublesome were unwanted signals caused by sensor and respiratory movements, air draft, and sound.

With the vibro-tactile sensor the tissue surface was oscillated and, since human tissue behaves like a harmonic oscillator, it can be characterized by its resonance frequency which is dependent on rigidity and mass. The sensor has an outer diameter of 10 mm, can be applied in endoscopy, and shows the resonance frequency on a display after several seconds. Silicon phantoms of different rigidity and geometry, could be distinguished as well as lung tumors in fresh tissue resections and bone fragments could be differentiated from soft tissue in otorhinolaryngology. However, the different masses of the analyzed tissue inadmissibly influenced the measurement, the transducer tended to cant, and the measurement cycle was felt to be too long [64, 66–69].

While the pulsatile and the vibro-tactile sensors can measure only from the tip in forward direction, the silicon pressure sensor line produced in micro system technology can measure within the jaws of a gripper. A line of eight spilled piezo resistive pressure sensor elements (distance 1.1 mm, maximum load 2.5 N) covered with a metal layer of 14 μm is integrated into a rod which can be introduced in the lower jaw of a tactile gripper [70]. By providing the possibility to rotate the jaw of the gripper containing the pressure sensor line, structures between the jaws of the gripper or outside can be palpated. Since it was assumed that gloved hands have only limited ability to palpate, the measurement result is not displayed on the instrument – palpation chambers filled with electro-rheologic fluid were initially planned – but visually with bars in the endoscopic video stream or on a separate monitor. The sensor showed a high dynamic range and a pulsation on the human wrist could be measured. However, it was fragile and prone to damage, the sensor characteristics have low permanence, and the sensor elements have to be calibrated relative to one another [64].

Extensive research comprising a number of different aspects in the field of tactile feedback especially in MIS surgery has been carried out in recent years by the group around Robert D. Howe at Harvard University, Division of Applied Sciences, Cambridge, MA, USA. The very broad investigations include human examination by touch [61, 71–76], the role and necessary performance of its feed-

back [42–44, 77, 78], a comparison between tactile and kinesthetic feedback [79], simulations of soft tissue [71, 80–83], tactile artery detection [3, 4], and a variety of different tactile feedback systems [45, 84–89] with evaluation results [90, 91] and even with clinical trial descriptions [92]. The necessity of tactile feedback in MIS according to Howe et al. was introduced in Sec. 2.3, hence, the introduced tactile feedback systems, especially those for tactile artery detection, are briefly discussed here.

The display described in [85] is very similar in its basic idea to the one in H. Fischer's PhD-thesis (see above in this Sec.), though differently actuated: 6×6 brads of 1 mm in diameter are deflected by commercial servomotors to a maximum of 2 mm at a frequency of at least 7.5 Hz. The performance of the display is thought to be satisfying, however, it is by far too big for an integration into a customary input device, and the perceiving finger is resting, not allowing for adequate perception (see above and [61]).

The vibro-tactile display presented in [86] is not intended for tactile feedback but substitutes manipulation forces during peg insertion by vibrations in four directions. It could be shown that peak forces during the insertion task could be reduced significantly. The presented sensory substitution of contact forces by fixed frequent vibrations can be compared to the modality substitution proposed in this thesis.

For remote palpation a distributed pressure sensor was introduced and discussed by the group [45, 79, 84, 88, 89]. The sensor showed several positive effects in object manipulation and was even used for artery palpation [3]. The sensor, intended for tumor and artery localization in MIRS, is made up of orthogonal layers of copper strips separated by a dielectric, thus building an array. An 8×8 structure with a 2 mm elements spacing was realized. Applying pressure to the sensor brings the copper strings closer together, changing the measured capacity. Measurement results can be displayed visually on a monitor as well as on a special tactile display. The display is comparable to the one described in H. Fischer's PhD-thesis (see above in this Sec.): spring readjusting shape memory alloy brads in 6×4 array arrangement are deflected at a bandwidth of 10 Hz with a force of at least 1 N per brad. Results with the system were promising, however, with increasing target size (i. e. tumor width) detection errors also increased, since perception of the measurement is relative and depends on sensor application force. Additionally, noise in the measurement and performance of the shape display were a problem. Nevertheless, detection of the radial artery was possible with the system, although the determination of the exact position of the artery under the sensor was difficult.

The same sensor technology in a 10×1 array was used to detect and follow hidden arteries semi-autonomously and with robot support. Tests on the radial artery were promising, however, the artery curvature radius had to be > 80 mm and the robot control algorithms showed room for improvement [4]. In an improved 10×1 shape an enhanced display with water cooling of the shape memory alloy deflections of 3 mm with a drop of 30% at 40 Hz and a force of < 1 N per brad could be achieved. However, for some test users the actuation frequency was still too low [87]. In a later publication the group around William Peine presented a

commercialized 3×12 version of the sensor focusing on the tactile localization of pulmonary nodules indicating lung cancer. Interestingly, a pseudo-color map of measured pressure distribution is registered and overlaid on the live video. Hence, a form of modality substitution is performed. However, the sensitivity of the sensor was too low for practical application and has to be adapted [93].

In the PhD-thesis of William Peine – supervised by Robert D. Howe – a combined system of the 8×8 sensor [88] and the 10×1 display [87] integrated in one instrument (one-handed use) is presented as well as a good overview of human sensing and palpation system design issues [94].

Hayward et al. presented a tactile display, different from typical shape displays (cf. abridged report of H. Fischer's PhD-thesis) or vibro-tactile displays: They used 64 actuated brads (12×12 mm) moving transversely to the fingertip, not up and down. This way the touching skin is stretched, provoking different sensations [95, 96]. This approach is unconventional, unfortunately however, the signal presentation is not quite intuitive and the user's ad hoc interpretation of the perception not yet fully understood. With the brads of the display moving transversely, the display does not seem to be suitable for displaying pulsations.

William Provancher (Department of Mechanical Engineering, Stanford University) presented a tactile sensor for object curvature measurement and a finger/object contact locations display in his PhD-thesis [97]. The sensor in array structure is deformed by a contact, displacing strain gage pairs located in the sensor surface under a thin elastomer membrane. The display renders contacts by a simple roller housed in a thimble and providing reaction forces to the finger pad. The roller is actuated by a servo-motor via push-pull wires. First tests in object handling are promising, however, hand and finger motion is not free since the servo-motor is attached to the lower arm of the user. Finger bending therefore is very limited, the lower arm has to be placed on an arm rest making sweeping gestures (e. g. for MIRS mastering) difficult.

The group around Ronald Fearing (Department of Electrical Engineering and Computer Sciences, University of California, Berkeley) also worked on teletactility, including basic issues [98], human psychophysics [99, 100], and signal detection [101]. They surveyed tactile sensing mechanisms [102] and presented own approaches [103–105]. Although the focus of their work is not MIRS, basic design parameters for tactile feedback systems [99] as well as a compliant tactile display [104] could be shown. In contrast to the others mentioned above, they present a round system matched to the axial finger form, deflecting 5×5 silicone brads pneumatically. Psychophysical experiments show promising results and the size of the display allows for integration into a tactile display glove.

The work of Javad Dargahi et al. (Concordia University Montreal, Quebec, Canada) focuses on tactile sensor development for MIRS introducing (design, fabrication, testing, and mathematical modeling of) a sensor based on a polyvinylidene fluoride (PVDF) membrane. When touched, the PVDF integrated sensor surface becomes distorted inducing stress/strain signals to only a small number (three or four respectively) of sensing elements. The actual sensor load can be concluded

from prior calculation including the sensing elements. The sensor therefore is not in array structure and sensitive on its entire surface, moreover its mass production is unproblematic [106–110]. Tests seem to be promising, however, PVDF is not only sensitive to mechanical stress but also to temperature distorting measurement results. The sensor principle was integrated into an endoscopic grasper [111–114]. Frontal application of the sensor is not recommendable since it would record parasitic manipulation forces due to pressing forces. However, in this case only structures that can be clasped around are palpable, limiting the applicability of the sensor. A color coding display method for softness, stress distribution, and lumps measured by the sensor is presented in [115]. Consequently, it can be said that a modality substitution is performed with the system (tactile information – optical information). A 10% average variation between data sets and known tactile properties is described. Pulse-detection processes with the system are worked on with the sensor being integrated in a grasper. Additionally, by clasping around a vessel the blood can be interrupted leading to incorrect pulsation measurements. In their book Dargahi et al. give a good summary of the present state of the art in biomedical tactile sensing and feedback especially in MI(R)S [116]. However, in addition to the consideration of the technical bases the book focuses on mechanical properties of tissues like stiffness and hardness for tumor detection. Neither pulsations within tissue nor ultrasound based sensors or modality substitution are mentioned.

A comparable approach to the PVDF based sensor of Dargahi et al. was presented by Menciassi et al. using a semiconductor strain gauge based force sensor built in an endoscopic grasper. With this grasper it is possible to detect vessels based on their pulsation [117]. However, the problems of interrupting the blood flow and clasping around a vessel are present in the same way.

Tavakoli et al. (Department of Electrical and Computer Engineering, University of Western Ontario, London, Ontario, Canada) worked on the realization of a haptic feedback system for soft tissue palpation [118, 119]. For this purpose they developed a sensorized, endoscopic gripper and a haptic interface with force/torque feedback. The sensorized, endoscopic gripper is designed with a strain gauge fitted inner shaft (only in contact with the manipulated tissue) and a rigid outer shaft (contactless with the inner shaft and absorbing outer reaction forces, e. g. trocar forces) [120]. The haptic interface is built as an extension of a three DoF commercial system (Phantom, Sensable Technologies, Inc.) using brushed DC motors to provide feedback in five DoF (including functional DoF) [121]. Investigations evaluating multi-modality feedback (visual and haptic) are performed with positive outcomes for haptic feedback [55, 122]. The system shows acceptable results for soft tissue palpation [123], however, by design it focuses on kinesthetic sensing, therefore, the sensor seems unsuitable for detecting pulsations or vessels.

The group around Martin O. Culjat presented a master/slave tactile feedback system mountable to a daVinci surgical system (cf. Sec. 2.2). The master console sided actuator consists of 3×2 balloons (3 mm in diameter, 1.5 mm max. deflection, > 2 N output force for each balloon) strapped to the user's finger tip and a pneumatic control unit providing five levels of force feedback over a force

input range of $0 - 25$ N. To measure tactile information a customary piezoresistive thin-film force sensor was mounted in a standard grasper of the daVinci surgical system [124–128]. Promising primary results are reported for grasping force tasks [129], however, the system seems more suited to kinesthetic than to tactile feedback since tasks like surface roughness classification will probably prove to be difficult. Additionally, with the described sensor arrangement only structures that can be clasped around are palpable as impairing influences of contact forces are to be avoided.

With two different tactile displays Hendrik Van Brussel and his group from the Katholieke Universiteit Leuven, Belgium, could show that perpendicular indentation displays are better suited in edge detection tasks of hard material covered by artificial tissue than lateral skin stretch displays [130]. Moreover, they could present a tactile display with five microhydraulically actuated brads in line. The brads have an outer diameter of 1.57 mm, a stroke of 2 mm, a spatial resolution of 2 mm, and can exert a maximal force of 0.5 N [131]. Recently, they reported on an elastoresistive 16×16 tactile sensor with a resolution of 1 mm and a bandwidth of 78 Hz for pressure distributions. Detecting a hard ball under 5 mm of covering gelatine showed promising results [132]. Further, they could present results of an ultrasound deformation imaging test in which the elasticity of four phantoms could be differentiated with a commercial ultrasound probe equipped with a sensor for longitudinal forces [133]. All approaches, however, focus on the detection of inhomogeneities within tissue which amounts to the detection of tumors and tumor margins. Tactile artery detection is not addressed.

Salcudean et al. (Department of Electrical and Computer Engineering, University of British Columbia, Vancouver, Canada) developed a setup [134, 135] and enhanced control strategies [135–139] for a teleoperated, robot-assisted, diagnostic ultrasound system, including a user interface [140–142], haptic interaction [143, 144], and ultrasound image processing [145, 146]. The robot is designed to carry the imaging probe of a customary ultrasound system for the examination of the carotid artery, basically to provide an enhanced user interface. The system seems to favorably combine telemanipulated medical robotics and ultrasound imaging. However, the system is primarily designed for the noninvasive application in limited areas and not intended for intraoperative use. For safety reasons, maximum probe forces are limited to 10 N by design by means of a fully balanced robot carrying a preselected ultrasound probe, therefore restricting other applications. Especially for minimally invasive procedures the suggested ultrasound probe is too big and the robot kinematics is unsuitable for use with an invariant entry point. In addition, simultaneous diagnosis and teleoperated tissue manipulation is complicated in addition, since the system's input devices are application specific and not intended to guide additional surgery robots.

To localize coronary arteries Budde et al. use a customary, miniaturized imaging ultrasound transducer by Aloka, Tokyo, Japan, and contact it to the region of interest by simply gripping it with common MIRS instruments (daVinci surgical system, cf. Sec. 2.2). A conventional ultrasound image is then displayed on a

color-Doppler system [147]. A registration of the endoscopic video image and the ultrasound-Doppler image is not reported, which suggests that they are presented on different screens and in different orientations. This forces the surgeon to take his head out of daVinci's master console (causing automatic blocking of the instrument control) to verify the ultrasound image on a second screen without being able to reorient the ultrasound transducer by means of this image (since the instrument control is blocked at this moment). The approach therefore seems quite non-intuitive. Altering daVinci's display signals seems difficult since Intuitive Surgical, Inc., would have to give extensive access to its proprietary, self-contained console.

A comparable approach is reported by Falk et al. where an ultrasonic catheter allowing B-mode, color Doppler, and continuous wave Doppler imaging (by Acuson, Mountain View, CA, USA) was inserted through a 5 mm port and manipulated with customary MIRS instruments (daVinci surgical system, cf. Sec. 2.2). The internal thoracic artery and the left anterior descending artery could be detected in a canine model [14].

Also comparable to Budde et al. [147] is the work of an Intuitive Surgical, Inc., and Johns Hopkins University research group around Leven et al. where ultrasound images and endoscopic images can be overlaid in real-time in a daVinci Surgical System [148]. The focus of their work, which shows promising results, was laparoscopic liver cancer surgery, however, due to the rigid ultrasound instrument not all sectors of the operative field could be reached, which was unsatisfactory. Additionally, the tracking algorithms to register ultrasound and endoscopic images were not robust enough. Detecting hidden arteries in general surgery was not their objective, however, the usage of complex and high-priced ultrasound imaging technology might not be purposeful. Furthermore, Leven et al. cite a number of other groups using robotically-assisted ultrasonography, but none of them applies ultrasound to deduce tactile perceptions.

A state-of-the-art overall view of tactile sensing in the 1980s and 1990s is given in the review articles by Nicholls and Lee [149–151], however, tactile artery detection is not discussed. The review article of Eltaib and Hewit [152] focuses on tactile sensing in MIS, yet tactile artery detection is only addressed indirectly by presenting tactile sensor principles. Westebring et al. [153] as well as Puangmali et al. [154] review research on kinesthetic (cf. Sec. 2.3) and tactile feedback in MIS, but tactile artery detection comparable to the approach presented in this dissertation is not reported.

Various other publications present tactile sensing approaches for MIS [155–161] – most of them for measuring the elastic properties of tissue –, special control algorithms [162], investigate human finger perception [57, 163–165], or draw conclusions on tactile characteristics from special MIS graspers [166–170]. However, none of the found publications focuses on the detection of blood vessels as a central issue or describe an approach comparable to the one proposed in this thesis.

In the book of Webster mainly basic sensor principles are discussed, biomedical considerations are taken into account but play a secondary role [171]. The particular problems of sensor integration in MI(R)S are not discussed at all. In

the last chapter of his book an electrocutaneous stimulation system to display tactile information e. g. from the hand is described. However, the system does not seem suitable for the intended purpose described in this dissertation since the 16 electrodes used (5 mm in diameter, centers 18 mm apart) and feeding back tactile sensor information are placed on the abdomen of the test person [171, p. 341 et seqq.]. The book by Grunwald et al. on human haptic perception gives a good general picture of physiological and psychological aspects as well as about haptic man-machine interfaces (MMI) and applications [172], but haptic feedback – especially tactile feedback – in MI(R)S is not discussed at all.

Publications focusing on tactility for robotic manipulation [173, 174] showed only limited relevance concerning the contents of this thesis. However, the book of Russell on robot tactile sensing [175] gives a good overview of human touch sensing, possible (robot) tactile sensor designs, and tactile sensor information processing although the objective of the book is different from the one in this thesis.

In all actuator approaches based on an array of brads two main problems remain in MIS applications: Firstly, the hand of the surgeon must be taken away from the input device to touch the tactile feedback device and to percept the tactile feedback signals, which is impractical. Secondly, intuitive palpation is associated with (finger) movement [61] so that different receptors are activated continuously. In the introduced cases the receptors relative to the actor are largely stationary, so the superficial mechano-receptors in the skin of the human finger tip are continually charged in the same way. Consequently, receptors exhaust and perception deteriorates becoming unintuitive.

Virtually all the above mentioned approaches have in common that kinesthetic or tactile sensor signals respectively are submitted to the user (surgeon) in an unchanged way, i. e. no modality substitution is considered. Only in some of the approaches an additional visual feedback is implemented. As said in Sec. 1.1, in this thesis, in contrast, a modality substitution is proposed, where expected tactile impressions are displayed kinesthetically.

As described, the basis of the approach presented in this dissertation is Doppler-ultrasound technology. The necessary basic knowledge and the related work are discussed in the following Cha. 2.5.

2.5 Doppler Ultrasound Technology

This section gives a very brief review of the ultrasound technology fundamentals focusing on the objective of this dissertation. For this purpose information mainly from the books of Kuttruff [176], Jensen [177], Evans et al. [178], Schäberle [179], Dössel [180], Duck et al. [181], and Kremkau [182] is summarized. The development of the advanced sensor described in Cha. 3 is based on the following considerations.

Sec. 2.5.1 is related to the basics of ultrasound generation and the fundamentals of ultrasound behavior in human tissue. The Doppler principle and its utilization

as a measurement method for blood flow in living tissue is briefly described in Sec. 2.5.2 .

2.5.1 Ultrasound and its Application in Medicine

Ultrasound is a mechanical, compressional wave of matter propagating periodically in a medium with a frequency above the audible range (>16-20 kHz). The upper limit of ultrasound is the beginning of microwave acoustics at about 1 GHz [176–178]. The frequency range of ultrasound used in medical applications (imaging, therapy) usually ranges from about 50 kHz to 150 MHz.

Ultrasound propagation is bound to a medium according to

$$\lambda = \frac{c}{f} \tag{2.1}$$

where $\lambda\ [m]$ is the wave length, $c\ \left[\frac{m}{s}\right]$ is the media specific sound propagation velocity (see below), and $f\ \left[Hz = \frac{1}{s}\right]$ is the frequency with

$$f = \frac{1}{T} \tag{2.2}$$

where $T\ [s]$ is the wave period. While ultrasound propagates well in liquids (low-grade attenuation, see below) up to a certain intensity[9] air highly attenuates the propagation with increasing ultrasound frequency. Inducing ultrasound from a transducer into tissue therefore needs an adequate coupling medium. In gases and liquids (and also in tissue) ultrasound propagates only as a longitudinal wave while in solids also transverse waves occur due to shear stress.

Ultrasound energy is transmitted through a medium[10] with a certain sound propagation velocity $c\ \left[\frac{m}{s}\right]$ which is dependent on its adiabatic compressibility $\kappa\ \left[\frac{m^2}{N}\right]$ and its density $\rho\ \left[\frac{kg}{m^3}\right]$ according to [177, p. 17]

$$c = \sqrt{\frac{1}{\rho \cdot \kappa}} \quad . \tag{2.3}$$

Typical values of sound propagation velocities in biological materials are shown in Tab. 2.3 . In the frequency range of interest for this thesis, namely 1-20 MHz (cf. Cha. 1.2 and 3), the sound propagation velocity is effectively independent of frequency, since dispersion effects need not to be taken into account. The effect of small temperature changes can also be ignored [178, p. 28].

[9] Pressure fluctuations of high intensity can reach $0 < p \leq 2p_0$, where $p\ \left[Pa = \frac{N}{m^2}\right]$ is the current pressure and $p_0\ \left[Pa = \frac{N}{m^2}\right]$ is the ambient pressure. However, for $p \rightarrow 0$ liquids tend to change their state of aggregation ("cavitation").

[10] The considerations refer to fluids (and also to tissue). Sound propagation velocity in solids follows $c = \sqrt{\frac{E}{\rho}}$ where $E\ [Pa]$ is the modulus of elasticity and $\rho\ \left[\frac{kg}{m^3}\right]$ is the material density.

Tab. 2.3: Summary of the important ultrasound parameters density, sound propagation velocity, and acoustic impedance of selected bio-materials, according to [178, p. 28], [177, p. 19] .

Material	Density $\rho \left[\frac{kg}{m^3}\right]$	Velocity $c \left[\frac{m}{s}\right]$	Acoustic Impedance $Z \left[\frac{kg}{m^2 \cdot s}\right]$
Air (NTP)	1.2	330	$0.0004 \cdot 10^6$
Blood	1600	1570	$1.61 \cdot 10^6$
Bone	1380–1810	3500	$7.80 \cdot 10^6$
Fat	920	1450	$1.38 \cdot 10^6$
Muscle	1070	1580	$1.70 \cdot 10^6$
Soft Tissue Average		1540	$1.63 \cdot 10^6$
Water (20°C)	1000	1480	$1.48 \cdot 10^6$

To create ultrasound waves usually the inverse piezoelectric effect is used: by impressing an alternating voltage on special crystals or ceramics[11], e. g. lead-titanate-zirconate ($Pb(Zr, Ti)O_3$), barium titanate ($BaTiO_3$), or quartz (SiO_2), a thickness vibration is initiated. Coupled into tissue, this oscillation propagates as an acoustic pressure wave. In turn, an echoing acoustic pressure wave hitting the piezo element induces a (comparably small) electric signal proportional to the acoustic pressure (piezoelectric effect). In medical applications a number of these transducer elements can be integrated into an ultrasound probe.

Transducer elements can be characterized by the acoustic field they generate. In the simple case of a single, continuously activated, circular, and planar transducer a beam comparable to the one shown in Fig. 2.6 will be generated, assuming that any point on the transducer surface emits a spherical wave (Huygens-Fresnel principle). Due to interferences the beam is narrowed down (natural focus) while the position of this constriction depends on the frequency and shape factors of the transducer. By introducing a central axis $x\ [m]$ starting at the transducer surface and continuing forward, the beam (depicted by a -6 dB boundary) can be divided in a near field (Fresnel zone) with $x \leq \frac{D^2}{2 \cdot \lambda}$ and a far field (Fraunhofer zone) with $x > \frac{D^2}{2 \cdot \lambda}$ while $D\ [m]$ is the diameter of the circular transducer. The focal distance is given by $x = \frac{D^2}{4 \cdot \lambda}$.

Interactions between tissue and ultrasound waves mainly occur at tissue interfaces (acoustic impedance steps) with different sound velocities and tissue densities. Here, both scattering (which includes reflection and refraction) and absorption contribute to the attenuation of a plane sound wave which will be reviewed briefly in the following.

As shown in Fig. 2.7 ultrasound waves are only partly transmitted through

[11] The piezoelectric effect is also shown by some high polymer plastics, e. g. polyvinylidene fluoride (PVDF), but for ultrasound transducers used in medical applications most often small ceramic plates metallized on both sides are used.

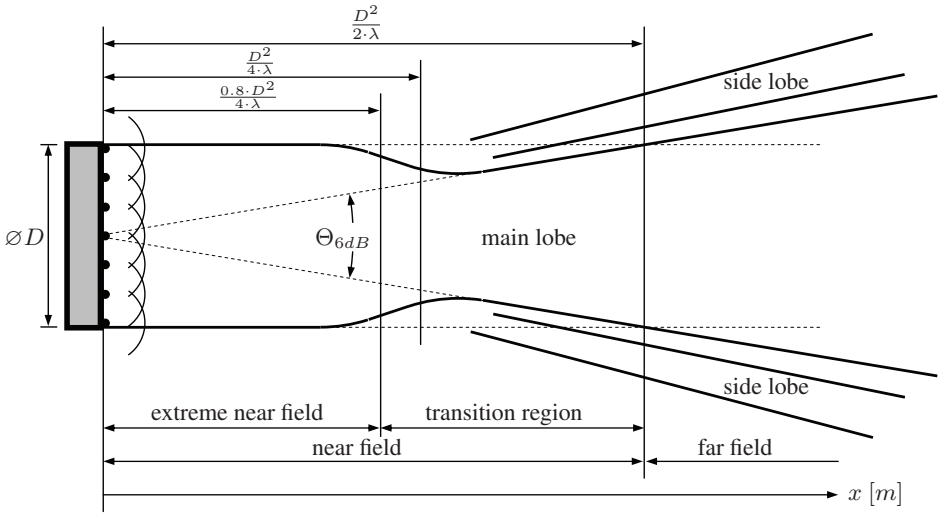

Fig. 2.6: Ultrasound beam characteristics (simplified) of a single, continuously activated, circular, and planar vibrating plate (section).

tissue interfaces with different acoustic impedances[12] $Z\left[\frac{kg}{m^2\cdot s}\right]$ according to

$$Z = \rho \cdot c \quad . \tag{2.4}$$

The transmission coefficient $T\ [1]$ is the ratio of transmitted intensity to incident intensity and can be calculated by

$$T = \frac{4 \cdot Z_1 \cdot Z_2 \cdot \cos\alpha \cdot \cos\beta}{(Z_1 \cdot \cos\beta + Z_2 \cdot \cos\alpha)^2} \quad . \tag{2.5}$$

In turn, the reflection coefficient $R\ [1]$ is the ratio of reflected intensity to incident intensity and can be calculated by

$$R = \left(\frac{Z_1 \cdot \cos\beta - Z_2 \cdot \cos\alpha}{Z_1 \cdot \cos\beta + Z_2 \cdot \cos\alpha}\right)^2 \tag{2.6}$$

since ideally $T + R = 1$. As shown, rough surfaces reflect a diffuse acoustic cone that broadens with decreasing wave length, which explains why an ultrasound echo can be detected with the same transducer even if the tissue interface is not perpendicular to the incident ultrasound beam. However, ultrasound echoes can also be detected coming from tissue between interfaces due to scattering effects at small inhomogeneities. Basically three scattering types are differentiated: omnidirectional scattering ($d \ll \lambda$), forward/backward scattering ($d \approx \lambda$), and reflection ($d \gg \lambda$) where $d\ [m]$ is the particle diameter.

[12] An obsolete but in practice still used unit is $1\ [Rayl] = 1\left[\frac{g}{cm^2\cdot s}\right] = 10\left[\frac{kg}{m^2\cdot s}\right] = 10\left[\frac{Pa\cdot s}{m}\right]$ named after John William Strutt, 3rd Baron Rayleigh, English physicist *1842 (Langford Grove, Meldon, England), †1919 (Terlin's Place, England).

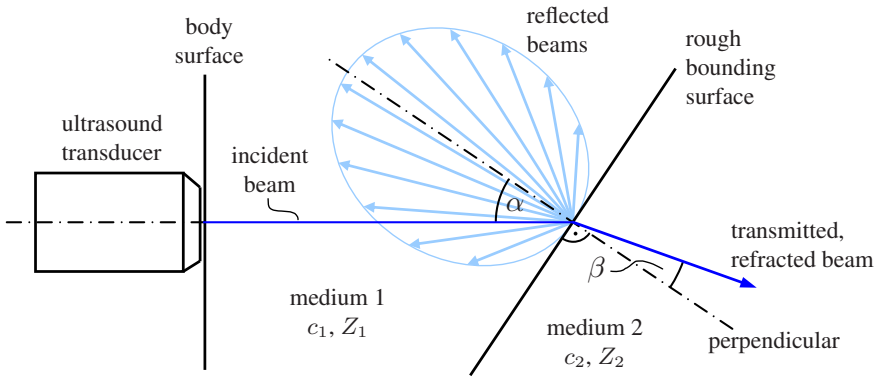

Fig. 2.7: Ultrasound wave reflection/scattering on rough tissue interfaces. As explained in the text, $\alpha > \beta$ due to refraction. Graphics according to [180, p. 189].

The second contribution to scattering (also shown in Fig. 2.7) is the refraction effect: Nonperpendicular incident acoustic beams are not transmitted in their original direction but under an angle of refraction which can be calculated according to Snell's law by

$$\frac{\sin\alpha}{\sin\beta} = \frac{c_1}{c_2} \tag{2.7}$$

where α $[^\circ]$ is the angle of incident, β $[^\circ]$ is the angle of refraction, and $c_{1,2}$ $\left[\frac{m}{s}\right]$ are the sound velocities in the two media.

Additionally, ultrasound energy is partly absorbed in tissue and mainly dissipated to heat (cf. Fig. 2.8, *left*). The absorption (which accounts for 75-95% of the total attenuation [183]) can be characterized by

$$I_x = I_0 \cdot e^{-\mu \cdot x} \tag{2.8}$$

usually referred to as Lambert-Beer law, where I_x $\left[\frac{W}{cm^2}\right]$ is the local intensity at penetration depth x $[cm]$, I_0 $\left[\frac{W}{cm^2}\right]$ is the initial intensity, and μ $\left[\frac{1}{cm}\right]$ is the frequency dependent intensity absorption coefficient. However, attenuation is usually given as a ratio between local and initial intensity in decibel $[dB]$ calculated by $10 \cdot \log_{10}(I_x/I_0)$. Therefore, I_x is not calculated by Eqn. 2.8 but by

$$I_x = I_0 \cdot 10^{-\mu \cdot x} \quad . \tag{2.9}$$

Thereby, μ is characterized by

$$\mu = \alpha \cdot f^n \tag{2.10}$$

where α $\left[\frac{dB}{MHz^n \cdot cm}\right]$ is the tissue specific attenuation coefficient, f $\left[\frac{1}{s}\right]$ is the ultrasound frequency, and n $[1]$ is a constant representing the frequency dependency[13]

[13]The intensity absorption coefficient of physiological soft tissue shows almost linear dependence on the frequency within the range of $1 < f < 20$ *MHz*. However, many liquids (including water) show a quadratic dependence.

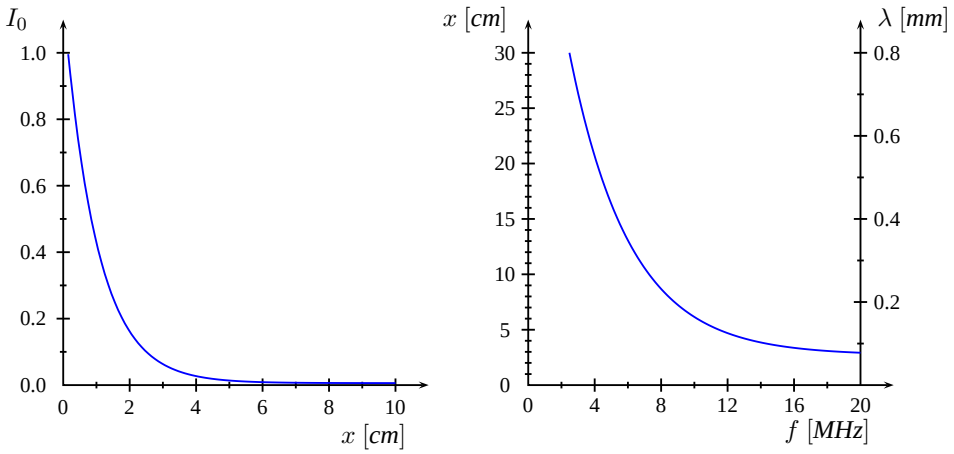

Fig. 2.8: Qualitative presentation of ultrasound energy absorption (left) and attenuation (right) within soft tissue. On the left the normalized initial ultrasound intensity is shown versus the penetration depth for 7.5 MHz; on the right the penetration depth is shown versus the ultrasound frequency (with the according wave length for a soft tissue average of $c \approx 1540 \frac{m}{s}$). It can be seen that the penetration depth decreases with increasing ultrasound frequencies since the attenuation increases. Graphics according to [182, p. 34] .

with $1 < n < 2$, appropriate since attenuation is tissue and frequency specific [181, p. 74]. The attenuation coefficient can be described by

$$\alpha = \frac{10}{x} \log_{10} \frac{I_0}{I_x} = \frac{20}{x} \log_{10} \frac{A_0}{A_x} \tag{2.11}$$

where again I_0 is the initial intensity, I_x is the local intensity at penetration depth x , A_0 $[cm]$ is the initial amplitude, and A_x $[cm]$ is the local amplitude at penetration depth x (cf. Fig. 2.8, *right*).

According to literature (e. g. [177, p. 30]), the attenuation coefficient of soft tissue usually is in the range of $0.2 < \alpha < 2 \left[\frac{dB}{MHz \cdot cm}\right]$.

2.5.2 Doppler Principle

The Doppler principle in diagnostic ultrasound is a non-invasive method for the detection and velocity measurement of matter moving within structures, especially blood flow in tissue. The principle is based on the fact that the frequency of a sound-source in relative motion to an observer is slightly shifted. This effect was first described by Christian Doppler[14] in conjunction with the color appearance of double stars[15] [185].

[14] Christian Andreas Doppler: Austrian physicist, *1803 (Salzburg), †1853 (Venice).

[15] Ballot tried in 1845 to prove Doppler's effect wrong [184] but it did turn out that Doppler was correct, although Doppler's claim [185] of explaining the color of the stars was wrong [186].

In Doppler sonography, ultrasound is coupled into the body, reflected at any interface and the reflected signal is measured and analyzed. Corpuscular components in the blood (e. g. erythrocytes) moving relative to the ultrasound source receive a shifted frequency according to Doppler. This is due to the fact that the propagation velocity increases with a motion towards the stationary source (and decreases with a motion away from the source) from the receiver's view, according to

$$c_c = c \pm v \quad , \tag{2.12}$$

where c_c is the sound velocity received by the corpuscle, c is the sound propagation velocity in the considered medium (cf. Tab. 2.3), and v is the velocity of the corpuscle (positive sign towards the sound source, negative sign away from the sound source). With Eqn. 2.1 the received frequency of the corpuscle can be calculated by

$$f_c = \frac{c_c}{\lambda} = \frac{c \pm v}{\lambda} = f_0 \frac{c \pm v}{c} = f_0 \left(1 \pm \frac{v}{c}\right) \quad . \tag{2.13}$$

Having received the ultrasound impulse, the corpuscle itself becomes the sender echoing the impulse, while the receiver (ultrasound transducer, cf. Fig. 2.9) is stationary. In this case not only the ultrasound source is moving but also the medium [176, p. 52], so the wavelength[16]

$$\lambda = c \cdot t \tag{2.14}$$

is then calculated taking into consideration the source's movement by

$$\lambda_r = \frac{(c \pm v)\, t}{f_c \cdot t} = \frac{c \pm v}{f_c} \tag{2.15}$$

with the positive sign away from the sound source and the negative sign towards the sound source. Hereby, λ_r is the wavelength received by the ultrasound transducer and f_c is the frequency received by the corpuscle. Accordingly, the frequency f_r received by the transducer is

$$f_r = \frac{c}{\lambda_r} = \frac{c \cdot f_c}{c \pm v} = \frac{f_c}{1 - \frac{v}{c}} \quad . \tag{2.16}$$

In case of an angle φ between moving direction and direction of the sound propagation (cf. Fig. 2.9) $\cos\varphi$ has to be amended to Eqn. 2.13 and 2.16, yielding

$$f_c = f_0 \left(1 \pm \frac{v}{c} \cdot \cos\varphi\right) \tag{2.17}$$

and

$$f_r = f_0 \cdot \frac{1}{1 \pm \frac{v}{c} \cdot \cos\varphi} \tag{2.18}$$

respectively. Sonography, therefore, is a matter of "double-Doppler" because the corpuscle receives a Doppler-shifted frequency, becomes the sender itself, and the

[16] According to $x = v \cdot t$ in the case of a linear movement in Newtonian mechanics.

transducer receives a Doppler-shifted frequency of the corpuscle's echo. In the case of a corpuscle moving away from the transducer (according to Fig. 2.9) the corpuscle receives the frequency

$$f_c = f_0 \left(1 - \frac{v_d}{c} \cdot \cos\varphi\right) \tag{2.19}$$

and the transducer then receives the echoed frequency

$$f_r = \frac{f_c}{1 + \frac{v_d}{c} \cdot \cos\varphi} \tag{2.20}$$

which can be written as

$$f_r = \frac{f_0 \left(1 - \frac{v_d}{c} \cdot \cos\varphi\right)}{1 + \frac{v_d}{c} \cdot \cos\varphi} \quad . \tag{2.21}$$

The interesting Doppler frequency Δf referring to the emitted and received frequencies of the transducer is then calculated by

$$\begin{aligned} \Delta f = f_0 - f_r &= f_0 - \frac{f_0 \left(1 - \frac{v_d}{c} \cdot \cos\varphi\right)}{1 + \frac{v_d}{c} \cdot \cos\varphi} \\ &= f_0 \left(\frac{c + v_d \cdot \cos\varphi}{c + v_d \cdot \cos\varphi} - \frac{c - v_d \cdot \cos\varphi}{c + v_d \cdot \cos\varphi}\right) \\ &= f_0 \left(\frac{2 v_d \cdot \cos\varphi}{c + v_d \cdot \cos\varphi}\right) \quad . \end{aligned}$$

Assuming that $c \gg v_d$ this can be written as

$$\Delta f = \frac{2 \cdot f_0 \cdot v_d \cdot \cos\varphi}{c} \tag{2.22}$$

which is usually found in literature, e. g. [178, p. 39].

Conventional Doppler measurement is either performed as pulsed-wave Doppler or as continuous-wave Doppler. In pulsed-wave (pw) Doppler mode only a short ultrasonic signal (burst) is sent and by measuring the running time of the returning echo a point can be calculated. Therefore, pulsed-wave doppler allows relatively precise localization and can be realized with only one single transducer being used as sender and receiver. However, the maximum velocity measurable is relatively small due to aliasing[17] effects, too small for blood flow velocities often occurring in stenoses or shunts. Then, the continuous-wave (cw) Doppler principle has to be used in which a constant signal is permanently sent and simultaneously echoes are recorded with a second transducer.

However, a conventional Doppler ultrasound probe as outlined in Fig. 2.9 is sensitive to motions in all directions except perpendicular to the ultrasound beam ($\varphi = 90°$), and it records the *distribution* of velocities if not all particles flow at the

[17] Depending on pulse repetition rate and penetration depth.

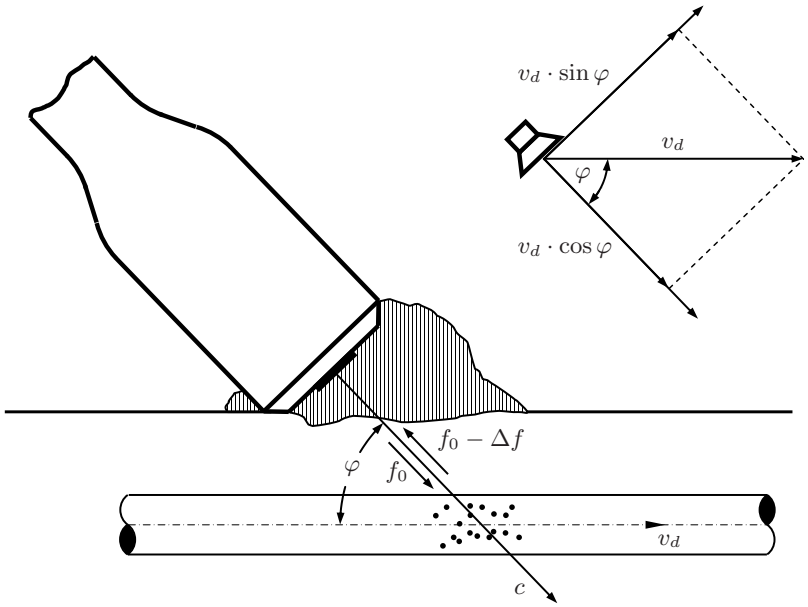

Fig. 2.9: Graphical representation and explanation of variables of Doppler's principle. Graphics according to [180, p. 204] and [179, p. 3 and p. 4] .

same speed. The relatively high velocities of blood cells moving in large vessels (cf. Sec. 3.2) result in frequency shifts of approximately 100 to 10,000 Hz assuming wavelengths of about $0.1 - 0.3$ mm as in usual vascular sonography. Therefore, direct acoustic display of the Doppler frequency Δf by subtracting the base frequency f_0 from the measured signal generates sounds in the audible range. These are characteristic for pulsating blood flow and intuitive for trained physicians.

A literature search concerning Laser Doppler Flowmetry (LDF) was performed as this is an alternative, established method to ultrasound based Doppler flowmetry.

LDF is a technique for the real-time measurement of microvascular erythrocyte perfusion in tissue by illuminating the tissue under observation with low power laser light from a probe containing optical fiber light guides. Laser light from one fiber is scattered within the tissue and some is scattered back to the probe. Another optical fiber collects the backscattered light from the tissue and returns it to the monitor. Most of the light is scattered by tissue that is not moving but a small percentage of the returned light is scattered by moving red blood cells. The light returned to the monitor undergoes signal processing whereby the emitted and returned signals are compared to extract the Doppler shift related to moving red blood cells [187–190].

The LDF technique is valuable in the measurement of microvascular blood perfusion, e. g. for the quantification of retinal and optical nerve perfusion [191, 192]. The method is non-invasive since the probe is not actually required to touch the surface of the tissue and in no way harms or disturbs the normal physiological state

of microcirculation. However, LDF does not seem to be appropriate for detecting comparably large and palpable vessels like coronary, cystic, or hepatic arteries (cf. Sec. 1.1). Furthermore, measurements obtained by LDF are intrinsically of a relative nature. Although the results of such measurements are proportional to perfusion, the factor of proportionality is different for different tissues.

3

Design and Technological Realization of a Suitable Ultrasonic Sensor

THE DEVELOPMENT AND REALIZATION of an ultrasonic sensor is a sophisticated task. Particularities like material selection, bonding of the oscillating elements, sound propagation characteristics, and electronic control have to be considered. Substantiated knowledge of ultrasonic sensor fundamentals, precise understanding of the application area, and the detailed conception of the specifications were essential to reach a sustainable formulation. A suitable design for the sensor probe meeting the demands of the described application was developed. The production of the crystal and the adoption of the sensor design to the limitations of the production technology was done in collaboration with the Fraunhofer Institute for Biomedical Engineering (FhG IBMT, St. Ingbert, Germany) due to their expertise in manufacturing of ultrasound transducers. A joint patent application for the new sensor probe has been filed [1]. The sensor electronics was developed, realized, and tested with the support of the Department of Biomedical Engineering (University of Stuttgart) and the Institute of Robotics and Mechatronics (German Aerospace Center).

After the general introduction to ultrasound technology in Sec. 2.5 a short overview of the specifically proposed ultrasound probe is given in Sec. 3.1, then the expected characteristics of the intended application areas of this probe are examined in Sec. 3.2. In Sec. 3.3 transducer measurement simulations are described, which were performed mainly to facilitate the interpretation of the real measurement results, to fine-tune the development of the transducer, and to verify the prototype. The design of the transducer probe and its electronics are outlined in Sec. 3.4 (probe) and Sec. 3.5 (electronics) respectively.

To test the transducer and adjust the sensor electronics, signal processing, and analysis, a test bench was built. Validation results and a test bed description are given in Cha. 4, Sec. 4.2 within the summary of the overall results.

[1] Publication of unexamined application (patent pending) No. DE 10 2008 005 041 A1, disclosure July 30th, 2009 [15].

(a) (b) (c)

Fig. 3.1: Photograph of the first multidirectional ultrasound probe. The 20MHz transducers are encapsulated in ultrasound casting compound Epo-Tek 353ND by Epoxy Technology, Inc. (outer diameter: 10 mm).

3.1 The Ultrasound Probe

As introduced in Sec. 1.2 one of the main tasks was the development of an innovative, multidirectional sensor aiming at the reliable detection of perfused vessels under covering tissue. Conventional Doppler probes are limited in detecting vessels since they are not sensitive to blood flow perpendicular to the direction of the ultrasound wave (cf. Sec. 2.5.2) which, however, is the predominant course in the planned application. In the case of separate transmitting and receiving elements, the detection rate for vessels with these probes can be increased by rotating the instrument's distal end around its longitudinal axis. Yet, this can be difficult or even impossible in MI(R)S, especially if the instrument is bent intracorporeally to achieve a flat contact of the transducer. Therefore, only a multidirectional sensor is suitable to solve the problem.

The development of the novel ultrasound probe (cf. Fig. 3.1) is based on a circular arrangement of more than two transducer elements. In contrast to conventional probes, 16 transducer elements were realized (cf. Fig. 3.11 and Sec. 3.4). Additionally, the elements are tilted at an angle of about 15° to the probe's longitudinal axis to achieve an appropriate directivity pattern (cf. Sec. 3.4).

In Sec. 2.5.2 the difference between continuous wave (cw) mode and pulsed wave (pw) mode was shortly introduced. Generally, the control electronics for cw mode is considered to be simpler, since the challenging fast switching between transmitter and receiver mode as needed for pw application is unnecessary. Additionally, the circuitry for pw burst generation is also difficult since a high rate of charge for an energy-rich burst is necessary. For these reasons, initially cw mode control was preferred. However, first tests showed that the arrangement of the transducer elements on one single solid carrier (cf. Fig. 3.11) leads to considerable crosstalk from transmitter to receiver elements at simultaneous activation, superimposing and, therefore, deteriorating the measurement data. Filtering was largely unsatisfying despite a slight frequency shift of the measurement signals since the crosstalk was much more intensive than the measurement signals. Therefore, the pw realization was chosen which had the further advantage of a signal delay de-

pendent depth estimation.

For each transducer element the specifications for the mechanics and control electronics are determined for use as either transmitter or receiver (cf. Sec. 3.5). Thereby, geometrically arbitrary Doppler transmitter/receiver pairs can be formed to reliably detect vessels in any planar orientation. The determination of both the transmitter and receiver element can be changed for every pulse.

Within the hardware development process parameters were kept variable, e. g. burst intensity, burst length, and actuation pattern of the transducer elements (cf. Sec. 3.5) to allow the largest possible variability for measuring and processing. Thus, parameters which were neglected during the dimensioning and development process can still be taken into consideration at a later stage. On the other side, variability of some of the parameters might turn out to be unnecessary and the electronics can be simplified in a later version of the system but at this time flexibility is kept as high as possible to allow later expansions of the system (cf. Sec. 5.1).

3.2 Expected Characteristics of the Application Area

In principle, the presented sensor is intended to be applicable in any operating field to reliably detect sub-surficial arteries in an arbitrary orientation. Nonetheless, particularly the detection of coronary arteries in closed chest revascularization surgery is intended to be a major application. This is due to the fact that a traumatizing thoracotomy as well as the harmful consequences of the usage of a heart lung machine, in case of off-pump surgery, can be avoided. A closer look at this application area, therefore, is the base for the dimensioning of the ultrasonic sensor and for the determination of development specifications. This includes anatomical and physiological conditions as well as the clarification of technically relevant parameters. Sec. 3.2.1 gives a brief description of the anatomy, Sec. 3.2.2 deals with the physiology in the target area. Both sections are strongly limited to the circumstances relevant for the intended application so as not to go beyond the scope of this thesis.

3.2.1 Anatomy of the Heart Surface

The heart is situated inside the thorax behind the sternum. It is completely enclosed by the pericardium, a sack-like connective tissue consisting of two layers, the inner epicardium and the outer myocardium, which are divided by a capillary gap containing 10-20 ml of serous liquid to allow minor friction caused by the beating of the heart. The transition of the two layers is located in the area of the large vessels.

Beneath the epicardium the coronary arteries are situated in or under a fatty tissue layer (*Tela subepicardiaca*). The epicardium is firmly attached to the heart muscle, the myocardium. The relatively thick myocardium forms the biggest part of the heart wall and consists of specialized muscle tissue which is only found in the heart. The interior of the heart chambers is covered with the endocardium which also forms the heart valves.

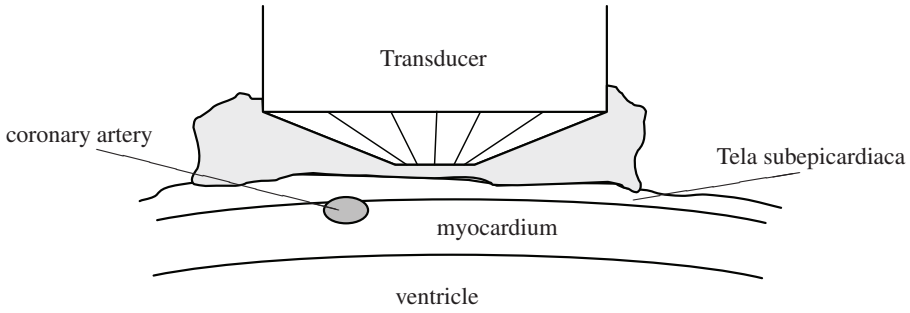

Fig. 3.2: Anatomy of the heart wall, according to [193, p. 9 and p. 11].

In closed chest heart surgery an intercostal access to the thorax is chosen and the pericardium is cut open to get direct access to the heart. As mentioned above, coronary arteries can be situated under tissue, severely impeding visual localization (cf. Fig. 3.2), in many cases they even show an intramyocardial course [11, p. 33], [14]. The ultrasound sensor presented in this dissertation is intended to detect coronary arteries without any direct palpation or preparation of covering tissue (cf. Fig. 3.2).

3.2.2 Coronary Arterial Flow Velocity

For dimensioning the ultrasonic system an estimation of the coronary artery flow velocity is necessary. In the following, anatomical and physiological parameters known from literature as well as calculated data are used to explain the observed circumstances.

According to literature, measurements of myocardial perfusion under resting conditions show approximately $0.8-0.9\ \frac{ml}{min \cdot g}$ related to the individual myocardial mass [194, p. 468 et seqq.], [195, p. 614]. Under stress this value can increase by a factor of 4. To estimate the coronary flow velocity with this information the cross section surface must be known.

In a group of 1,325 patients, 963 men and 362 women, O'Connor et al. characterize three different types of left coronary artery diameters: small (1.0 mm), medium ($1.5 - 2.0$ mm), and large ($2.5 - 3.5$ mm) whereas the overall, mean diameter was 2.04 mm for men and 1.81 mm for women [196].

Considering that the arteries narrow in progression, a diameter of 1.5 mm was chosen for an estimate. Thereby, a cross sectional area of

$$A = \pi \cdot r^2 = \pi \cdot (0.75\ mm)^2 = 1.767\ mm^2 \tag{3.1}$$

is calculated. Presuming an average heart mass of 350 g [197, p. 283], [198, p. 540] the volume flow calculates to

$$\dot{V} = m \cdot 0.85 \frac{ml}{min \cdot g} = 350\ g \cdot 0.85 \frac{ml}{min \cdot g} = 297.5 \frac{ml}{min} \quad . \tag{3.2}$$

Since the overall myocardial flow is distributed to three main coronary arteries and the measurement occurs in a certain distance to the coronary ostium, a volume flow of approximately $\dot{V} = 100\frac{ml}{min}$ is expected.

As seen in Fig. 3.3 the volume flow in the left coronary artery can reach values of about 150 $\frac{ml}{min}$ and in the coronary sinus even 200 $\frac{ml}{min}$. However, closely behind its orifice the left coronary artery divides into two big branches (Ramus interventricularis anterior and Ramus circumflexus) with a corresponding reduction of volume flow. The coronary sinus is a venous vessel unlikely to develop stenosis, therefore, a surgical invention in this area is rather unlikely. Thus, the it has not been chosen for the estimation of expected volume flow.

Hence, the estimation of

$$\dot{V}_{exp} = 100\frac{ml}{min} = A \cdot v \tag{3.3}$$

seems realistic. This results in an expected flow velocity of

$$v_{exp} = \frac{\dot{V}}{A} = \frac{100 \cdot 10^{-6}\frac{m^3}{s}}{60 \cdot 1.767 \cdot 10^{-6}m^2} = 0.94\frac{m}{s} = 94\frac{cm}{s} \quad . \tag{3.4}$$

Schiemann et al. performed magnetic-resonance-based flow velocity measurements of both the left and right coronary artery in 83 healthy patients. A catheter angiography performed beforehand confirmed the absence of coronary artery disease. 71 left coronary arteries could technically be detected and showed maximum systolic flow velocities of $4 - 39$ $\frac{cm}{s}$ (median: 19 $\frac{cm}{s}$) and maximum diastolic flow velocities of $7 - 44$ $\frac{cm}{s}$ (median: 24 $\frac{cm}{s}$). In the 66 right coronary arteries technically detectable maximum systolic flow velocities of $5 - 23$ $\frac{cm}{s}$ (median: 14 $\frac{cm}{s}$) and maximum diastolic flow velocities of $6 - 36$ $\frac{cm}{s}$ (median: 16 $\frac{cm}{s}$) were found [199].

Ofili et al. performed flow velocity measurements with the Doppler angioplasty flow wire method in the proximal and distal segments of 20 angiographically normal and 29 coronary arteries with significant stenoses. Their measurements showed maximum peak flow velocities in the proximal segment of normal left coronary arteries with patients at rest of 49 ± 20 $\frac{cm}{s}$ and 35 ± 16 $\frac{cm}{s}$ in the distal segment. Median peak flow velocities of patients at rest with stenosed arteries showed 29 ± 17 $\frac{cm}{s}$ [200].

With the calculation above and the measurement results taken from literature [194–196, 199–201] a maximum coronary artery flow velocity of about 100 $\frac{cm}{s}$ is estimated and used for dimensioning the ultrasound hardware (cf. Sec. 3.4).

3.3 Simulation of Transducer Measurement Results

As described in Sec. 3.1 (also cf. Sec. 3.4) 16 transducer elements acquire ultrasound Doppler data. To facilitate the interpretation of the measurement data acquired by the transducer probe and to rate the expected measurement data, a

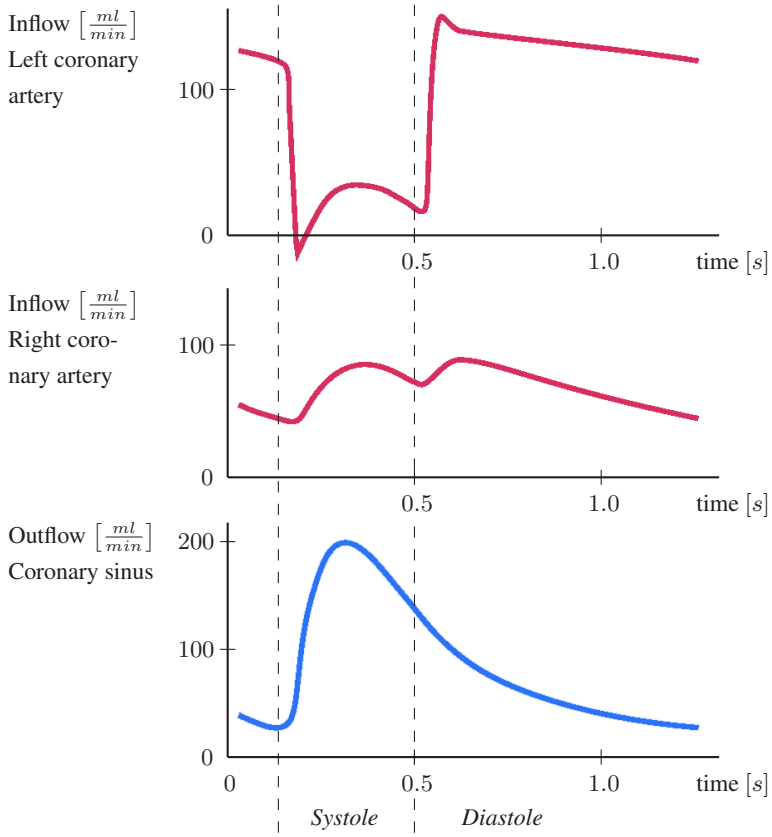

Fig. 3.3: Qualitative representation of pressure and volume flow for the coronary blood flow during systole and diastole. It can be seen that circulation to the myocardium takes place mainly during diastole. Diagram according to [194, p. 469], [195, p. 615].

MATLAB simulation was performed beforehand. For this purpose, a definable situs under the transducer probe can be created virtually, and the generated echoes effected by the defined situs and detectable by the transducer probe are displayed for each transducer element. The transducer probe, covering tissue layers, and vessels are taken into account in the simulation and are represented by different acoustic impedances, attenuation effects, and the reflection of ultrasound at the tissue interfaces.

Fig. 3.4 shows the graphical user interface (GUI) of the simulation tool. Here, parameters determining the scenario can be set. All other parameters like sound propagation velocities of all media, attenuation parameters etc. can be varied in the head of the simulation code. The GUI shows five main input fields: tissue and surface settings, transducer settings, blood vessel interpolation points, parameters of primary blood vessel, and parameters of secondary blood vessel. At the bottom of the GUI further entries can be made affecting the entire simulation.

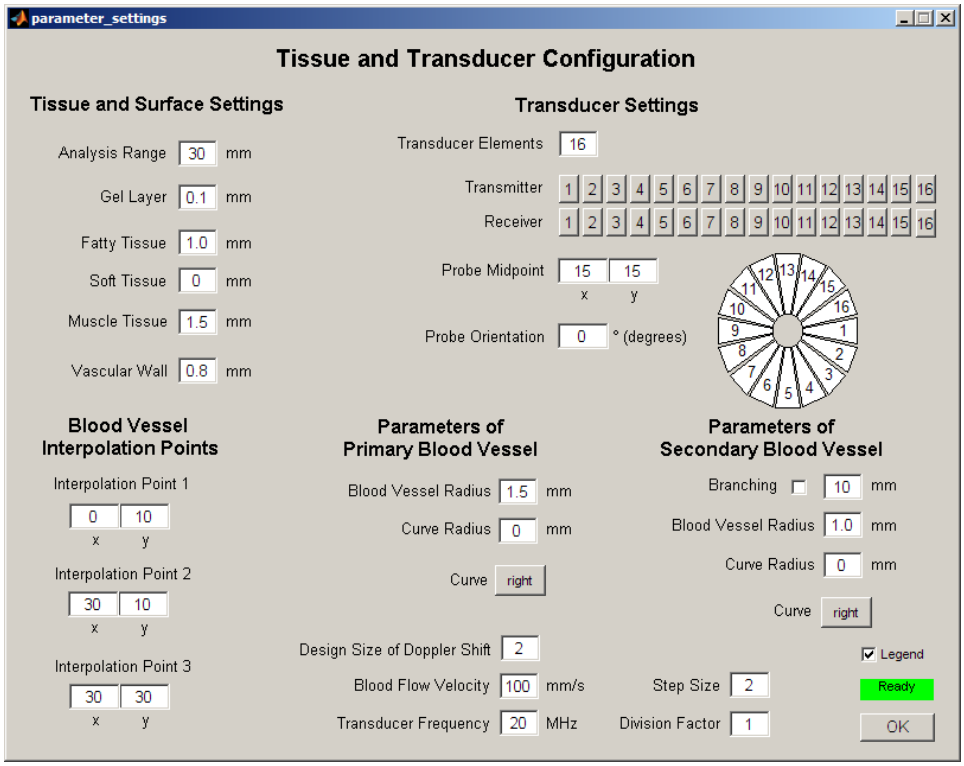

Fig. 3.4: Graphical user interface (GUI) of the transducer simulation. Input of the most important parameters to determine the simulation is requested, further parameters can be changed in the head of the simulation code.

Tissue and Surface Settings First, the user is requested to enter the size of the area considered for simulation, specified as the edge length of the assumed square. The following variables in this input field define the thicknesses of an ultrasound gel layer, a fatty tissue layer, a soft tissue layer, a muscle tissue layer, and the vascular wall. Each of the variables can be zero as well.

Transducer Settings The second input field defines the transducer probe. Initially the number of transducer elements is requested, then the transmitting and receiving elements have to be defined. Planar position and orientation of the transducer within the size of the area under consideration is requested in the following.

Blood Vessel Interpolation Points With interpolation point 1 and 2, each with x and y coordinate, start and end point of the simulated vessel are requested. In case of an optional branching of vessels interpolation point 3 is necessary as the end point of the branch. This setting has no effect if ”branching” (cf. below) is not selected. All interpolation points (x and y values) should be within the defined size of the simulation area.

Parameters of Primary Blood Vessel After having chosen start and end point in the previous input field the vessel radius has to be set here. The simulated arteries can either be compiled in a straight (cf. Fig. 3.5a) or an optionally curved manner (cf. Fig. 3.5b) with adjustable curve radii and vessel diameters. Curved vessels can be generated by setting the curve radius as well as the direction of the curve. For both optional input values circular geometries are assumed. Entering zero for the curve radius leads to a straight vessel. The curve direction button toggles left and right and has no effect if the curve radius is zero.

Parameters of Secondary Blood Vessel The simulation of one artery branching off is also possible (cf. Fig. 3.5). To activate the secondary vessel "branching" has to be selected generating a second, y-shaped vessel. The y-value of the point of branching off is requested next to the "branching" tick box. Again the radius of the vessel, its curve radius, and the direction of the curve are requested assuming circular geometries. For a straight secondary vessel the curve radius is zero. The curve direction button toggles left and right having no effect if the curve radius is zero.

Further Settings At the bottom of the GUI the scale factor (design size) for the drawing of the simulated Doppler frequency shift can be chosen (cf. Fig. 3.6b and 3.6c etc.). In the same input field blood flow velocity and ultrasound frequency can be set. "Step size" and "division factor" affect the precision of the result and, thus, the operating speed. Pressing "OK" finally activates the calculation and turns the green flag into red ("working").

The results of the calculation are displayed in MATLAB diagrams (cf. Fig. 3.6 – 3.10). First, the chosen vessel configuration and relative transducer probe position are displayed in 3D. All MATLAB functionalities in viewing (e. g. 3D rotation) are supported simplifying the understanding of the figures. The transducer elements' representation (according to the settings made in "transducer settings") can be green, blue, cyan, or white, with green meaning "transmitter", blue meaning "receiver", cyan meaning "transmitter and receiver", and white meaning "not active". To attribute the vessel direction to the simulation results it proved useful to consider both attenuation and Doppler frequency shift. Therefore, these two parameters are displayed in diagrams after processing. To verify the simulation software simple simulation examples were calculated delivering plausible results (cf. Fig. 3.6 – 3.10): a simulated 16-element transducer probe was moved vertically over an angled vessel (figures (a) in Fig. 3.6 – 3.10). Figures (b) in Fig. 3.6 – 3.10 show the color- and length-coded attenuation useful for the indication of the side on which the vessel runs relatively to the transducer probe. The attenuation of each transducer element is displayed circularly corresponding to the transducer probe, red indicating maximum attenuation and low echo detection respectively. Blue indicates minimum attenuation and high echoing, and green indicates a medium

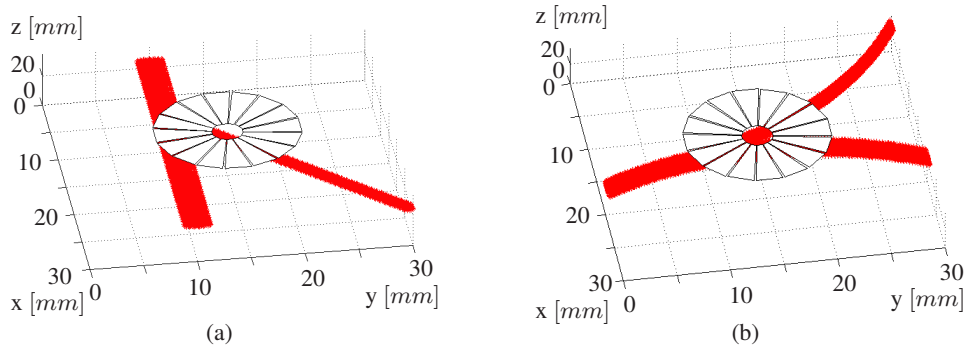

Fig. 3.5: Examples of simulated vessel branching, vessels straight (Fig. 3.5a) and curved (Fig. 3.5b). Transducer probe in central position. MATLAB diagram functionalities (e. g. 3D rotation) are supported.

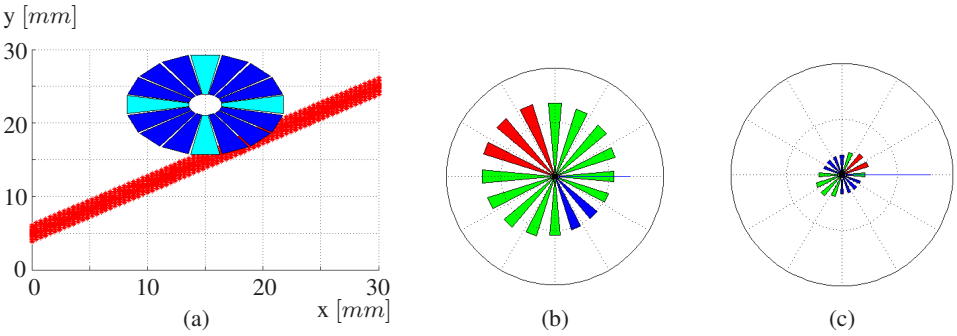

Fig. 3.6: Simulation results of a simple example (vertical transducer movement, cf. Fig. 3.6 – 3.10) for plausibility check. Transducer position $x = 15$ mm and $y = 22.5$ mm. Fig. 3.6a: simulated geometry in 3D; Fig. 3.6b: color- and length-coded attenuation; Fig. 3.6c: color- and length-coded Doppler frequency shift.

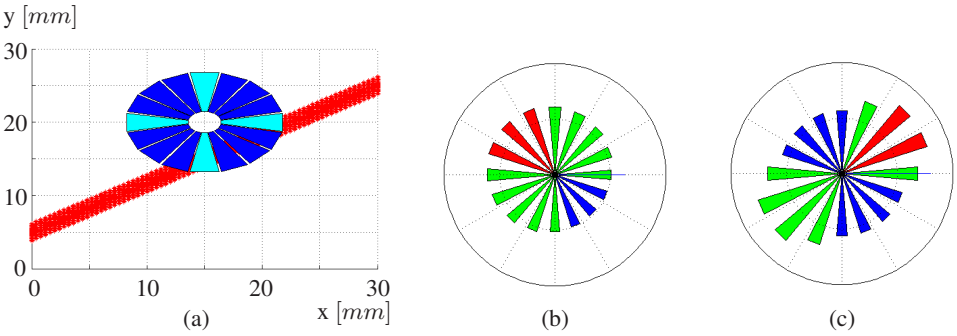

Fig. 3.7: Simulation results of a simple example (vertical transducer movement, cf. Fig. 3.6 – 3.10) for plausibility check. Transducer position $x = 15$ mm and $y = 20$ mm. Fig. 3.7a: simulated geometry in 3D; Fig. 3.7b: color- and length-coded attenuation; Fig. 3.7c: color- and length-coded Doppler frequency shift.

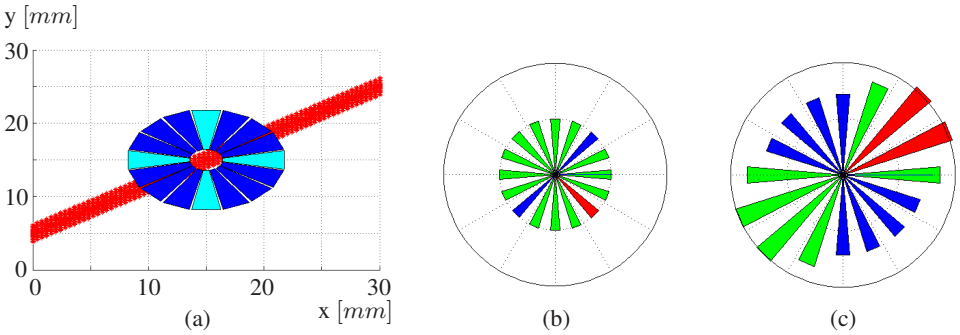

Fig. 3.8: Simulation results of a simple example (vertical transducer movement, cf. Fig. 3.6 – 3.10) for plausibility check. Transducer position $x = 15$ mm and $y = 15$ mm. Fig. 3.8a: simulated geometry in 3D; Fig. 3.8b: color- and length-coded attenuation; Fig. 3.8c: color- and length-coded Doppler frequency shift.

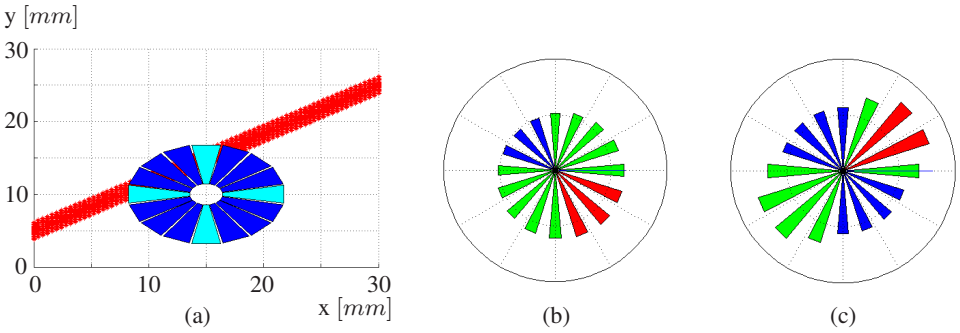

Fig. 3.9: Simulation results of a simple example (vertical transducer movement, cf. Fig. 3.6 – 3.10) for plausibility check. Transducer position $x = 15$ mm and $y = 10$ mm. Fig. 3.9a: simulated geometry in 3D; Fig. 3.9b: color- and length-coded attenuation; Fig. 3.9c: color- and length-coded Doppler frequency shift.

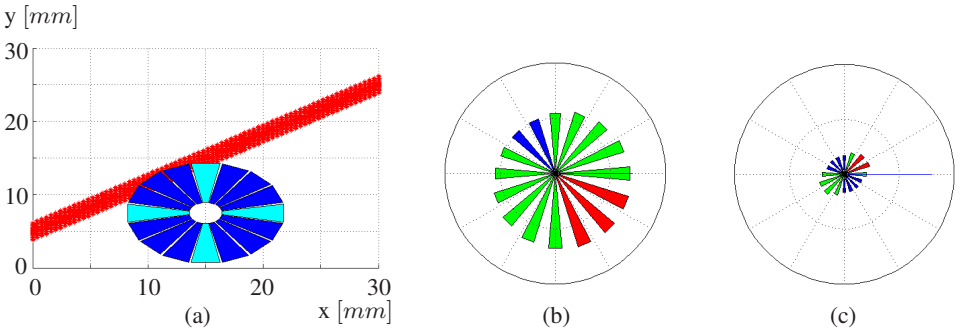

Fig. 3.10: Simulation results of a simple example (vertical transducer movement, cf. Fig. 3.6 – 3.10) for plausibility check. Transducer position $x = 15$ mm and $y = 7.5$ mm. Fig. 3.10a: simulated geometry in 3D; Fig. 3.10b: color- and length-coded attenuation; Fig. 3.10c: color- and length-coded Doppler frequency shift.

attenuation. A vessel can hence be expected on the ”blue side” of the transducer. The color values representing the attenuation are in relation to the actual simulation, while the absolute values can be read according to the length of the indicators. Figures (c) in Fig. 3.6 – 3.10 circularly display the color- and length-coded Doppler frequency shift for each transducer element, useful for indication of the direction in which the vessel runs relatively to the transducer probe. Blue indicates minimum, red indicates maximum, and green indicates medium Doppler frequency shifts. The direction of a vessel can hence be expected in the ”red direction” of the transducer. The color values representing the Doppler frequency shift are in relation to the actual simulation, while the absolute values can be concluded with the help of the indicator length.

Comparing the gradual movement of the transducer probe over the angled artery in Fig. 3.6 – 3.10 with the simulated values for attenuation and Doppler frequency shift as well as their gradual changing yields plausible results. Moreover, this form of representation is intended to enhance intuitive accessibility.

Multiple vessels beneath the transducer probe – especially crossing one another on top of each other – might lead to a result difficult to interpret. However, a pulsation would always be detected maintaining the initially intended purpose of the system. Moreover, manual perception of a situs like that would not allow conclusions about the route of the vessels either.

3.4 Realization of Transducer Mechanics

A number of different transducer element arrangements within the probe were discussed, they are summarized in Fig. 3.11 – 3.13 . At first, a central circular transmitter was considered surrounded by three or more segments of a ring as receivers indicating direction (cf. Fig. 3.11). However, the beam characteristics of a central circular transmitter is not adequate to evoke sufficient echoes for the surrounding elements and, thus, for reliable detection. In addition, the fabrication of ring segments is comparably difficult since with conventional saw cuts only linear borders can be produced. The idea of replacing the central circular transmitter by enclosing the receiving ring segments with an annular transmitter also proved unsuitable for the following reasons. As said before, ring-like geometries cannot be manufactured with conventional saw cuts increasing production cost. Moreover, it is difficult if not impossible to handle a ring with a thickness of only a few tenths of a millimeter (according to Eqn. 3.5, see below) and an estimated diameter of about 8 mm under prototypic conditions. Furthermore, the beam characteristics of a ring-like transmitter is inadequate to evoke sufficient echoes for reliable detection according to simulations performed at the FhG IBMT. Considering a design with neither an outer ring nor a central circular transmitter and using the remaining ring segments as transmitters and receivers (e. g. in pw mode) leads to an approach similar to the one finally chosen (see below in this Sec.).

Fig. 3.12 shows a different approach which was also discussed. Here, three

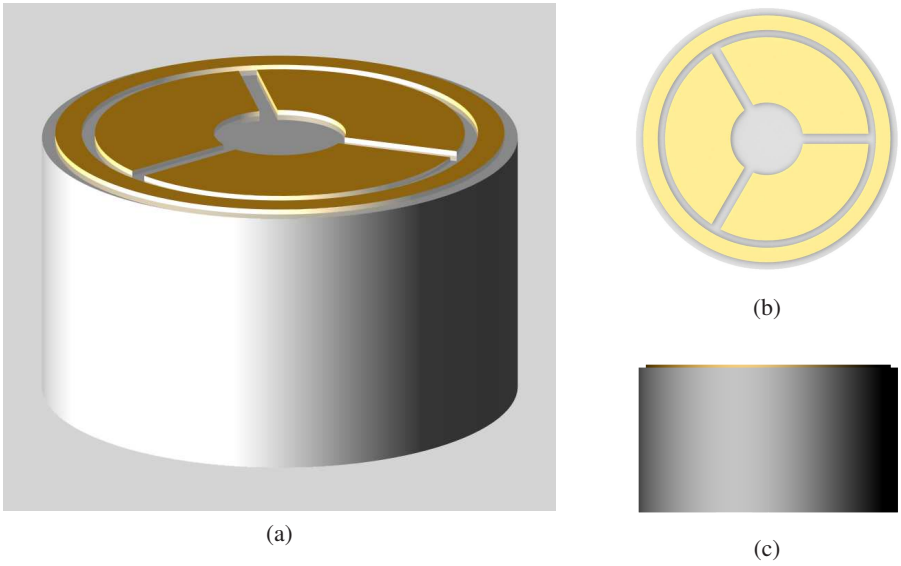

(a) (b) (c)

Fig. 3.11: Design and basic arrangement of the transducer elements within the ultrasound probe (rendered CAD depiction).

or more (six in Fig. 3.12) circular transducers were arranged surrounding a central circular element. For good area coverage under the transducer probe with reliable detection and direction information several surrounding elements were necessary. However, the more elements are used, the smaller their diameter has to be due to geometrical restrictions. Moreover, the smaller the elements' diameter and, thereby, their oscillating cross-sectional area, the smaller the released (and collected) energy of each element deteriorating the signal-to-noise ratio. As above, a central circular transmitter is inappropriate because of its beam characteristics and manufacturing of round geometries is difficult as well as expensive since conventional manufacturing methods cannot be applied. Considering a design without a central element and only circularly arranged transducer elements used as transmitters and receivers leads to an approach similar to the finally chosen one. Furthermore, in the proposed solution the energy transmission is higher since in that variant a bigger area of the transducer probe is covered with transducer elements and, therefore, a better area utilization on the transducer probe is provided.

This finally proposed version of the transducer probe as patented [15] and introduced in Sec. 3.1 is based on a circular arrangement of 16 transducer elements. Geometrically, each of the elements is an equiangular trapezoid with a height of about 2.7 mm, one ground-line length of about 1.25 mm, and one 0.24 mm (cf. Fig. 3.13 and 3.1). Therefore, the elements can be produced with conventional saw cuts and their size still allows manual handling and subsequent prototypical treatment. Handling in particular was one important point of interest during the development process. Additionally, a satisfying area coverage could be achieved

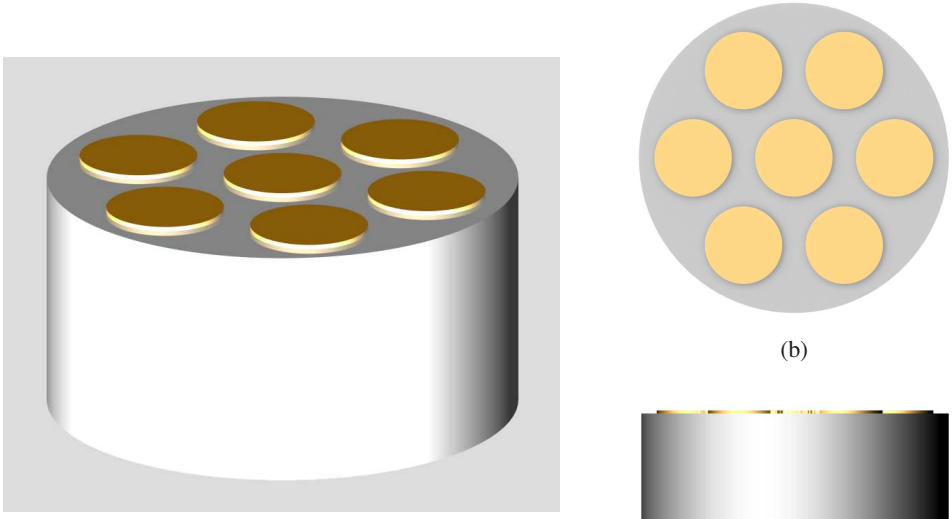

(a) (b) (c)

Fig. 3.12: Discussed alternative design and basic arrangement of the transducer elements within the ultrasound probe (rendered CAD depiction).

with this relatively simple and easily producible geometry. The outer diameter of 10 mm (including the front sealing, see below) is designed to fit into the existing DLR MIRS instruments (cf. Sec. 1.3 and [22, 23]).

The piezo-based transducer elements can all be used either as transmitters or receivers allowing the formation of geometrically arbitrary Doppler transmitter/receiver pairs to reliably detect vessels in any planar orientation. The direction selectiveness deriving from this circular arrangement of independent transducers is considered to be one major advantage of the sensor design.

Considering the required necessary number of elements for satisfying direction information and the necessary element size for sufficient energy release and area coverage on the probe, 16 elements seemed to be a feasible compromise. Focusing pairs of two transducer elements by tilting them to each other around their longitudinal axis to increase the level of received signals was also discussed. However, the tilting was expected to be inconstant due to manufacturing tolerances. Additionally, the manufacturing complexity would have been considerably higher, thereby increasing production cost. The additional expenses were not expected to be worth the design variation in relation to the expected increase of the received signals' level.

For intuitive detection comparable to the human finger tip (cf. Sec. 1.2), primarily vessels directly under the probe should be recognized since vessels next to a palpating finger tip would not be detected either. To achieve this quality, a predominantly axial ultrasound lobe characteristics under the probe is preferable. The elements are designed to mainly emit ultrasound energy by oscillating their

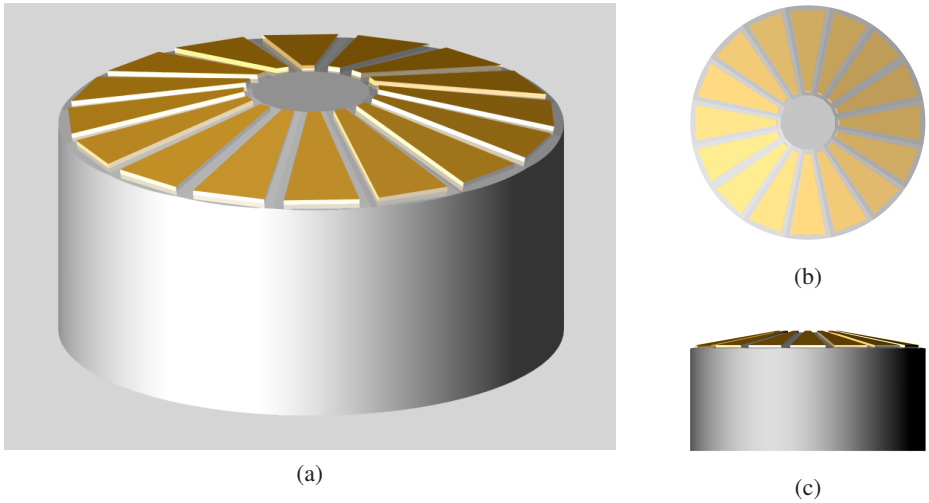

Fig. 3.13: Final design and basic arrangement of the transducer elements within the ultrasound probe (rendered CAD depiction).

thickness after applying an alternating voltage. However, due to their geometry more energy is emitted at the longer trapezoid ground-line than at the shorter one. To achieve a mainly axial sound lobe, the elements are tilted at an angle of about 15° to the probe's longitudinal axis (cf. Fig. 3.13) verified in prior simulations performed at the FhG IBMT.

The beam characteristics of the proposed geometrical arrangement was verified at the FhG IBMT with a very first, prototypical transducer probe in a hydro phonographic measurement. For this purpose, the transducer probe is contacted to the water surface in a sufficiently deep water basin so that the probe can beam ultrasound waves freely into the water. A hydrophone is moved in sufficiently small steps layer upon layer under the probe measuring the acoustic pressure at any position. Afterwards, all measurements are depicted in a computer-aided 3D reconstruction where the acoustic pressure at any point within the area of measurement is color-coded. The results in Fig. 3.14 indicate that at this stage of development not all transducer elements showed identical characteristics yet, most likely due to manufacturing tolerances. However, practically coaxial beam characteristics near the probe and a low expansion in the deep can be seen. This provides a discrete measurement of each transducer element with a corresponding vessel detection. Expectedly, narrowing the transducer elements might have widened their sound lobes (cf. Sec. 2.5.1, Fig. 2.6) yielding a slight overlapping of the lobes. Hence, neighboring elements might both have partly recorded the same vessel, possibly enhancing detection and location of the vessel since more elements contribute to the measurement. However, by narrowing the transducer elements the released and collected energy of each element considerably decreases, deteriorating measurement results. Therefore, considering the electronics' complexity, 16 elements

(a) (b) (c)

Fig. 3.14: Beam characteristics of a first transducer probe, determined in a hydro phonographic measurement. Acoustic pressures are color-coded. Rotated views (illustration: FhG IBMT).

yielding the element size described above and nonintersecting sound lobes again seem to be an adequate compromise for the intended application.

The characteristics of the sensor were designed to achieve a penetration depth of 3-4 mm (cf. Sec. 1.2) since deeper vessels would not be palpable manually either. Additionally, vessels under covering tissue deeper than 4 mm usually do not lie in the primary cutting region of a surgeon since conventionally multiple small and cautious cuts are performed rather than one deep incision. Furthermore, the small penetration depth is advantageous in detecting coronary arteries on the beating heart since measurement disturbances due to ventricular blood turbulences can be avoided. To achieve the desired penetration depth of about 3-4 mm the relatively high resonance frequency of 20 MHz was chosen (cf. Sec. 2.5.1) which allows higher pulse repetition frequencies (PRF) since the echo signal delay is shorter with small penetration depths. However, to achieve high resonance frequencies the thickness of the oscillators has to be comparably small according to [176, p. 100]

$$f = \frac{n}{2d} \cdot \sqrt{\frac{E}{\rho}} = \frac{n \cdot c_o}{2d} \tag{3.5}$$

where $f\ [Hz]$ is the natural frequency of the oscillator, $n\ [1]$ is the order of the oscillation $(1, 3, 5, \ldots)$, $E\ [Pa]$ is the oscillator material's module of elasticity, $\rho\left[\frac{kg}{m^3}\right]$ is the oscillator material's density, $c_o\left[\frac{m}{s}\right]$ is the sound propagation velocity in the oscillator material, and $d\ [m]$ is the thickness of the oscillator. As set out, thin piezo plates are difficult to handle and process especially under prototypic conditions, hence, manufacturing tolerances have to be taken into account.

To increase sound-emission in a forward direction the transducer elements are affixed to a carrier consisting of a composite material of hollow glass balls bound by an epoxy resin matrix. Thereby, density and longitudinal sound propagation

velocity in the carrier are very low (reflection coefficient $R \rightarrow 1$, cf. Eqn. 2.6, Sec. 2.5.1) improving forward sound-emission.

This structure is sealed with a synthetic resin (cf. Fig. 3.1) building an adequate impedance changeover to human soft tissue, insulating the transducer from the patient, protecting the assembly, and providing a constant contact geometry. As transducer casting compound in the first prototype an autoclavable, bio-compatible, two-component epoxy adhesive (Epo-Tek 353ND, Epoxy Technology, Inc.) was used [202][2]. The functionality of the transducer probe's sealing could be proved, however, a considerable signal attenuation was detected. This probably results from an acoustic impedance step between tissue and sealing. An acoustic adaption, either by adding a material layer joined to the transducer probe or by varying the entire sealing material, is considered to reduce the attenuation.

Vibration damping of the transducer elements is considered to be caused mainly by three components: first, the carrier material, second, the bonding of the elements on the carrier and thus the back filling of the elements, and third, the front sealing material contacting the elements' front side. In case of an insufficient mechanical vibration damping a resistor can be connected in parallel to the transducer elements after the burst pulse. This electronic damping dissipates the voltage induced by the passive post-pulse oscillation. As the assembly of the first transducer probes was prototypic, the vibration damping of the elements varies. According to measurements at the FhG IBMT a mean value of 1.5-2$\cdot 10^{-6}$ s of post-pulse oscillation time can be assumed. On the one hand high vibration damping of the elements is positive since a fast switch over to receiver mode is possible. Returning echoes are not superimposed by post-pulse oscillations in this case and, hence, structures near the transducer probe can be detected. On the other hand, high vibration damping considerably reduces the oscillation capability of the elements at low echo signals deteriorating sensor sensitivity. A post-pulse oscillation time of 1.5-2$\cdot 10^{-6}$ s denotes a penetration depth in human soft tissue of about 1.5 mm from which echoes cannot be detected due to superimposed post-pulse oscillations. However, this distance approximately corresponds to the length of the front sealing reducing the distance in which echoes evoked by vessels cannot be detected to virtually zero. The purely mechanical vibration damping is, therefore, considered to be sufficient. This is the reason for omitting an additional resistor for electronic vibration damping in the first prototypic electronics.

3.5 Realization of Transducer Electronics

The transducer electronics was developed in close cooperation with electronics team members of the German Aerospace Center, Institute of Robotics and Mechatronics, and the University of Stuttgart, Germany, Department of Biomedical En-

[2]Preliminary results with the first prototypic ultrasound probe could be published in [202], a partial prior publication of this dissertation, approved by the responsible faculty at the University of Stuttgart.

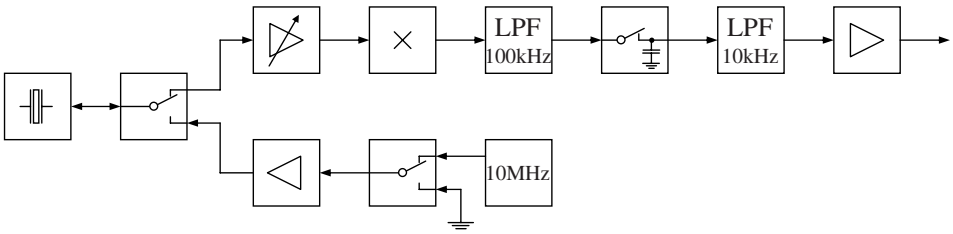

Fig. 3.15: Block diagram of the first prototypic electronics to operate one single transducer element. On the left the transducer element is symbolized connected with a change-over switch to the transmitter (lower) branch and to the receiver (upper) branch. According to [203,204].

gineering (IBMT UniS), since profound expertise in this special field is necessary for a promising concept, the dimensioning of the electronics and its design.

For preliminary test purposes and to prove the validity of the concept a control electronics for only one single transducer element was designed and realized. In previous evaluation tests of the transducer probe continuous wave (cw) operation did not prove effective since the frequency of transmitting elements was heavily overlaying measurement signals, probably due to reflections within the front sealing or the collective transducer element carrier. Hence, the circuitry was designed to operate in pulsed wave (pw) mode, using one element as transmitter and receiver in time multiplex.

Moreover, using pw mode provides further advantages. Considering the signal runtime, depth estimations as well as depth focusing can be performed yielding potentially favorable qualities: Vessels lying a little deeper usually evoke weaker echoes due to higher attenuation, although they are comparatively important. These signals can be identified and specifically be amplified. In contrast, signals of smaller vessels running near the transducer probe evoking misleadingly strong echoes if not compensated for distance can be adjusted. Additionally, signal quality during the detection of coronary arteries on the beating heart can be improved by specifically cutting off disturbances caused by deeper structures e. g. ventricular blood turbulences.

The necessary dynamic range of the receiver electronics is small compared to cw operation because it only has to amplify the echoed signals. By contrast, in cw mode a large part of the transmitter signal is directly coupled into the receiver and thus this high signal level must also be processed by the receiver electronics to extract the desired echo signals. Therefore, the dynamic range of the mixer would have to be significantly larger in cw mode, complicating the electronics.

Considering the above, pw seemed to be the more promising choice. However, the short signal runtime, aimed for a penetration depth of 3-4 mm, requires fast switching between transmitting and receiving. Additionally, due to the dimensions of the ultrasound elements, only little energy can be coupled into the tissue. Therefore, high transmitter pulse energy and low noise amplification of the small measurement signals has to be provided by the electronics.

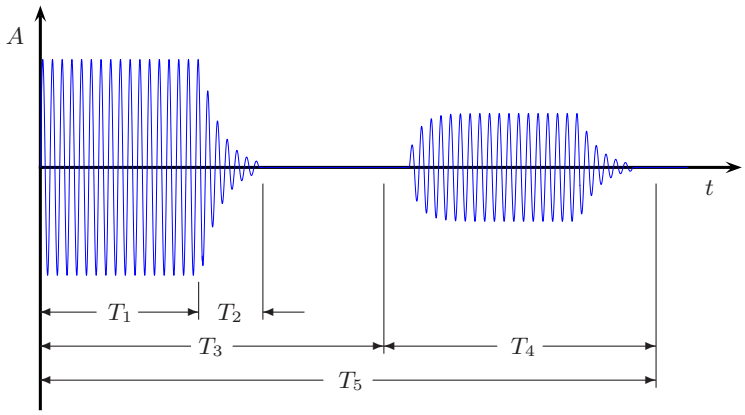

Fig. 3.16: Time diagram of pw mode: amplitude A of one single transducer element during a pw period with ultrasound burst, post-pulse oscillation, signal propagation delay, and echo. According to [204].

The initial electronics was designed for one of the first 10 MHz test transducers with the intention of proving the concept. Fig. 3.15 shows the block diagram of this first prototypic and established electronics: On the left the transducer element with a change-over switch from transmitter mode (lower branch) to receiver mode (upper branch) is represented. The 10 MHz on the transmitter branch are supplied by an external, conventional signal generator which is permanently transmitting. To raise the energy level provided by the signal generator an amplifier is interposed. After switching to receiver mode the acquired signals are amplified and lead through a multiplying mixer, yielding the sum and the difference of the measured frequency and the base frequency (10 MHz) while the difference between the two represents the Doppler frequency shift. The signal with the sum of the frequencies is, therefore, eliminated by a low-pass filter (LPF) after the mixer. Subsequently, the desired signal runtime is cut out by a sample and hold stage deciding on the depth range to be examined. After a final filtering and amplification the Doppler signal can be made audible since an expected maximum flow velocity of about $1\ \frac{m}{s}$ (according to Sec. 3.2.2) results in a Doppler frequency shift of $\Delta f \approx 6.72$ kHz (according to Eqn. 2.22) which is in the audible range.

For the dimensioning of the electronics the required time intervals were estimated (cf. Fig. 3.16). To determine the boundary conditions (e. g. intended penetration depth, covering tissue types) the system's principal purpose and the human perceptual ability for intuitive measurement results were taken into consideration.

T_1 in Fig. 3.16 determines the burst length and, thus, the energy applied to the tissue. The post-pulse oscillation time T_2, determined by the system's vibration damping, is intended to be $\approx 1.5 \cdot 10^{-6}$ s according to measurements of the FhG

IBMT. The beginning of the measurement is determined by T_3 and, hence, the penetration depth from which on vessels are expected. Assuming a mean sound propagation velocity in soft tissue of $1540\ \frac{m}{s}$ and the vessels to be in a depth of 3 mm results $T_3 \approx 1.95 \cdot 10^{-6}$ s, and in a depth of 5 mm, $T_3 \approx 3.25 \cdot 10^{-6}$ s. T_4 determines the depth range echo signals are acquired from. A windowing is possible to preselect the depth range. However, since the burst has a certain duration the burst echo also has a certain duration and, therefore, the depth of a point cannot be detected precisely. Furthermore, the windowed echo signals of one single burst are averaged yielding one value of the Doppler frequency shift signal. If $T_4 < T_1$ only parts of a burst echo will be sampled, deteriorating the averaging. It is, therefore, appropriate to choose at least $T_4 = T_1$. Moreover, since one sample is taken from every burst, the repetition rate determined by T_5 has to be at least twice the expected Doppler frequency in order not to violate the Nyquist-Shannon sampling theorem [205,206]. With an expected Doppler frequency shift of approximately 6.72 kHz the Nyquist frequency has to be about 13.45 kHz and, therefore, the repetition period has to be at least $T_5 \approx 0.07$ ms.

4

Construction, Technological Realization, and First Evaluation of the Entire ”False Haptic” System

TO DISPLAY THE EXPECTED TACTILE DATA to the remote surgeon a modality transformation is performed as introduced in Sec. 1.2: After the ultrasound based detection of a vessel the information is analyzed, processed, and substituted by kinesthetic impulses at the input device. Therefore, the term *false haptic representation* was introduced[1] following the term ”false color representation”, where inherently colorless images, e. g. in thermography, are visualized by systematic color coding of grey scales. To detect hidden vessels this modality substitution is intended to be as intuitive as possible under the operational conditions described in Sec. 1.3 and in Sec. 2.2. Nonetheless, a comparative evaluation of further feedback modalities through occupational psychological tests is planned (cf. Sec. 5.2).

The development of an ultrasonic sensor as introduced in Cha. 3, therefore, was only one step towards the proposed tactile feedback system. The completion of the system – as far as realized at this stage of development – is described in this chapter. However, presently only the suitability of the necessary components can be shown, the fusion of the components to a complete system has not yet been accomplished. Nevertheless, first results could be published in [202], a prior publication approved by the responsible university faculty.

4.1 Description of the Test-Bed

To evaluate the ultrasonic sensor system as introduced in Sec. 1.2 a test-bed containing material with the same ultrasonic properties as organic tissue was built and artificial arteries were embedded (cf. Fig. 4.1). On the one hand this simulator offers user-oriented analysis, i. e. trials with test persons to detect meandering, hidden arteries and to assess the process and its intuitiveness, on the other hand it allows technology-oriented analysis, i. e. verification and adaption of the sensor system under consistent, reproducible circumstances.

[1] Also cf. Sec. 1.2 and the corresponding definition in Sec. A.2 for additional explanations.

Fig. 4.1: Test-bed setup. Left top: power supply. Left middle: frequency synthesizer for the arterial pulsatile flow. Left bottom: frequency synthesizer for ultrasound transducer. Middle: acrylic glass basin filled with tissue simulating material (grey); at the front side the flexible tubes simulating the arteries running closely under the surface can be seen. In the black housing next to the basin the control electronics, the pump, and the flowmeter are situated. With the loudspeaker to the right the Doppler sounds can be made audible.

As shown in Fig. 4.2 the main part of the test-bed is a basin with walls consisting of acrylic glass for uncomplicated fabrication and handling. Its size with a base area of 200×300 mm was chosen to provide enough room for meandering, artificial arteries. The basin's height of 170 mm allows for two plains of arteries, each with two artery layers in close proximity and on top of each other (83, 90, and 143, 150 mm over the ground of the basin). The arrangement of two adjacent artery plains allows to test how well two crossing artery courses are perceivable independently from each other and how well the depth selectivity can be adjusted to detect and display them. The plains are arranged at half height of the basin or near its top surface to either save artificial tissue material (half height) or to prevent ultrasound reflections from the bottom of the basin (top surface) interfering with the measurement signals. The reflection coefficient of the bottom is estimated to be $R \approx 0.3$). With an attenuation coefficient of soft tissue according to [177, p. 30] of $\alpha \approx 0.5 \frac{dB}{MHz \cdot cm}$ the attenuation of reflected ultrasound transmitted from a plain 80 mm above the reflector is approximately 160 dB. Thus, interferences through reflected ultrasound waves from the bottom are only a problem for very high energy ultrasound probes. Due to the limited power of the first transducer prototype it was decided not to place an additional sound-absorbing matt on the bottom of the basin.

For the artificial vessels C-Flex tubes with different diameters were used. C-Flex is a special silicone-polymer with most acoustic characteristics being comparable to human blood vessels (cf. Tab. 4.1). Only its attenuation coefficient α is considerably higher than the one of a physiological human arterial wall. It was chosen because its handling in the test-bed is much less complicated than other

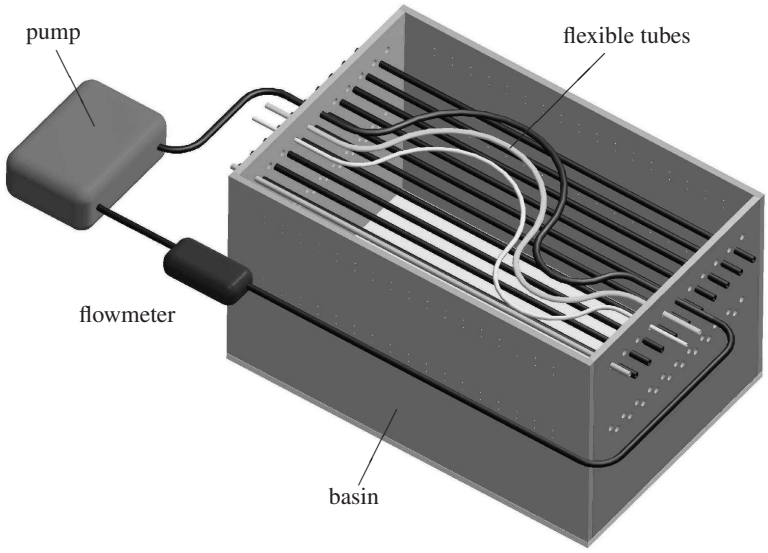

Fig. 4.2: Components of the ultrasound test-bed. The basin is filled up with a tissue simulating material (not shown) just covering the vessel simulating flexible tubes. The tubes can be arranged in straight lines or in a curved manner as shown in the figure and are perfused by a blood simulating fluid. The perfusion can either be stationary or pulsatile and is controlled by a pump and a flowmeter.

realizations described in literature such as wall-less phantoms [207] or rigid materials like acrylic glass, polyester resin, or quartz [208, 209]. Other flexible tubes, e. g. made of polyvinyl chloride (PVC) or polyethylene (PE), show a comparably high sound propagation velocity influencing the acoustic impedance and, thereby, yielding high reflection loss. With a wall thickness of only 0.8 mm the attenuation of C-Flex tubes was kept small enough to avoid noticeable influence on the measurements and is, therefore, an acceptable compromise between ease of handling and excessive attenuation. The inner diameters of the tubes were chosen to be comparable to physiological, human blood vessels (cf. Sec. 3.2), palpable under the circumstances of open surgery. Therefore, three different inner diameters were chosen for the tubes: $d_1 = 1.6$ mm, $d_2 = 2.4$ mm, and $d_3 = 3.2$ mm. To evaluate the intuitiveness of following the course of a vessel with the ultrasound system the tubes are arranged in a curved manner (cf. Fig. 4.2).

They are perfused by a fluid that simulates the ultrasound properties of human blood (cf. Tab. 4.2) and has the additional advantage of being easy to use under laboratory conditions (e. g. no coagulation, no decomposition, no risk of infection, no unpleasant odor etc.). The fluid consists of five components:

1. water as basic substance,

2. glycerol to adjust the sound propagation velocity, density, and viscosity,

Tab. 4.1: Acoustic characteristics of human arterial wall and C-Flex, according to [210–214].

Quality	Human tissue	C-Flex
Density $\rho \left[\frac{kg}{m^3}\right]$	≈ 1000	886
Sound propagation velocity $c \left[\frac{m}{s}\right]$	1581.04 ± 53.88	1553
Acoustic impedance $Z \left[10^6 \cdot \frac{kg}{m^2 \cdot s}\right]$	$1.56 - 1.69$	1.33
Attenuation coefficient $\alpha \left[\frac{dB}{MHz \cdot cm}\right]$	0.49 ± 1.33	≈ 5.6
Frequency dependency n	1.55 ± 0.18	1.8

Tab. 4.2: Physical properties of the blood mimicking fluid at room temperature ($20 - 25^\circ$ C) in comparison to human blood [215] according to the manufacturer [216].

Quality	Human blood	Simulating fluid
Density $\rho \left[\frac{kg}{m^3}\right]$	1053	1035 ± 5
Sound propagation velocity $c \left[\frac{m}{s}\right]$	1583	1550 ± 15
Attenuation coefficient $\alpha \left[\frac{dB}{MHz \cdot cm}\right]$	0.15	0.07 ± 0.05
Backscattering coefficient $\mu \left[\frac{1}{m \cdot sr}\right]$	$4 \cdot 10^{-31}$	blood equivalent
Viscosity $\eta \left[\frac{kg}{m \cdot s}\right]$	$3.5 - 4.5$	4 ± 1

3. dextran $[C_6H_{10}O_5]_n$ – a polysaccharide soluble in water which is usually used as plasma volume expander – also to adjust the viscosity,

4. nylon particles with a size of $\approx 5 \cdot 10^{-6}$ m to adjust backscattering, and

5. a detergent to reduce the surface tension and to ensure the moistening of the particles.

Backscattering is one of the most important parameters of blood-mimicking fluids [215] and is defined by the backscattering coefficient[2] $\mu \left[\frac{1}{m \cdot sr}\right]$. Backscattering of blood can be attributed to its corpuscular components, primarily the erythrocytes, which were emulated by nylon particles of about the same size. According to Evans et al. [178, p. 121], the particle's form is irrelevant in case of Rayleigh scattering which is predominant in blood. A concentration of 1.8% by volume causes backscattering comparable to the one of human blood [215].

The fluid is commercially available from Dansk Fantom Service, Inc. [216] as a concentrate that simply has to be diluted with distilled water in a ratio of $1 : 9$.

[2]The solid angle Ω [sr] (steradian, 1 sr $= 1\frac{m^2}{m^2} = 1$) is the area a cone cuts out of the unit ball's surface area divided by the radius of the unit ball to the second power. By definition, $\Omega = 1$ sr cuts out a surface area of 1 m^2 in a ball with a radius of 1 m; the aperture angle ω [°] then is $\omega \approx 65.54^\circ$.

Tab. 4.3: Physical properties of the tissue mimicking material [221] in comparison to human tissue [178, p. 28 et seqq.].

Quality	Human soft tissue (average)	Simulating material
Density $\rho \left[\frac{kg}{m^3}\right]$	$845 - 1235$	1054 ± 1
Sound propagation velocity $c \left[\frac{m}{s}\right]$	1540	1541 ± 3
Attenuation coefficient $\alpha \left[\frac{dB}{MHz \cdot cm}\right]$	$0.3 - 1.5$	0.5 ± 0.03
Acoustic impedance $Z \left[10^6 \cdot \frac{kg}{m^2 \cdot s}\right]$	$1.3 - 1.9$	1.62 ± 0.01

The flexible tubes with the blood simulating fluid[3] can either be perfused in a stationary or a pulsatile manner, controlled by a pump and a flowmeter (cf. Fig. 4.1 and 4.2). The pump is controlled by electronics in which the pulse rate can be adjusted by an external frequency synthesizer (cf. Fig. 4.1).

To create realistic conditions, the flexible tubes are embedded in tissue simulating material running $1 - 3$ mm beneath the surface of the tissue phantom, which was selected since its acoustic characteristics are comparable to physiological human soft tissue (cf. Tab. 4.3) and it is uncomplicated to handle (e. g. low molding tendency, no toxicity). Furthermore, the manufacturing process for the phantom had to be kept within reasonable limits. Despite their better durability in comparison to organic based phantoms, polymer based phantoms were not used because their production is generally more complicated. As the basic material for the phantom agar, gelatin, and tofu were considered and agar was chosen due to its better durability and higher melting point, compared to gelatin [218] and because it is more malleable than tofu based phantoms [219].

The phantom was realized with a material consisting of 82.97%[4] water (basic substance), 11.21% glycerol (to adjust the sound propagation velocity), 0.46% benzalkonium chloride (an antiseptic to prevent growth of microorganisms), 0.53% 400 grain silicon carbide (SiC) powder, 0.94% $3 \cdot 10^{-6}$ m aluminium oxide (Al_2O_3) powder, 0.88% $0.3 \cdot 10^{-6}$ m Al_2O_3 powder (to adjust attenuation and backscatter), and 3.00% agar as proposed in [214, 220]. All ingredients were mixed and heated to 96° C, kept at $96 \pm 3^\circ$ C for one hour, and then cooled down to 42° C under continuous stirring to prevent demixing. The development of air bubbles due to stirring had to be avoided. The material could then be poured into the basin up to the desired filling height. Since the empty tubes have a lower density than the initially liquid tissue simulating material, they were kept in place by nylon threads to prevent them from buoying upwards.

A first complete phantom was assembled (cf. Fig. 4.1) for the evaluation of

[3] Strictly speaking it is actually a suspension, however, in literature the term "fluid" can often be found, e. g. [215, 217].

[4] percent by weight

the components and demonstration purposes. The principal functionality could be shown, however, the attenuation of the C-Flex tubes was relatively high. Furthermore, it turned out that adding a fluid reservoir was helpful to simplify the removal of air from the tubes and to avoid pumping the liquid in a closed circle. The reservoir prevents air from being sucked in and removes air bubbles which were caught in the tubes during priming and, thereby, provides bubble free pumping of the blood mimicking fluid.

Even after several months the phantom did not show any mildew. It was observed, however, that the phantom dried out over time. This can be prevented in the future by wrapping the test-bed in a wet cloth or in plastic foil.

For the first functional tests, to adjust the electronics settings, and to exclude unnecessary causes of error, preliminary measurements with a simplified test-bed were performed at the IBMT UniS. Fig. 4.3 shows the test-bed consisting of a water filled plexiglass cylinder (190 mm in height to avoid reflections from the bottom) with one single arterial phantom (plexiglass tube, inner diameter: 3.5 mm). To simulate the pulse wave the artery phantom was perfused pulsatively with a blood substitute by a constant flow pump and intermittent manual throttling of the silicone supply tube (left and right in Fig. 4.3). The blood substitute consisted of water as the basic substance with added baking powder representing the corpuscular components in human blood to provide typical backscattering. With this setup – merely intended to commission the transducer probe and its test electronics, not to evaluate the detection process as in the test-bed described above (cf. Fig. 4.1) – a reliable preset of parameters could be found. The adjustable parameters as introduced in Sec. 3.5, were the transmitter frequency (by changing the frequency on the signal generator), the pre-amplification (by adjusting a potentiometer), in a limited range the low pass filter characteristics (by resoldering electronic devices), and the post-amplification (by adjusting a potentiometer). Objective of the adjustments was to achieve the best possible audibility of the Doppler signals on a loudspeaker connected to the circuit board. As expected, subsequent measurements on human radial arteries showed that the test-bed conditions were not adequately realistic. The plexiglass tube representing the arterial phantom as well as the tissue simulating water showed considerably lower attenuation than human tissue. Detecting the radial artery with the presetting found with this test-bed, therefore, was slightly more cumbersome than detecting the plexiglass tube. However, after adjusting the settings of the electronics to in vivo conditions, test persons' radial arteries could reliably be detected (cf. following Sec. 4.2).

4.2 First Test and Verification Results with the Ultrasound Sensor

To prove the functionality of the transducer probe and its electronics including the previously determined settings under realistic conditions, in vivo measurements on test persons' palpable distal radial arteries (forearm artery, about 3 cm above the

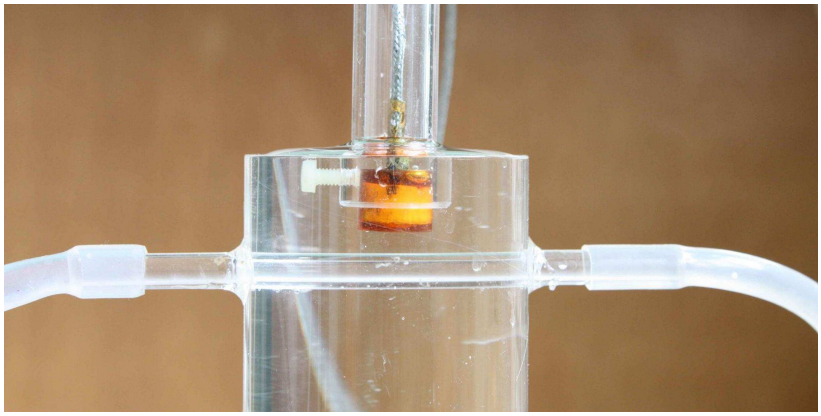

Fig. 4.3: Test-bed for first functional tests and adjustment of the electronics parameters. The amber-colored transducer probe (cf. Fig. 3.1, p. 44) is held above the perfused single artificial artery (horizontal plexiglass tube, inner diameter: 3.5 mm) by a support in a water filled plexiglass cylinder [204].

wrist) were performed. Since the test electronics only operates one single transducer element the probe had to be adjusted along the flow direction manually. Though clearly audible, the characteristic Doppler sound could not be recognized when the signal was displayed on an oscilloscope (model *WaveRunner 6050 A* by LeCroy, Inc., Chestnut Ridge, NY, USA). A more obvious representation was expected by displaying the spectrum of the Doppler signal which would show a clear frequency shift. Therefore, the measured signals were stored in periods of about 10 s in an oscilloscope with a USB port for the connection of mass storage devices. With these data the spectrum of the Doppler signals was calculated and displayed by applying the Fast Fourier Transformation (FFT) to consecutive time windows of 256 signal samples (cf. Fig. 4.4). Frequencies outside the range of 200 Hz to 5 kHz, which are irrelevant due to the physiological hemodynamics, are discarded. The spectrum looks very much like the representation of blood flow measured by ultrasound sonography and as described in the literature, e. g. [179, p. 20], [194, p. 505 et seqq.]. The incision after the first peak is caused by an early diastolic back flow of blood which is characteristic for large arteries and can be seen in a more moderate form even in peripheral arteries [195, p. 627].

The functionality and basic setting of the electronics for one transducer element in the ultrasound probe appear promising due to the positive results obtained and shown in Fig. 4.4 as a representative example. Even the most critical parameter, the switching time between transmitter and receiver mode, could be realized in a suitable range. The Doppler signal could be improved by using a more powerful output amplifier with a faster ramp response since the full capacity of the transducer elements has not yet been utilized. This is intended to be realized in the electronics presently being developed (cf. Sec. 5.1). Moreover, further improve-

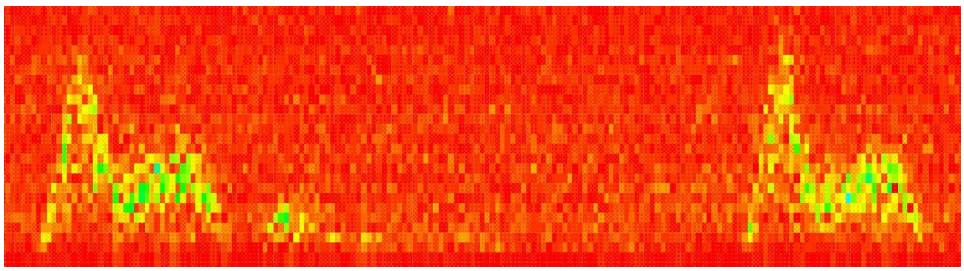

Fig. 4.4: Calculated spectral Doppler display of a test person's radial artery; abscissa: time, ordinate: Doppler frequency shift. According to [222].

ments are expected by a less provisional assembly of the amplifier providing a low-noise setup.

4.3 Data Acquisition, Signal Processing, and Signal Analysis

To facilitate the generation of feedback impulses corresponding to the ultrasound measurement signal, an automated, computer-assisted signal analysis has to be performed to identify pulses in this signal. Thereby, the latency period between measurement and display of the ultrasound signal to the user should be as short as possible to provide for acceptable intuitiveness (also cf. Sec. 5.1). To create, to adjust, and to pretest the signal analysis and to determine appropriate methods for the detection, measurement signals of a previous test setup were recorded, digitized, and stored on a conventional personal computer (PC). The data comprised typical ultrasound Doppler frequency shift signals Δf of test persons' radial arteries and were initially processed offline with MATLAB.

For the recording and digitalization of the Doppler signal Δf a standard PC sound card with a sampling rate of 44.1 kHz was used, connected to the speaker output of the transducer electronics (amplified mixer output). The digitized data were stored on the hard disk of a standard Windows-based PC in an uncompressed wave-file.

For data processing, first the bandwidth of the audio data was reduced with a standard bandpass filter implemented in MATLAB to the range of 1-6 kHz in which the pulse signals are expected. Second, the data were normalized to an amplitude value of 0.1 (cf. Fig. 4.5). This normalization made it possible to determine a limiting amplitude value of 0.075 which proved to be suitable. Amplitudes exceeding this limit underwent further analysis: All peaks in Fig. 4.5 have a width of about 10.000 samples and, therefore, it was checked whether additional sampling values exceeded the limiting amplitude within a range of 7.000 samples. If so, the position was marked to be a pulse. These results (cf. Fig.4.5) were taken as a basis for a feedback signal generation (cf. following Sec. 4.4).

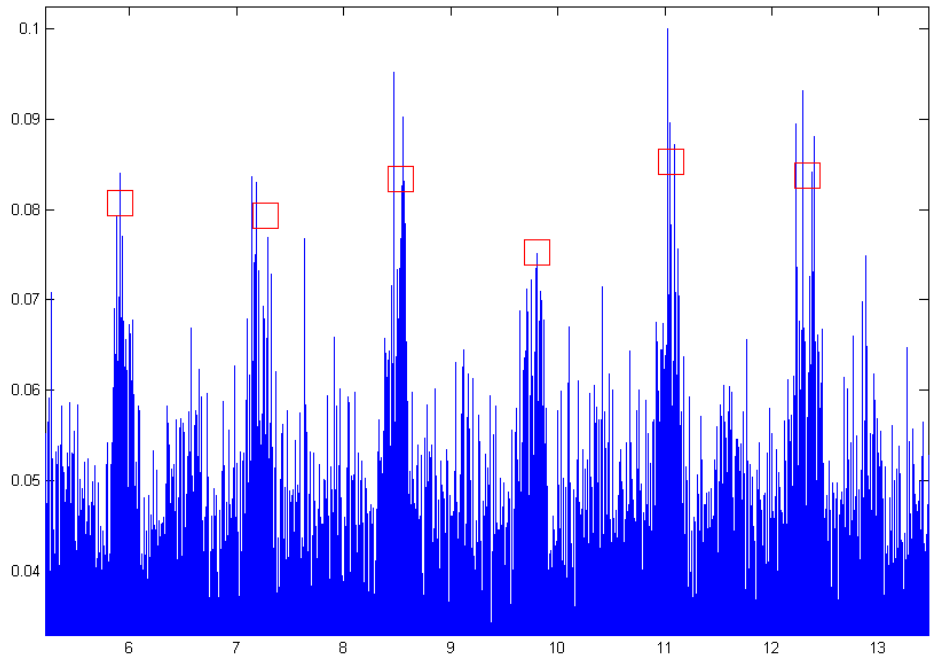

Fig. 4.5: Preliminary test of a MATLAB based peak detection with a previous transducer setup. Abscissa: time [s]; ordinate: normalized amplitudes. Although the sampling rate was 44.1 kHz not every sampling value is shown due to a pixel based depiction.

This peak detection, which is quite basic, was performed as a first signal analysis and yielded satisfying results on the recorded data sets with respect to feasibility and a proof of concept. However, it is expected that more advanced signal analysis algorithms can further improve the detection reliability.

Moreover, in this first attempt, the peaks found in the data stream were weighted equally and submitted to the haptic interface only as uniform impulses. In a later version, the impulses might be fed back more strongly or weakly depending on the ultrasound signal's shape.

Furthermore, the signal analysis is currently performed offline as described. In a next development step, the data processing is planned to be done online by means of the RT-Lab toolbox in MATLAB and a secondary PC, based on the real-time operating system QNX (cf. Sec. 5.1).

4.4 Generation of Kinesthetic Feedback Signals with the Haptic Interface ”Omega.7”

As mentioned in Sec. 1.2 the omega.7 haptic feedback device (cf. Sec. 1.3) is planned to be integrated into the described tactile feedback system. It is intended to substitute the tactilely expected perception by a kinesthetic feedback signal in

form of a soft twitch of the input device's open/close-input-master (index finger, cf. Sec. 1.3 and Fig. 1.2, right), which is intuitively recognizable as "pulsation". To verify the intuitiveness of the kinesthetic feedback impulses and to test how precisely the feedback impulses can be adjusted on the hardware, software activated, short deviated impulses on the active open/close-input-master were generated. For this, the omega.7 device can be connected to a standard PC via USB and is freely programmable, e. g. by means of MATLAB, since drivers for common operating systems are available (e. g. Windows, Unix/Linux, QNX). The adjustability of the open/close-input-master is tiered, however, the steps appear comparably small on the hardware and, therefore, the setting accuracy of the open/close-input-master proved to be satisfactory.

The open/close-input-master mainly consists of a small support bow for the index finger which is electromechanically driven by a cable transmission. Due to a back-strap for the index finger attached to this support bow (cf. Fig. 1.2, right), thrusts as well as tensile forces can be applied to the user's index finger. Since only small masses are moved, relatively high accelerations are possible. The response time of the open/close-input-master, hence, is favorably short and the mechanics is free of noticeable backlash, which allows shortly deviated movements. Therefore, it is concluded that with the software and the corresponding hardware of the open/close-input-master a relatively good adjustability for each user is provided to create movements interpretable as simulated pulsations.

As a result of the performed tests, although not representative and not scientifically reliable, it can be said that the feedback impulses are adjustable to such an extent that they are evocative of palpated pulsations and correlation with artery palpation is conceivable. However, to achieve science-based conclusions concerning intuitiveness and immersion of the feedback impulses, an occupational psychological evaluation is scheduled (cf. Sec. 5.2).

Further feedback modalities (visual and acoustical) are planned to be integrated into the system, to be compared with the pure kinesthetic feedback, and to be evaluated in occupational psychological tests (cf. Sec. 1.2 and 5.2).

5

Conclusion and Perspectives

WITHIN THIS DISSERTATION it could be shown that it is possible to create a system for the feedback of pulsations within tissue that is integrated in an existing MIRS instrument and using a commercially available haptic input device. This constitutes a new approach to establish tactility in MIRS. The proposed system is based on a new Doppler-ultrasound sensor with multiple, circularly arranged transducer elements to detect arbitrarily oriented, perfused vessels. The Doppler signals thereby acquired can be evaluated such that pulses can be detected and displayed on an omega.7 haptic input device (from ForceDimension, Inc., Switzerland) as soft impulses. The displayed feedback can be perceived by the user without further input devices and so the hands of the user do not have to be taken off the input device, increasing practicality. Moreover, further feedback modalities, e. g. acoustic (by displaying the characteristic Doppler sound) or visual (by displaying signals in the endoscopic image), can also be provided, either in addition or instead, which is expected to lead to a more intuitive perception. The proposed tactile feedback system can be used for the detection and improved localization of arteries, e. g. in closed-chest revascularization surgery or in other MIRS scenarios. The system, thus, is not intended to provide complete tactile feedback, but concentrates on an important, single, and precisely specified task in MIRS.

Unique position features of this dissertation are the disclosures contained in two patents, one on the transducer element arrangement within the ultrasound probe (pending, [15]), and the other one on the purpose of the system and the feedback modality respectively [223]. The novelty of the concept could be confirmed within the cooperation with the Fraunhofer Institute for Biomedical Engineering (FhG IBMT), an experienced research institution in the field of ultrasound. Furthermore, a reviewed publication of first results was accepted for oral presentation and the proceedings of the 11th International Congress of the International Union for Physical and Engineering Sciences in Medicine (IUPESM), World Congress on Medical Physics and Biomedical Engineering [202], as a prior publication approved by the responsible university faculty. Finally, a literature search (cf. Sec. 2.4) was performed which revealed no comparable approach for the intended purpose supporting the unique position features of this thesis.

The presumptions concerning a new transducer for teletactility substitution in

a single, precisely specified task in MIRS seem to be correct since the radial artery can be detected and is also palpable (cf. Sec. 4.2). Multidirectionality may be expected due to the measurements, but could not be proven yet since the present evaluation electronics only operates one single transducer element. The modality substitution and kinesthetic feedback of palpable, hidden, sub-surficial vessels by the soft impulse of a haptic input device's functional DoF (i. e. tactilely expected perception, ultrasound based detection, and kinesthetic feedback) seem feasible and feel satisfactory on the haptic interface. However, online data processing is not yet implemented. Development, construction and first evaluation results of the system components could be presented.

Following in this last chapter, the perspectives of the presented system and, hence, the future work are discussed. In Sec. 5.1 first the next necessary development steps for an integrated, fully operational system are shown. Sec. 5.1.1 – 5.1.3 then gives a medium-term perspective of how the system can be enhanced and how its functionality can be expanded. Finally, in Sec. 5.2 the contents of the pending occupational psychological tests to evaluate the system are described and the desired results are discussed.

5.1 Future Work

The next development steps to achieve the intended fully operational system (cf. Sec. 1.2) are listed below.

Presently a control electronics for only one single transducer element is available, designed, and created for preliminary test purposes. However, to achieve a multidirectional detection of vessels all transducer elements have to be operated. To determine the most suitable activation sequence of the elements, arbitrary activation should be provided by the electronic circuits for experimental purposes. Therefore, a field-programmable gate array (FPGA) controlled operation of all transducer elements is in the development stage. It is expected that it will be possible with this technique to control the transducer elements and to digitally preprocess (conditioning/mixing) the measurement data in a sufficiently fast manner. Additionally, the control electronics presently in development will provide an Ethernet communication interface to a standard PC. Thus, modifications of measurement data processing, signal analysis, and feedback signal generation can be carried out more flexibly to optimize the performance of the system. After having identified suitable and robust online processing and presentation of the measured data a comprehensive hardware realization can be contemplated as a further perspective.

To achieve quasi-online data processing the use of the MATLAB tool "RT-Lab" for real-time applications has been decided on. RT-Lab allows MATLAB like programming and finally generates code, executable on a microkernel-based, Unix-like real-time operating system named QNX running on a secondary, standard PC (cf. Fig. 5.1). The code generated in MATLAB by RT-Lab (development host)

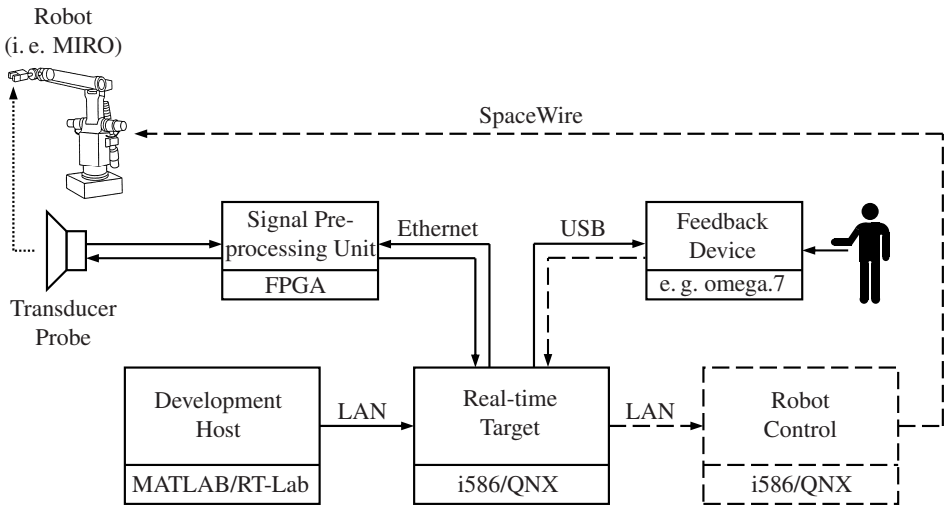

Fig. 5.1: Structure diagram of targeted hardware arrangement. As soon as the compilation is downloaded to the real-time target, the development host can be disconnected. The feedback device is interchangeable, e. g. by an audible feedback etc. Dashed lines indicate the robot guidance by the surgeon, in which SpaceWire is a standardized gigabit communication network protocol. The dotted line shows the position of the transducer probe carried by a medical robot (i. e. MIRO).

is downloaded to the secondary PC (real-time target) which is connected to the control electronics of the ultrasound probe (signal preprocessing unit) as well as to the omega.7 (or any other) output device. Hence, the preprocessed measurement data are transmitted via Ethernet to the QNX PC, processed there in quasi real-time, and the results are finally forwarded e. g. to the omega.7 haptic device since QNX drivers are available for this hardware.

The user input collected by the omega.7 device in form of position information is transmitted through to the robot control as set-point values (dashed lines in Fig. 5.1). As mentioned in Sec. 1.3 these data are used by the robot control to guide the robots. Thus, the instruments can be guided to the position desired by the user.

After the functional evaluation of the electronics and the processing unit the mechanical integration of the ultrasound probe into a DLR MIRS instrument is scheduled (cf. Sec. 1.3 and Fig. 1.4). The force/torque sensor presently implemented in the DLR instruments can optionally be integrated to measure contact reactions of the probe with the surrounding tissue as well. This additional kinesthetic feedback can contribute to prevent a clamping of the blood vessel caused by excessive pressure against the vessel on the one hand and an air gap between probe and tissue due to poor contact on the other hand. In both cases considerable measuring errors are expected. However, the force/torque sensor unnecessarily complicates the setup resulting in further causes of error. It might be appropriate,

therefore, to integrate the force/torque sensor in a further step.

Another improvement of the pulse detection might possibly yield an electrocardiogram (ECG) triggering: Assuming physiological hemodynamics, a pulse wave is expected in a particular time slot after the R wave in the ECG. The additional technological expenditure would be comparatively small since an ECG is usually recorded during surgery anyway. Moreover, the R wave detection is an often addressed problem which can nowadays be dealt with effectively [224]. Hence, it is assumed that the automated, computer-assisted R wave detection within the ECG can be performed more robustly in comparison to an automated, computer-assisted pulse wave detection within the Doppler signal. Therefore, it is expected that the pulse detection quality can be improved taking ECG triggering into consideration, e. g. for plausibility checks and for filtering out false-positive detections in absence of an R wave respectively.

On the basis of the novel multidirectional ultrasound probe's first test results (cf. Sec. 4.2 – 4.4 and [202]) further work on the research project is considered to be justified. Moreover, it is expected that the sensor system can be employed in many more fields of application as referenced in Sec. 5.1.1 – 5.1.3.

5.1.1 Cartography of Artery Position

The ultrasound probe is planned to be guided by a MIRO robot permanently providing position data due to position sensors in every joint. It is possible with any pulse detection, therefore, to determine the current ultrasound probe's position. Moreover, the position can be marked, e. g. with a clearly visible dot in the endoscopic image. A number of "pulse positions" then show the course of a vessel point wise which can be supported e. g. by fitting a spline through these points in the endoscopic image to show the probable course. This is intended to help the surgeon getting a clear idea of the intra-operative site in addition to his pure anatomical knowledge.

Moreover, before revascularization surgery usually a patient specific coronary angiography – often even in 3D – is made to get a clearer picture of the coronaries' positions and to plan the procedure in advance. Therefore, the surgeon has a relatively clear idea of the preoperative situs and can plan the best suitable location of a bypass anastomosis. However, it is often difficult to match the preoperative data with the intraoperative situation since the arteries clearly visible in the coronary angiogram often cannot be seen that clearly in the operating field e. g. due to covering tissue. A time-consuming, careful preparation of covering tissue then is necessary for better orientation and for finding the exact location of anastomoses [10, p. 20], [11, p. 33], [12, p. 125], [13, 14], cf. Sec. 1.1. With the described drawing of detected artery positions in the endoscopic image this time-consuming preparation could become obsolete.

In a further future step, an automated, computer-assisted matching of preoperative planning data and in situ recorded vessel positions ("matching points") could be performed and overlaid e. g. the endoscopic video image. This might support a

faster orientation within the intraoperative site without unnecessary lesions to the patient's tissue only for orientation purposes.

The described cartography of artery positions is part of a corresponding patent [223].

5.1.2 Further Possible Fields of Application

Omata et al. introduced a tactile sensor principle based on changing resonance frequencies of an ultrasound probe contacted to tissues of different hardness. They use two piezoelectric transducers, one behind the other, in longitudinal direction. The rear one is subjected to alternating voltage to generate longitudinal vibrations while the front one is used to pick up the frequency, feeding it back to the amplifier driving the rear transducer. Hence, the system always oscillates at its resonance frequency. Contacting this transducer probe to tissue changes the resonance frequency of the feedback system according to the acoustic impedance of the tissue. The changes are detected by the pick up indicating inhomogeneities in the tissue while passing over it with the transducer probe. These changes are interpreted as different levels of rigidity [69,155,225,226]. Matsumoto et al. described the detection of gallstones in the gallbladder and the cholecystic duct respectively as well as the discrimination between gallstones and air bubbles during laparoscopic cholangiography by this system [156]. Moreover, Ohtsuka et al. used it in a clinical study to localize small lung nodules thoracoscopically yielding promising results [227]. More recently the system's measurement results could be computed by Murayama et al. to obtain a contour image and topographical elasticity information [228].

It is considered to be possible to modify the sensor presented in this dissertation so that comparable measurements might be performed. An adapted electronics sending simultaneous impulses with most of the transducer elements and using three or four of the elements as pick up to determine the current resonance frequency according to the contacted tissue may yield results comparable to Omata et al. However, the front sealing might possibly have to be modified to show lower damping characteristics. As explained in Sec. 5.1.1 a cartography for the course of a vessel is already planned; an extension, therefore, on tissue elasticity following Murayama et al. is expected to be possible.

5.1.3 Transducer Element Integration in MIRS Instruments

A number of research groups address multi-functional MI(R)S instruments [229–235]. In most cases a reduction of operating time due to a decrease of time-consuming instrument changes during surgery is intended. The devices allow e. g. cutting as well as gripping [232–234] and, therefore, an instrument change for these purposes becomes unnecessary.

In the long term it is considered to be possible that a further miniaturization of the transducer probe presented in this dissertation will allow an integration in the jaws of a MIRS instrument. The transducers could e. g. be integrated into the inner

surface of an instrument's jaws. With a 180° opening of the jaws and a contacting with the tissue concerned the presence of vessels could then be checked and the preparation could be continued directly afterwards without an instrument change. Moreover, by this 180° opening of the jaws, structures would be palpable in a planar way as well as by clasping around – depending on the surgical requirements. As mentioned in Sec. 1.1 cautious preparation (i. e. cutting, dissecting) of tissue structures is a frequent necessity during surgery. With a multi-functional MIRS instrument, for cutting, gripping, and palpating, this task could be performed more carefully and possibly even more quickly with a step by step palpation, ensuring the absence of arteries, and dissection without any instrument changes. This steady preparation without interruptions for instrument changes allows more concentrated work and, thus, leaves less room for mistakes.

However, the miniaturization of the ultrasound transducer probe is considered to be difficult. Probably different manufacturing and assembling processes will have to be used since structures will be too small for manual treatment. In addition, transducers with a smaller radiating area due to miniaturization have a limited ability to emit ultrasound energy, which complicates the measurement. Further investigation about the minimum energy needed and a benefit-cost analysis of the miniaturization might have to be conducted.

5.2 Occupational Psychological Tests for Evaluation Purposes and Discussion of Desired Result

As introduced in Sec. 1.2 and at the beginning of this chapter further feedback modalities, e. g. acoustic (by playing the characteristic Doppler sound) or visual (by displaying signals in the endoscopic image), are planned to be implemented to enhance intuitiveness and immersion by addressing different perceptive channels. For a scientifically reliable, substantiated evaluation of the feedback modalities' effects on the user, the intuitiveness, and the achievable grade of immersion, tests by occupational psychologists are considered appropriate, since parameters like manageability, intuitiveness or immersion can hardly be conceptualized with conventional engineering methods.

Occupational psychology in this respect is concerned with man-machine systems from a psychological perspective. Moreover, by contributing knowledge about typical human abilities and restrictions concerning information reception and processing, occupational psychology tries to enhance the development of man-machine systems which are as effective as possible. Thereby, cognitive psychology, concerned with the analysis of human discernment, knowledge, and information processing, plays an important part [236].

For these reasons, tests by occupational psychologists of the Human Factors Institute (IfA) of the University of the Bundeswehr Munich are scheduled within the framework of the Collaborative Research Center (SFB) 453. In these tests it is initially planned to evaluate the three feedback modes described, soft twitch-

ing of the input device's open/close-input-master, production of the characteristic Doppler sound, and displaying of signals in the endoscopic image.

The objective is to find the most intuitive and immersed feedback modality or combination of modalities. It is planned to ask (skilled and unskilled) test persons to find and to follow artificial vessels within the test-bed (cf. Sec. 4.1) which is considered to be suitable for these tests. Optimization of the feedback characteristics is planned to be achieved by varying the feedback parameters, i. e. activating and deactivating a single or a combination of the three feedback modalities, and by varying the feedback amplification, especially of the kinesthetic feedback modality. Thereby, especially the type and the effect of the modality substitution is to be examined, evaluated, and optimized. It is expected that through these tests even further suitable feedback modalities or possibly necessary adaptations of the hardware might be identified to optimize the detection process. Necessary hardware optimizations might e. g. be modifications of the sensor front-end geometry like a beveling of the front surface, a reduction of the instrument diameter, or of the front-end length.

Within these tests it is desired to achieve tactile feedback as intuitively as possible. However, in the present state of development the system is focused on the detection of hidden vessels within covering tissue. This is seen as an important and safety-relevant feature (cf. Sec. 1.1). Since previous approaches did not prevail (cf. Sec. 2.4), a new approach was presented to achieve one step towards the establishment of tactile feedback. Nevertheless, reestablishment of full tactile feedback comparable to the human hand still has to be striven for. In Sec. 5.1.2 one further possible field of application for the presented sensor type could be shown, namely tactile feedback of tissue rigidity. Enhanced data processing and displaying to the user (cf. Sec. 5.1.1 and 5.1.2), i. e. the surgeon, may further support intuitiveness and immersion. It is, therefore, assumed that the presented sensor type has the potential to cover more fields of application than detecting hidden vessels and can at least go some steps further towards full tactile feedback. Nonetheless, the development of tactile feedback for minimally invasive (robotic) surgery comparable to the human hand is just at the very beginning.

A Glossary

THE SUBJECT MATTER of this dissertation deals with a medical engineering subject and, therefore, is related to medical as well as engineering sciences. Especially at the interface between these two areas of expertise – two areas with completely different terminologies and ways of thinking – comprehensible communication is a necessity and a major task of medical engineers.

Therefore, this chapter has two main reasons: first to make the thesis more understandable for representatives of both disciplines and second to give a clear explanation of the meaning of abbreviations and technical expressions used in this thesis. Furthermore, MIRS, telepresence, and teletactility are relatively young fields of research with a not yet completely consistent nomenclature in literature. This makes it mandatory to define the technical terms as they are used in this thesis.

A.1 Abbreviations

A.	artery (*Latin:* arteria)
AG	stock corporation (*German:* Aktiengesellschaft)
Al_2O_3	aluminium oxide
ASME	American Society of Mechanical Engineers
$BaTiO_3$	barium titanate
BMES	Biomedical Engineering Society
B-mode	brightness modulation (imaging ultrasound: ultrasound echo amplitude is transformed into a gray scale value of a pixel)
$[C_6H_{10}O_5]_n$	dextran (polysaccharide soluble in water which can also be used as plasma volume expander)
CAD	computer aided design
CCD	charge coupled device
cf.	compare (*Latin:* confer)
Cha.	chapter

cw	continuous-wave
DC	direct current
DOI	digital object identifier
Dept.	department
DFG	German Research Association (*German:* Deutsche Forschungsgemeinschaft)
DLR	German Aerospace Center (*German:* Deutsches Zentrum für Luft- und Raumfahrt *e. V.*)
DoF	degree(s) of freedom
ECABG	endoscopic coronary artery bypass graft
ECG	electrocardiogram
e. g.	for example (*Latin:* exempli gratia)
EMBS	IEEE Engineering in Medicine and Biology Society
Eqn.	equation(s)
et al.	and others (*Latin:* et alii)
etc.	and so forth (*Latin:* et cetera)
et seqq.	and the following (*Latin:* et sequens)
e. V.	registered association (*German:* eingetragener Verein)
FhG IBMT	Fraunhofer Institute for Biomedical Engineering (*German:* Fraunhofer Gesellschaft, Institut für Biomedizinische Technik)
Fig.	figure(s)
FPGA	field-programable gate array (customarily configurable semiconductor device)
GB	United Kingdom of Great Britain and Northern Ireland
GmbH	private limited company (*German:* Gesellschaft mit beschränkter Haftung)
GUI	graphical user interface
IBMT UniS	Department of Biomedical Engineering, University of Stuttgart (*German:* Institut und Lehrstuhl für Biomedizinische Technik, Universität Stuttgart)
i. e.	that is (*Latin:* id est)
IEEE	Institute of Electrical and Electronics Engineers
IFMBE	International Federation for Medical and Biological Engineering
Inc.	incorporated
IRE	Institute of Radio Engineers

ISBN	International Standard Book Number
ISO	International Organization for Standardization
IUPESM	International Union for Physical and Engineering Sciences in Medicine
L.	ligament
LAD	left anterior descending artery (*Latin:* Ramus interventricularis anterior, RIVA)
LAN	local area network
LDF	Laser Doppler Flowmetry
LPF	low-pass filter
MATLAB	matrix laboratory (computer software tool primarily for numeric calculations of matrices)
MERODA	Medical Robotics Database
MIDCAB	minimally invasive direct coronary artery bypass
MIRA	Minimally Invasive Robotics Association
MIRO	proper name of the latest medical robot arm version developed by the German Aerospace Center, Institute of Robotics and Mechatronics
MIRS	minimally invasive robotic surgery
MIS	minimally invasive surgery
MMI	man-machine interface(s)
NTP	normal temperature and pressure ($T = 273,15$ K, $p = 101325$ Pa)
p.	page(s)
Pb(Zr, Ti)O_3	lead-titanate-zirconate
PC	personal computer
PE	polyethylene (special plastic material)
PhD	Doctor of Philosophy
PRF	pulse repetition frequency
PVC	polyvinyl chloride (special plastic material)
PVDF	polyvinylidene fluoride (special plastic material)
pw	pulsed-wave
QNX	microkernel-based, Unix-like real-time operating system introduced by Quantum Software Systems, Inc.
Sec.	section(s)
SFB	Collaborative Research Center (*German:* Sonderforschungsbereich)

SiC	silicon carbide
SiO_2	quartz
SPIE	International Society for Optical Engineering (*formerly:* Society of Photographic Instrumentation Engineers)
St.	Saint (*German:* Sankt)
Tab.	table(s)
TAMIC	tactile microsystem for minimally invasive surgery (*German:* Taktiles Mikrosystem für die minimal invasive Chirurgie)
TAPP	transabdominal preperitoneal hernioplasty
TEP	total extraperitoneal hernioplasty
UK	United Kingdom of Great Britain and Northern Ireland
USA	United States of America
USB	Universal Serial Bus
vs.	in comparison to (*Latin:* versus)
3D	three-dimensional

A.2 Explanation / Definition of Technical Terms

As pointed out, most of the relevant scientific fields in the context of this thesis are relatively young. This entails that terminology found in literature is partly inhomogeneous and incoherent. To avoid misunderstandings, the most important technical terms are explained as they are used in this dissertation and in the majority of the relevant literature.

false haptic representation

The neologism *false haptic representation* was formed analogously to the term ”pseudo-color representation” or ”false color representation”. In thermodynamics, for example, thermal radiation or heat fluxes can be visualized by assigning colors to temperatures. A thermally expected information is perceived visually and, more or less, intuitively. More generally, a physical value (in this thesis: a tactilely expected impression, actually Doppler frequency shifts) is proposed to be represented in a transformed value (in this thesis: amongst others a kinesthetic impression), therefore, the term *false haptic representation* was introduced. In a special sense the superordinate term to false haptic representation is ”modality substitution”.

fulcrum point

The penetration point of the minimally invasive surgical instruments into the corresponding body cavity (usually abdominal or chest wall). Kinematically it must

be regarded as a combination of an elastic, gimballed, and prismatic bearing (cf. Fig. 2.2 , p. 19). From a medical point of view the tissue around the fulcrum point should not be loaded with forces to avoid tearing.

haptics

The word *haptics* or *haptic perception* in its literal sense means to touch or to handle, just as the word *tactility* or *tactile perception* does (see below) [237, p. 4]. In accordance with newer literature *haptics* is used in this thesis as the superordinate for a variety of perceptions, e. g. pressure, vibration, pain, or temperature, and, especially relevant in this dissertation, for kinesthesia and tactility (see below and cf. diagram).

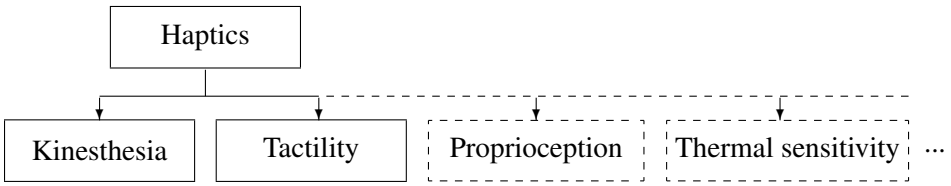

immersion

Degree of being familiarized with, of being involved or absorbed in a presented situation. Therefore, *immersion* is a measure of the quality of telepresence: good telepresence delivers a high grade of immersion and vice versa. The grade of immersion can be experienced very differently, depending e. g. on the user, his/her personality, the duration of use, or the quality of telepresence [238].

intuitive

The expression *intuitive*, or in the stricter sense as used in this dissertation, the expression *intuitive use* means the power of attaining direct cognition without evident rational thought and inference, a usage which is known by immediate and/or direct apprehension and understood without apparent effort. Optimal intuitive use is possible with an apparatus which, regardless of its complexity, possesses a very user-friendly and self-explanatory user prompting and can be operated without studying its manual.

kinesthesia

Kinesthesia[1] solely means the perception of reaction forces from the environment and their magnitude. Position, orientation, and movement of one's own body and forces/torques acting on it are perceived with kinesthesia and proprioception [239]. It is not possible to recognize surface structures (e. g. roughness) or short deviated

[1] Coming from the Greek "kinesis" (movement) and "aesthesie" (perception).

vibrations and (almost) impossible to recognize the rigidity of touched bodies in that way [57].

medical robotics

Robots can be employed for various tasks in medical contexts, especially in the field of service robotics. However, in this thesis the term *medical robot* is only used for systems with direct patient contact and interaction with a patient.

According to ISO 8373:1996 (international standard), a *robot* in the strict sense of the word is: ”An automatically controlled, reprogramable, multipurpose manipulator, programable in three or more axes, which may be either fixed in place or mobile for use in industrial automation applications” [240, ’Robot’].

Actually, regarding the tasks which have to be performed in minimally invasive robotic surgery, the system is better characterized by the definition of a *manipulator*: ”A machine, the mechanism of which usually consists of a series of segments jointed or sliding relative to one another, for the purpose of grasping and/or moving objects (pieces or tools) usually in several degrees of freedom. It may be controlled by an operator, a programable electronic controller, or any logic system (for example cam device, wired, etc.)” [240, ’Manipulator’]. Thus, strictly speaking a manipulator is not a robot. However, in this thesis and in accordance with literature the term *medical robot* is used meaning a *tele*manipulator with direct contact to and interaction with a patient.

modality substitution

Techniques for restructuring data so that one perceptive modality can be substituted for another one are called *modality substitution* in this dissertation. The term is primarily used in the psychology of perception as well as in behavioral and occupational psychology, but not yet very common. Exemplary are the representation of forces by means of arrows (comparable to engineering mechanics), the representation of stress and strain (calculated e. g. with the finite element method) by colors, or the visualization of pressure distributions on a surface by color representation.
The expression is used in relation to the well-established term ”sensory substitution” where the defective sensory modality of a disabled person is substituted by using their ability to perceive with another, functioning sensory modality [171, p. 341 et seqq.], [241].

operator

A (human) *operator* commands a telemanipulation system. Input commands of the operator (master side) are executed in a remote location by the teleoperator (slave side, cf. *teleoperation*).

proprioception

Proprioception, also called deep sensibility and sometimes kinesthetic sensibility, is divided into posture proprioception, movement proprioception, and force sensation [194, p. 216 et seqq.]. It is the unconscious perception of body position (spacial orientation) and movement, also under loaded conditions, generated by stimuli of internal mechanoreceptors [242, p. 1246] located at the skeletal joints and in the inner ear. The use of these receptors as well as impulses from the central nervous system (memory effect) is named *proprioception* here [237, p. 4].

tactility

The word *tactility* or *tactile perception* in its literal sense means to touch or to handle (cf. *haptics*). In accordance with literature *tactility* is used here for the perception of surface structures as well as of the rigidity of touched bodies and/or short deviated vibrations with the sense of touch (skin). It has to be kept in mind that the perception of surface structures in many cases can only be achieved by moving the sensing body (e. g. fingertip) over the corresponding surface[2]. "Short deviated vibrations" can be e. g. (subsurficial) pulsating vessels.

telemanipulation

In the technical sense *telemanipulation* is the capability of performing remotely handling objects or environments with chronological synchronism of the user [239].
Manipulation in the psychological sense of persuasion or indoctrination, is not meant here.

teleoperation

The expansion of a person's ability to sensorize and to manipulate to a remote location is known as teleoperation. A teleoperator (i. e. remote or slave system) must have sensors and actors as well as multimodal communication channels from and to the human operator (i. e. master system) [239].

telepresence

Telepresence pools e. g. television, telemanipulation, teletactility, or teleconsultation in a scenario where the user feels on-site. In the ideal case, the user is not aware of his remote state due to concentration or immersion. This can be supported by the teleoperator sided acquisition of relevant sensor data of the remote location and a subsequent natural and realistic presentation to the operator [239].

[2] Simply laying a finger on a surface can not give information about the surface structure in most cases; possibly with the exception of temperature but for sensing e. g. the surface roughness or material the sensing body must be moved [61].

telesurgery

In literature the terms *telesurgery*, *remote surgery*, and *minimally invasive robotic surgery* (MIRS) are widely used synonymously. The terms describe minimally invasive surgery with robotic support, almost always in the classical teleoperated order by division into a master and a slave system. In this thesis the term *minimally invasive robotic surgery (MIRS)* is preferred (cf. [243, p. 187]).

A.3 Notation

A	cross sectional area $\left[mm^2\right]$
A_0	initial amplitude $[cm]$
A_x	local amplitude $[cm]$ at penetration depth x $[m]$
α	angle $[^\circ]$, tissue specific attenuation coefficient $\left[\frac{dB}{MHz^n \cdot cm}\right]$
β	angle $[^\circ]$
c	sound-propagation velocity in considered medium $\left[\frac{m}{s}\right]$ ($c_{water,\ 293.15K} = 1484\frac{m}{s}$, cf. Tab. 2.3, p. 35)
c_0	sound propagation velocity in the oscillator material $\left[\frac{m}{s}\right]$
c_c	sound velocity received by corpuscle $\left[\frac{m}{s}\right]$
d	particle diameter $[m]$, oscillator thickness $[m]$
D, $\varnothing D$	diameter of a circular transducer $[m]$
Δf	Doppler frequency shift $\left[Hz = \frac{1}{s}\right]$
e	Euler's constant (2.71828 . . .) [1]
E	modulus of elasticity, Young's modulus $\left[Pa = \frac{N}{m^2}\right]$
f	frequency $\left[Hz = \frac{1}{s}\right]$
φ	angle $[^\circ]$
f_0	transmitted frequency $\left[Hz = \frac{1}{s}\right]$,
f_c	frequency received by corpuscle $\left[Hz = \frac{1}{s}\right]$
f_r	frequency received by transducer $\left[Hz = \frac{1}{s}\right]$
I_0	initial intensity $\left[\frac{W}{m^2}\right]$
I_x	local intensity $\left[\frac{W}{m^2}\right]$ at penetration depth x $[m]$
κ	adiabatic compressibility $\left[\frac{m^2}{N}\right]$
λ	wave length $[m]$
λ_r	received wave length $[m]$
m	mass $[kg]$

μ	frequency dependent intensity absorption coefficient $\left[\frac{1}{cm}\right]$, backscattering coefficient $\left[\frac{1}{m \cdot sr}\right]$
n	constant representing frequency dependency $[1]$, order of oscillation $[1]$
Ω	steradian, solid angle $[sr]$
ω	aperture angle $[^\circ]$
p	pressure $\left[Pa = \frac{N}{m^2}\right]$
p_0	ambient pressure $\left[Pa = \frac{N}{m^2}\right]$
π	circular constant ($3.14159 \ldots$ $[1]$)
r	radius $[mm]$
R	reflection coefficient $[1]$
ρ	density $\left[\frac{kg}{m^3}\right]$
t	time $[s]$
T	temperature $[K]$, wave period $[s]$, transmission coefficient $[1]$
Θ_{6dB}	beam angle $[^\circ]$ within a -6 dB boundary
T_n	spans of time $[s]$ within oscillator time diagram
v	velocity $\left[\frac{m}{s}\right]$
$\dot{V}$	volume flow $\left[\frac{ml}{min}\right]$
$\dot{V}_{exp}$	expected volume flow $\left[\frac{ml}{min}\right]$
v_d	motion speed of interface $\left[\frac{m}{s}\right]$
v_{exp}	expected flow velocity $\left[\frac{m}{s}\right]$
x	linear length $[m]$
y	linear length $[m]$
Z	acoustic impedance $\left[\frac{kg \cdot m^2}{s}\right]$

List of Figures

List of Tables

Bibliography

[1] Intuitive Surgical, Inc. Company profile of Intuitive Surgical, Inc., Sunnyvale, CA, USA. Website, 08/2009. `http://www.intuitivesurgical.com`.

[2] Joachim M. Müller, ed. Chirurgenmanual. Charité – Klinik für Allgemein-, Visceral-, Gefäß- und Thoraxchirurgie, Campus Mitte, Berlin, Germany. Website, 08/2006. `http://www.charite.de/ch/chir/chir/ch_manu.htm`.

[3] William J. Peine, Jae S. Son, and Robert D. Howe. A palpation system for artery localization in laparoscopic surgery. In *Proceedings of the 1st International Symposium on Medical Robotics and Computer-Assisted Surgery*, Pittsburgh, PA, USA, September 22-24 1994.

[4] Ryan A. Beasley and Robert D. Howe. Tactile tracking of arteries in robotic surgery. In *Proceedings of the IEEE International Conference on Robotics and Automation (ICRA)*, volume 4, pages 3801–3806, Washington, DC, May 11-15 2002. DOI: 10.1109/ROBOT.2002.1014309.

[5] Andreas Kuthe. *Chirurgie der Leistenhernie – Minimalinvasive Operationstechniken*, chapter Praktische Hinweise zur Vermeidung von Komplikationen und Rezidiven bei der TEP, pages 205–214. Karger, Basel, 2006. DOI: 10.1159/000093416.

[6] Klaus Kraft. *Chirurgie der Leistenhernie – Minimalinvasive Operationstechniken*, chapter Praktische Hinweise zur Vermeidung von Komplikationen und Rezidiven bei der TAPP, pages 188–204. Karger, Basel, 2006. DOI: 10.1159/000093415.

[7] Joachim Jähne. Chirurgie der Leistenhernie. *Der Chirurg*, 72(4):456–471, April 2001. DOI: 10.1007/PL00002599.

[8] Barbara Kraft. *Chirurgie der Leistenhernie – Minimalinvasive Operationstechniken*, chapter Aktuelle Methodenwahl unter spezieller Berücksichtigung der Herniensituation, pages 40–57. Karger, Basel, DOI: 10.1159/000093390 2006.

[9] R. Keller, H.-P. Bruch, O. Schwandner, and R. Broll. *Chirurgie*, chapter 29 – Gallenblase und Gallenwege, pages 871–903. Elsevier, Munich, 5th edition, 2006.

[10] Johannes Frömke. *Standardoperationen in der Herzchirurgie*. Steinkopff Verlag, Darmstadt, 1st edition, January 2003.

[11] Johannes Albes. *OP-Atlas Herzchirurgische Operationen*, chapter Koronare Standardrevaskularisation, pages 25–43. Lehmanns Media-Lob.de, Berlin, 1st edition, November 2005. ISBN-13: 978-3865410764.

[12] Christof Schmid. *Tipps und Tricks für den Herz- und Thoraxchirurgen*. Springer Verlag, Berlin, Heidelberg, New York, 2005.

[13] Michael F. Szwerc, Jeffery C. Lin, and James A. Magovern. Finding the LAD during MIDCAB operations. *The Annals of Thoracic Surgery*, 68(4):1422–1423, 1999.

[14] Volkmar Falk, James I. Fann, Jürg Grünenfelder, and Thomas A. Burdon. Endoscopic Doppler for detecting vessels in closed chest bypass grafting. *The Heart Surgery Forum*, 3(4):331–333, 2000.

[15] Bernhard Kübler, Georg Passig, Robin Gruber, Steffen H. Tretbar, and Christian Degel. Publication of unexamined application, DE 10 2008 005 041 A1, Ultraschallkopf mit Ultraschall-Doppler-Anordnung. Patent pending, disclosure July 30th 2009.

[16] Tobias Ortmaier, Holger Weiss, Ulrich A. Hagn, Markus Grebenstein, Mathias Nickl, Alin Albu-Schäffer, Christian Ott, Stefan Jörg, Rainer Konietschke, Luc Le-Tien, and Gerd Hirzinger. A hands-on-robot for accurate placement of pedicle screws. In *Proceedings of the IEEE International Conference on Robotics and Automation (ICRA)*, pages 4179–4186, Orlando, FL, USA, May 2006.

[17] Rainer Konietschke, Tobias Ortmaier, Christian Ott, Ulrich Hagn, Luc Le-Tien, and Gerd Hirzinger. Concepts of human-robot cooperation for a new medical robot. In Klaus Diepold and Rüdiger Dillmann, editors, *Proceedings of 2nd International Workshop on Human Centered Robotic Systems (HCRS)*, pages 93–98, Munich, Germany, October 2006.

[18] Force Dimension, Inc. omega.x haptic devices, data sheet. Website, 10/2008. `http://www.forcedimension.com/downloads/specs/specsheet-omega.x.pdf`.

[19] Ulrich Hagn, Rainer Konietschke, Andreas Tobergte, Mathias Nickl, Stefan Jörg, Bernhard Kübler, Georg Passig, Martin Gröger, Florian Fröhlich, Ulrich Seibold, Luc Le-Tien, Alin Albu-Schäffer, Alexander Nothhelfer, Franz Hacker, Markus Grebenstein, and Gerd Hirzinger. DLR MiroSurge: a versatile system for research in endoscopic telesurgery. *International Journal of Computer Assisted Radiology and Surgery*, 2009.

[20] Christoph Grossmann. International Patent, WO 2008/011888 A1, Autostereoscopic System, SeeFront GmbH, Hamburg, Germany, chartered January 31st 2008.

[21] Ulrich A. Hagn, Mathias Nickl, Stefan Jörg, Georg Passig, Thomas Bahls, Alexander Nothhelfer, Franz Hacker, Luc Le-Tien, Alin Albu-Schäffer, Rainer Konietschke, Markus Grebenstein, Rebecca Warpup,

Robert Haslinger, Mirko Frommberger, and Gerd Hirzinger. The DLR MIRO: a versatile lightweight robot for surgical applications. *Industrial Robot: An International Journal*, 35(4):324–336, 2008. DOI: 10.1108/01439910810876427.

[22] Bernhard Kuebler, Ulrich Seibold, and Gerd Hirzinger. Development of actuated and sensor integrated forceps for minimally invasive robotic surgery. *The International Journal of Medical Robotics and Computer Assisted Surgery*, 1(3):96–107, September 2005. DOI: 10.1002/rcs.33.

[23] Ulrich Seibold, Bernhard Kübler, and Gerd Hirzinger. Prototype of instrument for minimally invasive surgery with 6-axis force sensing capability. In *Proceedings of the IEEE International Conference on Robotics and Automation (ICRA)*, pages 496–501, Barcelona, Spain, April 2005.

[24] Michael R. Treat. *Computer-Integrated Surgery – Technology and Clinical Applications*, chapter 42, A Surgeon's Perspective on the Difficulties of Laparoscopic Surgery, pages 559–560. MIT Press, January 1996.

[25] Ulrich Seibold. Illustration, Institute of Robotics and Mechatronics, German Aerospace Center (DLR), April 2004.

[26] Desmond H. Birkett. Electromechanical instruments for endoscopic surgery. *Minimally Invasive Therapy & Allied Technologies*, 10(6):271–274, November 2001. DOI: 10.1080/136457001753337302.

[27] Jens Rassweiler and Thomas Frede. Geometrie der Laparoskopie, Telechirurgie, Training und Telementoring. *Der Urologe*, 41(2):131–143, March 2002. DOI: 10.1007/s00120-002-0186-2.

[28] Gyung Tak Sung and Inderbir S. Gill. Robotic laparoscopic surgery: A comparison of the daVinci and Zeus systems. *Adult Urology*, 58(6):893–898, August 2001.

[29] Minimally Invasive Robotics Association (MIRA). Homepage. Website, 11/2006. `http://www.teleroboticsurgeons.com/`.

[30] Russel H. Taylor and Dan Stoianovici. Medical robotics in computer-integrated surgery. *IEEE Transactions on Robotics and Automation*, 19(5):765–781, October 2003.

[31] Peter P. Pott, ed. Medical Robotics Database (MERODA). Laboratory for Biomechanics and experimental Orthopedics, Dept. of Orthopedic Surgery, University Clinic Mannheim, Germany. Website, 11/2006. `http://www.ma.uni-heidelberg.de/apps/ortho/meroda/`.

[32] Garth H. Ballantyne. Robotic surgery, telerobotic surgery, telepresence, and telementoring – Review of early clinical results. *Surgical Endoscopy*, 16(10):1389–1402, October 2002. DOI: 10.1007/s00464-001-8283-7.

[33] Jonathan M. Sackier and Yulun Wang. *Computer-Integrated Surgery – Technology and Clinical Applications*, chapter 45, Robotically Assisted Laparoscopic Surgery: From Concept to Development, pages 577–580. MIT Press, January 1996.

[34] Harold A. Tabaie, Jeffrey A. Reinbolt, W. Peter Graper, Thomas F. Kelly, and Michael A. Connor. Endoscopic coronary artery bypass graft (ECABG) procedure with robotic assistance. *The Heart Surgery Forum*, 2(4):310–317, September 1999.

[35] Ronald J. Franzino. The Laprotek surgical system and the next generation of robotics. *Surgical Clinics of North America*, 83(6):1317–1320, December 2003. DOI: 10.1016/S0039-6109(03)00171-3.

[36] H.-J. Düpree, T.H.K. Schiedeck, F. Fischer, and H.P. Bruch. Erstmaliger Einsatz des neuen Master-Slave-Systems Laprotek für die minimalinvasive Chirurgie: Erfahrungen der klinischen Pilotstudie am Beispiel der computerassistierten Cholecystektomie. In *121. Kongress der Deutschen Gesellschaft für Chirurgie*, Berlin, Germany, April 2004. German Medical Science. Poster Presentation, `http://www.egms.de/en/meetings/dgch2004/04dgch394.shtml`.

[37] Gary S. Guthart and J. Kenneth Salisbury. The Intuitive™ telesurgery system: Overview and application. In *Proceedings of the IEEE International Conference on Robotics and Automation (ICRA)*, volume 1, pages 618–621, San Francisco, CA, USA, April 2000. DOI: 10.1109/ROBOT.2000.844121.

[38] Jens Rassweiler, Jochen Binder, and Thomas Frede. Robotic and telesurgery: will they change the future? In *Current Opinion in Urology*, volume 11, pages 309–320, May 2001.

[39] Tobias Ortmaier, Barbara Deml, Bernhard Kuebler, Georg Passig, Detlef Reintsema, and Ulrich Seibold. *Advances in Telerobotics*, volume 31 of *Springer Tracts in Advanced Robotics (STAR)*, chapter 21 – Robot Assisted Force Feedback Surgery, pages 361–379. Springer Verlag, Berlin, Germany, August 2007. DOI: 10.1007/978-3-540-71364-7_22.

[40] Barbara Deml, Tobias Ortmaier, and Holger Weiss. Minimally invasive surgery: Empirical comparison of manual and robot assisted force feedback surgery. In *Proceedings of the EuroHaptics2004, 4th International Conference*, pages 403–406, Munich, Germany, June 2004.

[41] Barbara Deml, Tobias Ortmaier, and Ulrich Seibold. The touch and feel in minimally invasive surgery. In *Proceedings of the IEEE International Workshop on Haptic Audio Visual Environments and their Applications (HAVE)*, pages 33–38, Ottawa, Ontario, Canada, October 2005. DOI: 10.1109/HAVE.2005.1545648.

[42] Christopher R. Wagner and Robert D. Howe. Mechanisms of performance enhancement with force feedback. In *Proceedings of the 1st joint Euro-Haptics Conference and Symposium on Haptic Interfaces for Virtual Environment and Teleoperator Systems (WHC)*, pages 21–29, Pisa, Italy, March 2005. DOI: 10.1109/WHC.2005.88.

[43] Christopher R. Wagner, Nicholas Stylopoulos, Patrick G. Jackson, and Robert D. Howe. The benefit of force feedback in surgery: Examination of blunt dissection. *Presence*, 16(3):252–262, June 2007. DOI: 10.1162/pres.16.3.252.

[44] Christopher R. Wagner, Nicholas Stylopoulos, and Robert D. Howe. The role of force feedback in surgery: Analysis of blunt dissection. In *Proceedings of the 10th Symposium on Haptic Interfaces for Virtual Environment and Teleoperator Systems*, pages 68–74, Orlando, FL, USA, March 24-25 2002.

[45] Robert D. Howe, William J. Peine, Dimitrios A. Kontarinis, and Jae S. Son. *Remote Palpation Technology*, volume 14, chapter IEEE Engineering in Medicine and Biology Magazine, pages 318–323. IEEE Engineering in Medicine and Biology Society, May/June 1995. DOI: 10.1109/51.391770.

[46] Wagahta Semere, Masaya Kitagawa, and Allison M. Okamura. Teleoperation with sensor/actor asymmetry: Task performance with partial force feedback. In *Proceedings of the 12th International Symposium on Haptic Interfaces for Virtual Environment and Teleoperator Systems (HAPTICS)*, pages 121–127, Chicago, IL, USA, March 2004. DOI: 10.1109/HAPTIC.2004.1287186.

[47] Gregory Tholey, Jaydev P. Desai, and Andres E. Castellanos. Force feedback plays a significant role in minimally invasive surgery: Results and analysis. *Annals of Surgery*, 241(1):102–109, January 2005. DOI: 10.1097/01.sla.0000149301.60553.1e.

[48] Jens Rassweiler and Thomas Frede. Robotics, Telesurgery and Telementoring – their position in modern urological laparoscopy. *Archivos Españoles de Urología*, 55(6):610–628, July 2002.

[49] Hermann Mayer, Istvan Nagy, Alois Knoll, Eva U. Braun, Robert Bauernschmitt, and Rüdiger Lange. Haptic feedback in a telepresence system for endoscopic heart surgery. *Presence*, 16(5):459–470, October 2007. DOI: 10.1162/pres.16.5.459.

[50] Eva U. Braun, Hermann Mayer, Alois Knoll, Rüdiger Lange, and Robert Bauernschmitt. *Medical Robotics*, chapter 2 – The Must-Have in Robotic

Heart Surgery: Haptic Feedback, pages 9–20. International Journal of Advanced Robotic Systems Publishing, Vienna, Austria, 2008. ISBN-13: 978-3-902613-18-9.

[51] Brian T. Bethea, Allison M. Okamura, Masaya Kitagawa, Torin P. Fitton, Stephen M. Cattaneo, Vincent L. Gott, William A. Baumgartner, and David D. Yuh. Application of haptic feedback to robotic surgery. *Journal of Laparoendoscopic and Advanced Surgical Techniques*, 14(3):191–195, November 2004. DOI: 10.1089/1092642041255441.

[52] Masaya Kitagawa, Daniell Dokko, Allison M. Okamura, and David D. Yuh. Effect of sensory substitution on suture-manipulation forces for robotic surgical systems. *The Journal of Thoracic and Cardiovascular Surgery*, 129(1):151–158, 2005. DOI: 10.1016/j.jtcvs.2004.05.029.

[53] Takintope Akinbiyi. Intelligent Instruments and Visual Force Feedback in Laparoscopic Minimally Invasive Surgery. Master's thesis, The Johns Hopkins University, Baltimore, MD, USA, October 2005.

[54] Takintope Akinbiyi, Carol E. Reiley, Sunipa Saha, Darius Burschka, Christopher J. Hasser, David D. Yuh, and Allison M. Okamura. Dynamic augmented reality for sensory substitution in robot-assisted surgical systems. In *Proceedings of the 28th IEEE EMBS Annual International Conference of the Engineering in Medicine and Biology Society*, pages 567–570, New York City, NY, USA, August/September 2006.

[55] M. Tavakoli, A. Aziminejad, R.V. Patel, and M. Moallem. Tool/tissue interaction feedback modalities in robot-assisted lump localization. In *Proceedings of the 28th IEEE EMBS Annual International Conference of the Engineering in Medicine and Biology Society*, pages 3854–3857, New York City, NY, USA, August/September 2006. DOI: 10.1109/IEMBS.2006.260672.

[56] M. Tavakoli, R.V. Patel, M. Moallem, and A. Aziminejad. *Haptics for Teleoperated Surgical Robotic Systems*, volume 1 of *New Frontiers in Robotics*. World Scientific Publishing, Singapore, 1st edition, April 2008.

[57] M.A. Srinivasan and R.H. LaMotte. Tactual discrimination of softness. *Journal of Neurophysiology*, 73(1):88–101, 1995.

[58] Iman Brouwer, Jeffrey Ustin, Loren Bentley, Alana Sherman, Neel Dhruv, and Frank Tendick. Measuring in vivo animal soft tissue properties for haptic modeling in surgical simulation. *Studies in Health Technology and Informatics*, 81:69–74, 2001. ISBN-13: 978-1-58603-143-5.

[59] Harald Fischer. *Sensor-Aktorsysteme für den Einsatz in der laparoskopischen Chirurgie*. PhD thesis, Fakultät für Elektrotechnik der Universität Karlsruhe (TH), Forschungszentrum Karlsruhe GmbH, Karlsruhe, April 1997.

[60] H. Fischer, R. Trapp, L. Schüle, and B. Hoffmann. Actuator array for use in minimally invasive surgery. *Journal de Physique*, IV 07(C5):609–614, 1997. DOI: 10.1051/jp4:1997596.

[61] Robert D. Howe and Mark R. Cutkosky. Dynamic tactile sensing: Perception of fine surface features with stress rate sensing. *IEEE Transactions on Robotics and Automation*, 9(2):140–151, April 1993. DOI: 10.1109/70.238278.

[62] Harald Fischer, Bernhard Neisius, and Rainer Trapp. Chapter 19 – tactile feedback for endoscopic surgery. In K.S. Morgan, Richard M. Satava, Hans B. Sieburg, R. Mattheus, and J.P. Christensen, editors, *Proceedings of the Interactive Technology and the New Paradigm for Healthcare: Medicine Meets Virtual Reality III*, pages 114–117, San Diego, CA, USA, January 1995. IOS Press. ISBN-13: 978-9051992014.

[63] Department of General Surgery, Section for Minimally Invasive Surgery. Network project TAMIC, Entwicklung eines taktilen Mikrosensorsystems für die Minimal Invasive Chirurgie. Schlussbericht, Eberhard-Karls-University Tuebingen, June 1997.

[64] University Hospital Tuebingen, Department of General Surgery, Section for Minimally Invasive Surgery. Tactile Sensor for Minimally Invasive Surgery (project TAMIC 1995-98). Website, 08/2008. `http://mic.uni-tuebingen.de/mic/index.php?id=95&lang=eng`.

[65] Margit Biehl. International Patent, WO 97/13130, Static and Dynamic Pressure Sensing Electronic Component, chartered April 10th 1997.

[66] Heinz Wörn, Ferdinand Schmoeckel, Axel Buerkle, Josep Samitier, Manel Puig-Vidal, Stefan A. Johansson, Urban Simu, Joerg-Uwe Meyer, and Margit Biehl. From decimeter- to centimeter-sized mobile microrobots: the development of the MINIMAN system. In Bradley J. Nelson and Jean-Marc Breguet, editors, *Proceedings of the SPIE Microrobotics and Microassembly*, volume 4568, pages 175–186, October 2001. DOI: 10.1117/12.444124.

[67] Erwin Petter, Margit Biehl, and Jörg-Uwe Meyer. Vibrotactile palpation instrument for use in minimal invasive surgery. In *Proceedings of the 18th Annual International Conference of the IEEE Engineering in Medicine and Biology Society. Bridging Disciplines for Biomedicine*, volume 1, pages 179–180, October 1996. DOI: 10.1109/IEMBS.1996.656905.

[68] Margit Biehl and Stefan Kiefer. International Patent, WO 97/17016, Sensor for the Non-Invasive and Continuous Measurement of the Arterial Pulse Wave Passage Time, chartered May 15th 1997.

[69] Sadao Omata and Yoshikazu Terunuma. New tactile sensor like the human hand and its applications. *Sensors and Actuators A: Physical*, 35(1):9–15, October 1992. DOI: 10.1016/0924-4247(92)87002-X.

[70] Matthias Balazs, Matthias Hähnle, Günther Roth, Ernst Flemming, and Gerhard F. Bueß. German Patent, DE 19 632 298 B4 2004.09.23, Greifeinrichtung zum Einsatz in der Minimal-Invasiven-Chirurgie, chartered September 23rd 2004.

[71] Parris S. Wellman and Robert D. Howe. Modeling probe and tissue interaction for tumor feature extraction. In *Proceedings of the ASME Summer Bioengineering Conference*, Sun River, OR, USA, June 1997.

[72] Jae S. Son and Robert D. Howe. Tactile sensing and stiffness control with multifingered hands. In *Proceedings of the IEEE International Conference on Robotics and Automation (ICRA)*, volume 4, pages 3228–3233, Minneapolis, MN, USA, April 1996. DOI: 10.1109/ROBOT.1996.509204.

[73] D.T.V. Pawluk and R.D. Howe. Dynamic lumped element response of the human fingerpad. *Journal of Biomechanical Engineering, Transactions of the ASME*, 121(2):178–183, April 1999. DOI: 10.1115/1.2835100.

[74] D.T.V. Pawluk and R.D. Howe. Dynamic contact of the human fingerpad against a flat surface. *Journal of Biomechanical Engineering, Transactions of the ASME*, 121(6):605–611, December 1999. DOI: 10.1115/1.2800860.

[75] William J. Peine and Robert D. Howe. Finger pad shape in lump detection. In *Proceedings of the ASME Summer Bioengineering Conference*, volume 35, Sun River, OR, USA, June 1997.

[76] William J. Peine and Robert D. Howe. Do humans sense finger deformation or distributed pressure to detect lumps in soft tissue? In R.J. Furness, editor, *Proceedings of the ASME International Mechanical Engineering Congress and Exposition*, volume 64, pages 273–278, Anaheim, CA, USA, November 1998. ASME Dynamic Systems and Control Division.

[77] R.L. Feller, C.K.L. Lau, C.R. Wagner, D.P. Perrin, and R.D. Howe. The effect of force feedback on remote palpation. In *Proceedings of the IEEE International Conference on Robotics and Automation (ICRA)*, volume 1, pages 782–788, New Orleans, LA, USA, April/May 2004. DOI: 10.1109/ROBOT.2004.1307244.

[78] William J. Peine, Parris S. Wellman, and Robert D. Howe. Temporal bandwidth requirements for tactile shape displays. In *Proceedings of the 6th Annual Symposium on Haptic Interfaces for Virtual Environment and Teleoperator Systems*, pages 107–113, Dallas, TX, USA, November 1997. ASME Dynamic Systems and Control Division.

[79] Jae S. Son, Mark R. Cutkosky, and Robert D. Howe. Comparison of contact sensor localization abilities during manipulation. *Journal of Robotics and Autonomous Systems*, 17(4):217–233, June 1996. DOI: 10.1016/0921-8890(95)00068-2.

[80] Dianne T.V. Pawluk, William J. Peine, Parris S. Wellman, and Robert D. Howe. Simulating soft tissue with a tactile shape display. In B. Simon, editor, *Proceedings of the ASME International Mechanical Engineer Congress and Exhibition (IMECE)*, volume 36 of *Advances in Bioengineering*, pages 253–254, Dallas, TX, USA, November 1997.

[81] Amy E. Kerdok, Stephane M. Cotin, Mark P. Ottensmeyer, Anna M. Galea, Robert D. Howe, and Steven L. Dawson. Truth cube: Establishing physical standards for soft tissue simulation. *Medical Image Analysis*, 7(3):283–291, September 2003. DOI: 10.1016/S1361-8415(03)00008-2.

[82] Anna M. Galea and Robert D. Howe. Liver vessel parameter estimation from tactile imaging information. In *Proceedings of the International Symposium on Medical Simulation (ISMS)*, volume 3078 of *Lecture Notes in Computer Science*, pages 59–66, Cambridge, MA, USA, June 2004. Springer. DOI: 10.1007/b98155.

[83] Christopher R. Wagner, Douglas P. Perrin, Ross L. Feller, Robert D. Howe, Olivier Clatz, Hervé Delingette, and Nicholas Ayache. Integrating tactile and force feedback with finite element models. In *Proceedings of the IEEE International Conference on Robotics and Automation (ICRA)*, pages 3942–3947, Barcelona, Spain, April 2005.

[84] William J. Peine, Dimitrios A. Kontarinis, and Robert D. Howe. Chapter 44 – a tactile sensing and display system for surgical applications. In K.S. Morgan, Richard M. Satava, Hans B. Sieburg, R. Mattheus, and J.P. Christensen, editors, *Proceedings of the Interactive Technology and the New Paradigm for Healthcare: Medicine Meets Virtual Reality III*, pages 283–288, San Diego, CA, USA, January 1995. IOS Press. ISBN-13: 978-9051992014.

[85] Christopher R. Wagner, S.J. Lederman, and Robert D. Howe. Design and performance of a tactile shape display using RC servomotors. *The Electronic Journal Of Haptics Research*, 3(4), August 2004. `http://www.haptics-e.org/Vol_03/he-v3n4.pdf`.

[86] Thomas Debus, Tae-Jeong Jang, Pierre Dupont, and Robert Howe. Multichannel vibrotactile display for teleoperated assembly. *International Journal of Control, Automation, and Systems*, 2(3):390–397, September 2004.

[87] Parris S. Wellman, William J. Peine, Gregg Favalora, and Robert D. Howe. Mechanical design and control of a high-bandwidth shape memory alloy

tactile display. In *Proceedings of the 5th International Symposium on Experimental Robotics*, volume 232 of *Lecture Notes in Control and Information Sciences*, pages 56–66, Barcelona, Spain, June 1998. Springer. DOI: 10.1007/BFb0112950.

[88] D.T.V. Pawluk, J.S. Son, P.S. Wellman, W.J. Peine, and R.D. Howe. A distributed pressure sensor for biomechanical measurements. *Journal of Biomechanical Engineering, Transactions of the ASME*, 120(2):302–305, April 1998. DOI: 10.1115/1.2798317.

[89] Dimitrios A. Kontarinis, Jae S. Son, William Peine, and Robert D. Howe. A tactile shape sensing and display system for teleoperated manipulation. In *Proceedings of the IEEE International Conference on Robotics and Automation (ICRA)*, volume 1, pages 641–646, Nagoya, Japan, May 1995. DOI: 10.1109/ROBOT.1995.525356.

[90] Dimitrios A. Kontarinis and Robert D. Howe. Tactile display of vibratory information in teleoperation and virtual environments. *Presence*, 4(4):387–402, 1995.

[91] Parris S. Wellman, Robert D. Howe, Navin Dewagan, Michael A. Cundari, Edward Dalton, and Kenneth A. Kern. Tactile imaging: A method for documenting breast lumps. In *Proceedings of the 1st joint BMES/EMBS Conference*, page 1131, Atlanta, GA, USA, October 1999.

[92] Parris S. Wellman, Edward P. Dalton, David Krag, Kenneth A. Kern, and Robert D. Howe. Tactile imaging of breast masses – first clinical report. *Archieves of Surgery*, 136(2):204–208, February 2001.

[93] Andrew P. Miller, William J. Peine, Jae S. Son, and Zane T. Hammoud. Tactile imaging system for localizing lung nodules during video assisted thoracoscopic surgery. In *Proceedings of the IEEE International Conference on Robotics and Automation*, pages 2996–3001, Rome, Italy, April 2007. DOI: 10.1109/ROBOT.2007.363927.

[94] William J. Peine. *Remote Palpation Instruments for Minimally Invasive Surgery*. PhD thesis, Division of Engineering and Applied Sciences, Harvard University, Cambridge, MA, USA, October 1998.

[95] Vincent Hayward and Juan Manuel Cruz-Hernández. Tactile display device using distributed lateral skin stretch. In *Proceedings of the Symposium on Haptic Interfaces for Virtual Environment and Teleoperator Systems (IMECE)*, November 2000.

[96] Qi Wang and Vincent Hayward. Compact, portable, modular, high-performance, distributed tactile transducer device based on lateral skin deformation. In *Proceedings of the 14th Symposium on Haptic Interfaces for*

Virtual Environment and Teleoperator Systems, pages 67–72, Alexandria, VA, USA, March 2006. DOI: 10.1109/HAPTICS.2006.153.

[97] William R. Provancher. *On Tactile Sensing and Display*. PhD thesis, Department of Mechanical Engineering, Stanford University, Stanford, CA, August 2003.

[98] R.S. Fearing, G. Moy, and E. Tan. Some basic issues in teletaction. In *Proceedings of the IEEE International Conference on Robotics and Automation (ICRA)*, volume 4, pages 3093–3099, Albuquerque, NM, USA, April 1997. DOI: 10.1109/ROBOT.1997.606758.

[99] Gabriel Moy, Ujjwal Singh, Eden Tan, and Ronals S. Fearing. Human psychophysics for teletaction system design. *Haptics-e – The Electronic Journal of Haptics Research*, 1(3):MS 1999–07, February 2000. `http://www.haptics-e.org/Vol_01/he-v1n3.pdf`.

[100] U. Singh and R.S. Fearing. Tactile after-images from static contact. In *Proceedings of the 7th Symposium on Haptic Interfaces for Virtual Environment and Teleoperator Systems*, volume 64, pages 163–170. ASME Dynamic Systems and Control Division (DSC), 1998.

[101] Joseph Yan, Paul K. Scott, and Ronald S. Fearing. Inclusion probing: Signal detection and haptic playback of 2D FEM and experimental data. In *Proceedings of the ASME International Mechanical Engineer Congress and Exposition (IMECE)*, pages 203–210, Nashville, TN, USA, November 1999.

[102] Ronald S. Fearing. Tactile sensing mechanisms. *The International Journal of Robotics Research*, 9(3):3–23, June 1990. DOI: 10.1177/027836499000900301.

[103] Bonnie L. Gray and Ronald S. Fearing. A surface micromachined microtactile sensor array. In *Proceedings of the IEEE International Conference on Robotics and Automation (ICRA)*, volume 1, pages 1–6, Minneapolis, MN, USA, April 1996. DOI: 10.1109/ROBOT.1996.503564.

[104] G. Moy, C. Wagner, and R.S. Fearing. A compliant tactile display for teletaction. In *Proceedings of the IEEE International Conference on Robotics and Automation (ICRA)*, volume 4, pages 3409–3415, San Francisco, CA, USA, April 2000. DOI: 10.1109/ROBOT.2000.845247.

[105] Kenneth H. Chiang and Ronald S. Fearing. A hybrid pneumatic/electrostatic milli-actuator. In *Proceedings of the ASME International Mechanical Engineering Congress and Exposition*, volume MEMS, Orlando, FL, USA, November 2000.

[106] Javad Dargahi, Andrew R. Eastwood, and Ian J. Kemp. Combined force and position polyvinylidene fluoride (PVDF) robotic tactile sensing system. In *Proceedings of the SPIE Conference on Sensor Fusion: Architectures, Algorithms, and Applications*, volume 3067 of *Fusion System Applications*, pages 160–170, Orlando, FL, USA, April 1997. DOI:10.1117/12.276132.

[107] J. Dargahi, M. Normandeau, J.A. Milne, M. Parameswaran, and S. Payandeh. A micro-strain gauge endoscopic tactile sensor using two sensing elements for tissue manipulation. In *Proceedings of the SPIE Conference on Sensor Fusion: Architectures, Algorithms, and Applications IV*, volume 4051, pages 349–357, Orlando, FL, USA, April 2000. DOI: 10.1117/12.381648.

[108] Javad Dargahi and Simak Najarian. A supported membrane type sensor for medical tactile mapping. *Sensor Review*, 24(3):284–297, 2004. DOI: 10.1108/02602280410545416.

[109] Javad Dargahi, Siamak Najarian, and Kayvan Najarian. Development and three-dimensional modelling of a biological-tissue grasper tool equipped with a tactile sensor. *Canadian Journal of Electrical and Computer Engineering*, 30(4):225–230, Fall 2005. DOI: 10.1109/CJECE.2005.1541755.

[110] Mohsen Hosseini, Siamak Najarian, Samira Motaghinasab, and Javad Dargahi. Detection of tumors using a computational tactile sensing approach. *The International Journal of Medical Robotics and Computer Assisted Surgery*, 2(4):333–340, December 2006. DOI: 10.1002/rcs.112.

[111] J. Dargahi, S. Payandeh, and M. Parameswaran. A micromachined piezoelectric teeth-like laparoscopic tactile sensor: Theory, fabrication and experiments. In *Proceedings of the IEEE International Conference on Robotics and Automation (ICRA)*, volume 1, pages 299–304, Detroit, MI, USA, May 1999. DOI: 10.1109/ROBOT.1999.769995.

[112] Javad Dargahi. An endoscopic and robotic tooth-like compliance and roughness tactile sensor. *Journal of Mechanical Design*, 124(3):576–582, 2002. DOI: 10.1115/1.1471531.

[113] Javad Dargahi and Siamak Najarian. An endoscopic force-position sensor grasper with minimum sensors. *Canadian Journal of Electrical and Computer Engineering*, 28(3):151–161, Fall 2003. DOI: 10.1109/CJECE.2003.1425102.

[114] Javad Dargahi, Siamak Najarian, and Xiang Zhi Zheng. Measurements and modeling of compliance using novel multi-sensor endoscopic grasper. *Journal of Sensor and Materials*, 17(1):7–20, 2005.

[115] J. Dargahi, S. Najarian, and R. Ramezanifard. Graphical display of tactile sensing data with application in minimally invasive surgery. *Canadian Journal of Electrical and Computer Engineering*, 32(3):151–155, Summer 2007. DOI: 10.1109/CJECE.2007.4413126.

[116] Siamak Najarian, Javad Dargahi, and Ali Abouei Mehrizi. *Artificial Tactile Sensing in Biomedical Engineering*. Biophotonics. McGraw-Hill Professional, April 2009.

[117] A. Menciassi, A. Eisinberg, M.C. Carrozza, and P. Dario. Force sensing microinstrument for measuring tissue properties and pulse in microsurgery. *IEEE/ASME Transactions on Mechatronics*, 8(1):10–17, March 2003. DOI: 10.1109/TMECH.2003.809153.

[118] M. Tavakoli, R.V. Patel, and M. Moallem. A force reflective master-slave system for minimally invasive surgery. In *Proceedings of the IEEE/RSJ International Conference on Intelligent Robots and Systems (IROS)*, volume 4, pages 3077–3082, October 2003. DOI: 10.1109/IROS.2003.1249629.

[119] M. Tavakoli, R.V. Patel, and M. Moallem. Design issues in a haptics-based master-slave system for minimally invasive surgery. In *Proceedings of the IEEE International Conference on Robotics and Automation (ICRA)*, volume 1, pages 371–376, New Orleans, LA, USA, May 2004. DOI: 10.1109/ROBOT.2004.1307178.

[120] M. Tavakoli, R.V. Patel, and M. Moallem. Haptic interaction in robot-assisted endoscopic surgery: a sensorized end-effector. *The International Journal of Medical Robotics and Computer Assisted Surgery*, 1(2):53–63, January 2005. DOI: 10.1002/rcs.16.

[121] M. Tavakoli, R.V. Patel, and M. Moallem. A haptic interface for computer-integrated endoscopic surgery and training. *Virtual Reality*, 9(2-3):160–176, March 2006. DOI: 10.1007/s10055-005-0017-z.

[122] M. Tavakoli, A. Aziminejad, R.V. Patel, and M. Moallem. Multi-sensory force/deformation cues for stiffness characterization in soft-tissue palpation. In *Proceedings of the 28th IEEE EMBS Annual International Conference of the Engineering in Medicine and Biology Society*, pages 837–840, New York City, NY, USA, August/September 2006. DOI: 10.1109/IEMBS.2006.260292.

[123] M. Tavakoli, R.V. Patel, and M. Moallem. Bilateral control of a teleoperator for soft tissue palpation: Design and experiments. In *Proceedings of the IEEE International Conference on Robotics and Automation (ICRA)*, pages 3280–3285, Orlando, FL, USA, May 2006. DOI: 10.1109/ROBOT.2006.1642202.

[124] Martin O. Culjat, Chih-Hung King, Miguel L. Franco, Catherine E. Lewis, James W. Bisley, Erik P. Dutson, and Warren S. Grundfest. A tactile feedback system for robotic surgery. In *Proceedings of the 30th Annual International Conference of the IEEE Engineering in Medicine and Biology Society (EMBS)*, pages 1930–1934, Vancouver, BC, Canada, August 2008. DOI: 10.1109/IEMBS.2008.4649565.

[125] Martin Culjat, Chih-Hung King, Miguel Franco, James Bisley, Warren Grundfest, and Erik Dutson. Pneumatic balloon actuators for tactile feedback in robotic surgery. *Industrial Robot: An International Journal*, 35(5):449–455, September 2008. DOI: 10.1108/01439910810893617.

[126] Chih-Hung King, Martin O. Culjat, Miguel L. Franco, James W. Bisley, Erik Dutson, and Warren S. Grundfest. Optimization of a pneumatic balloon tactile display for robotic surgery based on human perception. *IEEE Transactions on Biomedical Engineering*, 55(11):2593–2600, November 2008. DOI: 10.1109/TBME.2008.2001137.

[127] Miguel L. Franco, Chih-Hung King, Martin O. Culjat, Catherine E. Lewis, James W. Bisley, E. Carmack Holmes, Warren S. Grundfest, and Erik P. Dutson. An integrated pneumatic tactile feedback actuator array for robotic surgery. *The International Journal of Medical Robotics and Computer Assisted Surgery*, 5(1):13–19, March 2008. DOI: 10.1002/rcs.224.

[128] Chih-Hung King, Martin O. Culjat, Miguel L. Franco, James W. Bisley, Gregory P. Carman, Erik P. Dutson, and Warren S. Grundfest. A multielement tactile feedback system for robot-assisted minimally invasive surgery. *IEEE Transactions on Haptics*, 2(1):52–56, January-March 2009. DOI: 10.1109/TOH.2008.19.

[129] Chih-Hung King, Martin O. Culjat, Miguel L. Franco, Catherine E. Lewis, Erik P. Dutson, Warren S. Grundfest, and James W. Bisley. Tactile feedback induces reduced grasping force in robot-assisted surgery. *IEEE Transactions on Haptics*, 2(2):103–110, April-June 2009. DOI: 10.1109/TOH.2009.4.

[130] Koen Peeters, Mauro Sette, Pauwel Goethals, Jos Vander Sloten, and Hendrik Van Brussel. Design considerations for lateral skin stretch and perpendicular indentation displays to be used in minimally invasive surgery. In *Proceedings of the 6th International Conference EuroHaptics*, volume 5024 of *Lecture Notes in Computer Science*, pages 325–330, Madrid, Spain, June 2008. Springer. DOI: 10.1007/978-3-540-69057-3_40.

[131] Pauwel Goethals, Hans Lintermans, Mauro M. Sette, Dominiek Reynaerts, and Hendrik Van Brussel. Powerful compact tactile display with microhydraulic actuators. In *Proceedings of the 6th International Conference EuroHaptics*, volume 5024 of *Lecture Notes in Computer Science*, pages 447–

457, Madrid, Spain, June 2008. Springer. DOI: 10.1007/978-3-540-69057-3_58.

[132] Pauwel Goethals, Mauro M. Sette, Dominiek Reynaerts, and Hendrik Van Brussel. Flexible elastoresistive tactile sensor for minimally invasive surgery. In *Proceedings of the 6th International Conference EuroHaptics*, volume 5024 of *Lecture Notes in Computer Science*, pages 573–579, Madrid, Spain, June 2008. Springer. DOI: 10.1007/978-3-540-69057-3_74.

[133] M.M. Sette, J. D'hooge, S. Langeland, P. Goethals, H. Van Brussel, and J. Vander Sloten. Tactile feedback in minimally invasive procedures using an elastography-based method. In *Proceedings of the 21st International Congress and Exhibition on Computer Assisted Radiology and Surgery*, volume 2, page 504, Berlin, Germany, June 2007. Springer, International Journal of Computer Assisted Radiology and Surgery. DOI: 10.1007/s11548-007-0115-3.

[134] S.E. Salcudean, G. Bell, S. Bachmann, W.H. Zhu, P. Abolmaesumi, and P.D. Lawrence. Robot-assisted diagnostic ultrasound – design and feasibility experiments. In *Proceedings of the 2nd International Conference on Medical Image Computing and Computer-Assisted Intervention (MICCAI)*, volume 1679, pages 1062–1071, Cambridge, UK, September 1999. DOI: 10.1007/10704282_115.

[135] S.E. Salcudean, R. Six, R. Barman, S. Kingdon, I. Chau, D. Murray, and M. Steenburgh. Control electronics and hybrid dynamic systems-based api for a 6-dof desktop haptic interface. In *Proceedings of the ASME International Mechanical Engineer Congress and Exhibition (IMECE)*, Symposium on Haptic Interfaces for Virtual Environments and Teleoperation Systems, pages 407–414, Nashville, TN, USA, November 1999.

[136] W.-H. Zhu, S.E. Salcudean, S. Bachmann, and P. Abolmaesumi. Motion/force/image control of a diagnostic ultrasound robot. In *Proceedings of the IEEE International Conference on Robotics and Automation (ICRA)*, volume 2, pages 1580–1585, San Francisco, CA, USA, April 2000. DOI: 10.1109/ROBOT.2000.844822.

[137] Mohammed R. Sirouspour and S.E. Salcudean. On the nonlinear control of hydraulic servo-systems. In *Proceedings of the IEEE International Conference on Robotics and Automation (ICRA)*, volume 2, pages 1276–1282, San Francisco, CA, USA, April 2000. DOI: 10.1109/ROBOT.2000.844774.

[138] Keyvan Hashtrudi-Zaad and Septimiu E. Salcudean. Bilateral parallel force/position teleoperation control. *Journal of Robotic Systems*, 19(4):155–167, April 2002. DOI: 10.1002/rob.10030.

[139] P. Abolmaesumi, M.R. Sirouspour, S.E. Salcudean, and W.H. Zhu. Adaptive image servo controller for robot-assisted diagnostic ultrasound. In *Proceedings of the IEEE/ASME International Conference on Advanced Intelligent Mechatronics*, volume 2, pages 1199–1204, Como, Italy, July 2001. DOI: 10.1109/AIM.2001.936881.

[140] S.E. Salcudean and L. Stocco. Isotropy and actuator optimization in haptic interface design. In *Proceedings of the IEEE International Conference on Robotics and Automation (ICRA)*, volume 1, pages 763–769, San Francisco, CA, USA, April 2000. DOI: 10.1109/ROBOT.2000.844143.

[141] M.R. Sirouspour, S.P. DiMaio, S.E. Salcudean, P. Abolmaesumi, and C. Jones. Haptic interface control – design issues and experiments with a planar device. In *Proceedings of the IEEE International Conference on Robotics and Automation (ICRA)*, volume 1, pages 789–794, San Francisco, CA, USA, April 2000. DOI: 10.1109/ROBOT.2000.844147.

[142] P. Abolmaesumi, S.E. Salcudean, W.H. Zhu, S.P. DiMaio, and M.R. Sirouspour. A user interface for robot-assisted diagnostic ultrasound. In *Proceedings of the IEEE International Conference on Robotics and Automation (ICRA)*, volume 2, pages 1549–1554, Seoul, Korea, 2001. DOI: 10.1109/ROBOT.2001.932831.

[143] S.P. DiMaio, S.E. Salcudean, and M.R. Sirosupour. Haptic interaction with a planar environment. In *Proceedings of the ASME International Mechanical Engineer Congress and Exhibition (IMECE)*, volume 69 of *9th Symposium on Haptic Interfaces for Virtual Environments and Teleoperation Systems*, pages 1223–1230, Orlando, FL, USA, November 2000.

[144] D. Constantinescu, I. Chau, S.P. DiMaio, L. Filipozzi, S.E. Salcudean, and F. Ghassemi. Haptic rendering of planar rigid-body motion using a redundant parallel mechanism. In *Proceedings of the IEEE International Conference on Robotics and Automation (ICRA)*, volume 3, pages 2440–2445, San Francisco, CA, USA, April 2000. DOI: 10.1109/ROBOT.2000.846393.

[145] P. Abolmaesumi, M.R. Sirouspour, and S.E. Salcudean. Real-time extraction of carotid artery contours from ultrasound images. In *Proceedings of the 13th IEEE Symposium on Computer-Based Medical Systems (CBMS)*, pages 181–186, Houston, TX, USA, June 2000. DOI: 10.1109/CBMS.2000.856897.

[146] P. Abolmaesumi, S.E. Salcudean, and W.H. Zhu. Visual servoing for robot-assisted diagnostic ultrasound. In *Proceedings of the 22nd Annual International Conference of the IEEE Engineering in Medicine and Biology Society*, volume 4, pages 2532–2535, Chicago, IL, USA, July 2000. DOI: 10.1109/IEMBS.2000.901348.

[147] Ricardo P.J. Budde, Cornelius Borst, Patricia F.A. Bakker, and Paul F. Gründeman. *Medical Robotics*, chapter 3 – Robot-Assisted Epicardial Ultrasound for Coronary Artery Localization and Anastomosis Quality Assessment in Totally Endoscopic Coronary Bypass Surgery, pages 21–28. International Journal of Advanced Robotic Systems Publishing, Vienna, Austria, 2008. ISBN-13: 978-3-902613-18-9.

[148] Joshua Leven, Darius Burschka, Rajesh Kumar, Gary Zhang, Steve Blumenkranz, Xiangtian Dai, Mike Awad, Gregory D. Hager, Mike Marohn, Mike Choti, Chris Hasser, and Russell H. Taylor. DaVinci Canvas: A telerobotic surgical system with integrated, robot-assisted, laparoscopic ultrasound capability. In *Proceedings of the 8th International Conference on Medical Image Computing and Computer-Assisted Intervention (MICCAI)*, volume 3749, pages 811–818, Palm Springs, CA, USA, October 2005. DOI: 10.1007/11566465_100.

[149] Howard R. Nicholls and Mark H. Lee. A survey of robot tactile sensing technology. *The International Journal of Robotics Research*, 8(3):3–30, June 1989. DOI: 10.1177/027836498900800301.

[150] Mark H. Lee and Howard R. Nicholls. Tactile sensing for mechatronics – a state of the art survey. *Mechatronics*, 9(1):1–31, February 1999. DOI: 10.1016/S0957-4158(98)00045-2.

[151] Mark H. Lee. Tactile sensing: New directions, new challenges. *The International Journal of Robotics Research*, 19(7):636–643, 2000. DOI: 10.1177/027836490001900702.

[152] M.E.H. Eltaib and J.R. Hewit. Tactile sensing technology for minimal access surgery – a review. *Mechatronics*, 13(10):1163–1177, December 2003. DOI:10.1016/S0957-4158(03)00048-5.

[153] E.P. Westebring van der Putten, R.H.M. Goossens, J.J. Jakimowicz, and J. Dankelman. Haptics in minimally invasive surgery – a review. *Minimally Invasive Therapy and Allied Technologies*, 17(1):3–16, January 2008. DOI: 10.1080/13645700701820242.

[154] Pinyo Puangmali, Kaspar Althoefer, Lakmal D. Seneviratne, Declan Murphy, and Prokar Dasgupta. State-of-the-art in force and tactile sensing for minimally invasive surgery. *IEEE Sensors Journal*, 8(4):371–381, April 2008. DOI: 10.1109/JSEN.2008.917481.

[155] Sadao Omata, Yoshinobu Murayama, and Christos E. Constantinou. Real time robotic tactile sensor system for the determination of the physical properties of biomaterials. *Sensors and Actuators A: Physical*, 112(2-3):278–285, May 2004. DOI: 10.1016/j.sna.2004.01.038.

[156] S. Matsumoto, R. Ooshima, K. Kobayashi, N. Kawabe, T. Shiraishi, Y. Mizuno, H. Suzuki, and S. Umemoto. A tactile sensor for laparoscopic cholecystectomy. *Surgical Endoscopy*, 11(9):939–941, September 1997. DOI: 10.1007/s004649900492.

[157] Maria Vatshaug Ottermo. *Virtual Palpation Gripper*. PhD thesis, Norwegian University of Science and Technology, Faculty of Information Technology, Mathematics and Electrical Engineering, Department of Engineering Cybernetics, Trondheim, Norway, June 2006.

[158] Antonio Bicchi, Gaetano Canepa, Danilo De Rossi, Pietro Iacconi, and Enzo P. Scillingo. A sensor-based minimally invasive surgery tool for detecting tissueelastic properties. In *Proceedings of the IEEE International Conference on Robotics and Automation (ICRA)*, volume 1, pages 884–888, Minneapolis, MN, USA, April 1996. DOI: 10.1109/ROBOT.1996.503884.

[159] Tomohiro Kawahara, Shinji Tanaka, and Makoto Kaneko. Non-contact stiffness imager. *The International Journal of Robotics Research*, 25(5-6):537–549, May 2006. DOI: 10.1177/0278364906065826.

[160] Sebastian Schostek, Chi-Nghia Ho, Daniel Kalanovic, and Marc O. Schurr. Artificial tactile sensing in minimally invasive surgery – a new technical approach. *Minimally Invasive Therapy and Allied Technologies*, 15(5):296–304, October 2006. DOI: 10.1080/13645700600836299.

[161] P.N. Brett and R.S.W. Stone. A technique for measuring contact force distribution in minimally invasive surgical procedures. In *Proceedings of the Institution of Mechanical Engineers, Part H: Journal of Engineering in Medicine*, volume 211, pages 309–316. Professional Engineering Publishing, 1997. DOI: 10.1243/0954411971534430.

[162] G. De Gersem, H. Van Brussel, and J. Vander Sloten. Enhanced haptic sensitivity for soft tissues using teleoperation with shaped impedance reflection. In Antonio Bicchi and Massimo Bergamasco, editors, *Proceedings of the 1st joint EuroHaptics Conference and Symposium on Haptic Interfaces for Virtual Environment and Teleoperator Systems (World Haptics)*, Pisa, Italy, March 2005.

[163] Neel Dhruv and Frank Tendick. Frequency dependence of compliance contrast detection. In *Proceedings of the ASME Dynamic Systems and Control Division*, volume DSC 69-2, pages 1087–1093, 2000.

[164] Ujjwal Singh. Temporal characteristics of the human finger. Master's thesis, Department of Electrical Engineering and Computer Sciences, University of California at Berkeley, May 1997.

[165] Eden Tan. Estimating human tactile resolution limits for stimulator design. Master's thesis, Department of Electrical Engineering and Computer Sciences, University of California at Berkeley, May 1995.

[166] Gregory Tholey, Anand Pillarisetti, and Jaydev P. Desai. On-site three dimensional force sensing capability in a laparoscopic grasper. *Industrial Robot: An International Journal*, 31(6):509–518, 2004. DOI: 10.1108/01439910410566380.

[167] Gregory Tholey and Jaydev P. Desai. A modular, automated laparoscopic grasper with three-dimensional force measurement capability. In *Proceedings of the IEEE International Conference on Robotics and Automation (ICRA)*, pages 250–255, Roma, Italy, April 2007. DOI: 10.1109/ROBOT.2007.363795.

[168] Gregory Tholey, Anand Pillarisetti, William Green, and Jaydev P. Desai. Design, development, and testing of an automated laparoscopic grasper with 3-d force measurement capability. In *Proceedings of the International Symposium on Medical Simulation (ISMS)*, volume 3078, pages 38–48, Cambridge, MA, USA, June 2004. DOI: 10.1007/b98155.

[169] Mark MacFarlane, Jacob Rosen, Blake Hannaford, Carlos Pellegrini, and Mika Sinanan. Force-feedback grasper helps restore sense of touch in minimally invasive surgery. *Journal of Gastrointestinal Surgery*, 3(3):278–285, June 1999. DOI: 10.1016/S1091-255X(99)80069-9.

[170] Blake Hannaford, Jason Trujillo, Mika Sinanan, Manuel Moreyra, Jacob Rosen, Jeff Brown, Rainer Leuschke, and Mark MacFarlane. Computerized endoscopic surgical grasper. In *Proceedings of the Studies in Health Technology and Informatics – Medicine Meets Virtual Reality*, volume 50, pages 265–271, San Diego, CA, USA, January 1998. IOS Press.

[171] John G. Webster, editor. *Tactile Sensors for Robotics and Medicine*. John Wiley & Sons, Inc., New York, Chichester, Brisbane, Toronto, Singapore, November 1988.

[172] Martin Grunwald, editor. *Human Haptic Perception: Basics and Applications*. Birkhäuser, Basel, 1st edition, November 2008. DOI: 10.1007/978-3-7643-7612-3.

[173] Robert D. Howe. Tactile sensing and control of robotic manipulation. *Journal of Advanced Robotics*, 8(3):245–261, 1993. DOI: 10.1163/156855394X00356.

[174] Howard R. Nicholls, editor. *Advanced Tactile Sensing for Robotics*, volume 5 of *World Scientific Series in Robotics and Automated Systems*. World Scientific Publishing, Singapore, January 1993.

[175] Andrew R. Russell. *Robot Tactile Sensing*. Prentice Hall, New York, London, Toronto, Sydney, Tokyo, Singapore, December 1990.

[176] Heinrich Kuttruff. *Physik und Technik des Ultraschalls*. Hirzel Verlag, Stuttgart, 1988.

[177] Jørgen A. Jensen. *Estimation of blood velocities using ultrasound: a signal processing approach*. University Press, Cambridge, GB, 1996.

[178] David H. Evans and W. Norman McDicken. *Doppler Ultrasound: Physics, Instrumentation and Signal Processing*. Wiley & Sons, West Sussex, England, 2nd edition, 2000.

[179] Wilhelm Schäberle. *Ultrasonography in Vascular Diagnosis – A Therapy-Oriented Textbook and Atlas*. Springer Verlag, Berlin, Heidelberg, October 2005. DOI: 10.1007/3-540-28925-9.

[180] Olaf Dössel. *Bildgebende Verfahren in der Medizin – Von der Technik zur medizinischen Anwendung*. Springer Verlag, Berlin, 1st edition, January 2000.

[181] Francis A. Duck, Andrew C. Baker, and Hazel C. Starritt. *Ultrasound in Medicine*. Medical Science Series. Institute of Physics Publishing, Bristol, UK and Philadelphia, PA, USA, December 1998.

[182] Frederick W. Kremkau. *Diagnostic Ultrasound: Principles and Instruments*. W.B. Saunders & Co. Publishing, 7th edition, October 2005.

[183] Kevin J. Parker. Ultrasonic attenuation and absorption in liver tissue. *Ultrasound in Medicine & Biology*, 9(4):363–369, July/August 1983. DOI: 10.1016/0301-5629(83)90089-3.

[184] Buijs Ballot. Akustische Versuche auf der Niederländischen Eisenbahn, nebst gelegentlichen Bemerkungen zur Theorie des Hrn. Prof. Doppler. *Annalen der Physik und Chemie*, 142(11):321–351, 1845. DOI: 10.1002/andp.18451421102.

[185] Christian Doppler. *Abhandlungen von Christian Doppler*, chapter I. Ueber das farbige Licht der Doppelsterne und einiger anderer Gestirne des Himmels, pages 3–24. Number 161 in Ostwald's Klassiker der exakten Wissenschaften. Verlag von Wilhelm Engelmann, Leipzig, 1907. Reprint of the original, Doppler, C. *Ueber das farbige Licht der Doppelsterne und einiger anderer Gestirne des Himmels*. Abhandlung der Königlich Böhmischen Gesellschaft der Wissenschaften Sers. 2:465-482, 1843.

[186] D.N. White. Johann Christian Doppler and his effect – A brief history. *Ultrasound in Medicine & Biology*, 8(6):583–591, 1982. DOI: 10.1016/0301-5629(82)90114-4.

[187] Jürgen Czarske, Lars Büttner, and Thorsten Pfister. Berührungslos messen mit Licht. Laser-Doppler-Sensoren. *Physik in unserer Zeit*, 38(6):282–289, October 2007. DOI: 10.1002/piuz.200601144.

[188] Robert F. Bonner and Ralph Nossal. *Laser-Doppler Blood Flowmetry – Developments in Oncology*, volume 107, chapter Principles of Laser-Doppler Flowmetry, pages 17–45. Springer Verlag, 2nd edition, 1990. ISBN-13: 978-0792305088.

[189] Franz Durst, Manfred Stieglmeier, and Maris Ziema. Strömungs- und Teilchenmessung mittels Doppler-Anemometrie. *Physik in unserer Zeit*, 24(1):15–23, 1993. DOI: 10.1002/piuz.19930240106.

[190] P. Ake Öberg. Laser-Doppler Flowmetry. *Critical Reviews in Biomedical Engineering*, 18(2):125–163, 1990.

[191] Georg Michelson, Jürgen Welzenbach, Istvan Pal, and Joanna Harazny. Automatic full field analysis of perfusion images gained by scanning laser Doppler flowmetry. *British Journal of Ophthalmology*, 82(11):1294–1300, November 1998.

[192] Charles E. Riva. Basic principles of laser Doppler flowmetry and application to the ocular circulation. *International Ophthalmology*, 23(4-6):183–189, July 2001. DOI: 10.1023/A:1014433913240.

[193] Frank H. Netter. *Herz*, volume 1 of *Farbatlanten der Medizin*. Georg Thieme Verlag, Stuttgart, New York, 3rd edition, 1990.

[194] Robert F. Schmidt, Gerhard Thews, and Florian Lang, editors. *Physiologie des Menschen*. Springer Verlag, Berlin, Heidelberg, New York, 28th edition, 2000.

[195] Robert F. Schmidt and Florian Lang, editors. *Physiologie des Menschen – mit Pathophysiologie*. Springer Verlag, Berlin, 30th edition, September 2007. DOI: 10.1007/978-3-540-32910-7.

[196] Nancy J. O'Connor, Jeremy R. Morton, John D. Birkmeyer, Elaine M. Olmstead, and Gerald T. O'Connor. Effect of coronary artery diameter in patients undergoing coronary bypass surgery. *Circulation*, 93:652–655, 1996.

[197] Theodor H. Schiebler and Horst-Werner Korf. *Anatomie – Histologie, Entwicklungsgeschichte, makroskopische und mikroskopische Anatomie, Topographie*. Steinkopff Verlag, 10th edition, September 2007.

[198] Herbert Lippert and Wunna Lippert-Burmester. *Anatomie – Text und Atlas*. Urban & Fischer Verlag, Munich, 6th edition, 1995.

[199] M. Schiemann, F. Bakhtiary, V. Hietschold, A. Koch, A. Esmaeili, H. Ackermann, A. Moritz, T.J. Vogl, and N.D. Abolmaali. MR-based coronary artery blood velocity measurements in patients without coronary artery disease. *European Radiology*, 16(5):1124–1130, May 2006. DOI: 10.1007/s00330-005-0039-7.

[200] Elizabeth O. Ofili, Arthur J. Labovitz, and Morton J. Kern. Coronary flow velocity dynamics in normal and diseased arteries. *The American Journal of Cardiology*, 71(14):3D–9D, May 1993.

[201] Mair Zamir. *The Physics of Coronary Blood Flow*. Springer Verlag, Berlin, Heidelberg, 2005. DOI: 10.1007/b136492.

[202] Bernhard Kuebler, Robin Gruber, Christoph Joppek, Johannes Port, Georg Passig, Joachim H. Nagel, and Gerd Hirzinger. Tactile feedback for artery detection in minimally invasive robotic surgery – preliminary results of a new approach. In Olaf Dössel and Wolfgang C. Schlegel, editors, *Proceedings of the 11th International Congress of the IUPESM, World Congress on Medical Physics and Biomedical Enginneering*, volume 25/VI of *IFMBE Proceedings*, pages 299–302, Munich, Germany, September 2009. Springer.

[203] Robin Gruber. Illustration, Institute of Robotics and Mechatronics, German Aerospace Center (DLR), October 2008.

[204] Christoph Joppek. Illustration, Department of Biomedical Engineering, University of Stuttgart (IBMT UniS), October 2008.

[205] Claude E. Shannon. Communication in the presence of noise. In *Proceedings of the IRE*, volume 37, pages 10–21, January 1949.

[206] Henry Nyquist. Certain topics in telegraph transmission theory. *Transactions of the American Institute of Electrical Engineers*, 47(2):617–644, April 1928. DOI: 10.1109/T-AIEE.1928.5055024.

[207] K.J.M. Surry, H.J.B. Austin, A. Fenster, and T.M. Peters. Poly(vinyl alcohol) cryogel phantoms for use in ultrasound and MR imaging. *Physics in Medicine and Biology*, 49(24):5529–5546, December 2004. DOI: 10.1088/0031-9155/49/24/009.

[208] Y. Douville, K.W. Johnston, M. Kassam, P. Zuech, R.S.C. Cobbold, and A. Jares. An in vitro model and its application for the study of carotid Doppler spectral broadening. *Ultrasound in Medicine & Biology*, 9(4):347–356, July/August 1983. DOI: 10.1016/0301-5629(83)90087-X.

[209] D.W. Rickey, P.A. Picot, D.A. Christopher, and A. Fenster. A wall-less vessel phantom for Doppler ultrasound studies. *Ultrasound in Medicine & Biology*, 21(9):1163–1176, 1995. DOI: 10.1016/0301-5629(95)00044-5.

[210] Jérémie Fromageau, Elisabeth Brusseau, Didier Vray, Gérard Gimenez, and Philippe Delachartre. Characterization of PVA cryogel for intravascular ultrasound elasticity imaging. *IEEE Transactions on Ultrasonics, Ferroelectrics and Frequency Control*, 50(10):1318–1324, October 2003. DOI: 10.1109/TUFFC.2003.1244748.

[211] Jacinta E. Browne, Amanda J. Watson, Peter R. Hoskins, and Alex T. Elliott. Validation of a sensitivity performance index test protocol and evaluation of colour Doppler sensitivity for a range of ultrasound scanners. *Ultrasound in Medicine & Biology*, 30(11):1475–1483, November 2004. DOI: 10.1016/j.ultrasmedbio.2004.09.005.

[212] J.C. Machado, F.S. Foster, and A.I. Gotlieb. Measurement of the ultrasonic properties of human coronary arteries in vitro with a 50-MHz acoustic microscope. *Brazilian Journal of Medical and Biological Research*, 35(8):895–903, August 2002. DOI: 10.1590/S0100-879X2002000800006.

[213] Stefan Pfaffenberger, Branka Devcic-Kuhar, Christian Kollmann, Stefan P. Kastl, Christoph Kaun, Walter S. Speidl, Thomas W. Weiss, Svitlana Demyanets, Robert Ullrich, Heinz Sochor, Christian Wöber, Josef Zeitlhofer, Kurt Huber, Martin Gröschl, Ewald Benes, Gerald Maurer, Johann Wojta, and Michael Gottsauner-Wolf. Can a commercial diagnostic ultrasound device accelerate thrombolysis? – An in vitro skull model. *Stroke*, 36:124–128, 2005. DOI: 10.1161/01.STR.0000150503.10480.a7.

[214] Kumar V. Ramnarine, Tom Anderson, and Peter R. Hoskins. Construction and geometric stability of physiological flow rate wall-less stenosis phantoms. *Ultrasound in Medicine & Biology*, 27(2):245–250, February 2001. DOI: 10.1016/S0301-5629(00)00304-5.

[215] Kumar V. Ramnarine, Dariush K. Nassiri, Peter R. Hoskins, and Jaap Lubbers. Validation of a new blood-mimicking fluid for use in Doppler flow test objects. *Ultrasound in Medicine & Biology*, 24(3):451–459, March 1998. DOI: 10.1016/S0301-5629(97)00277-9.

[216] Dansk Fantom Service, Inc. Flow Doppler phantoms. Website, 06/2009. `http://www.fantom.dk`.

[217] H. Samavat and J.A. Evans. An ideal blood mimicking fluid for Doppler ultrasound phantoms. *Journal of Medical Physics*, 31(4):275–278, 2006.

[218] Ernest L. Madsen, James A. Zagzebski, and Gary R. Frank. Oil-in-gelatin dispersions for use as ultrasonically tissue-mimicking materials. *Ultrasound in Medicine & Biology*, 8(3):277–287, 1982. DOI: 10.1016/0301-5629(82)90034-5.

[219] Junru Wu. Tofu as a tissue-mimicking material. *Ultrasound in Medicine & Biology*, 27(9):1297–1300, September 2001. DOI: 10.1016/S0301-5629(01)00424-0.

[220] Carolus J.P.M. Teirlinck, Robert A. Bezemer, Christian Kollmann, Jaap Lubbers, Peter R. Hoskins, Peter Fish, Knud-Erik Fredfeldt, and Ulrich G. Schaarschmidt. Development of an example flow test object and comparison of five of these test objects, constructed in various laboratories. *Ultrasonics*, 36(1-5):653–660, February 1998. DOI: 10.1016/S0041-624X(97)00150-9.

[221] Chr. Kollmann, R.A. Bezemer, K.E. Fredfeldt, U.E. Schaarschmidt, and C.J.P.M. Teirlinck. Ein Testobjekt für die apparative Qualitätssicherung bei Ultraschall-Doppler(Duplex)-Geräten, ausgehend vom Normenentwurf IEC 61685. *Ultraschall in der Medizin*, 20:248–257, 1999. DOI: 10.1055/s-1999-8918.

[222] Johannes Port. Illustration, Department of Biomedical Engineering, University of Stuttgart (IBMT UniS), April 2009.

[223] Bernhard Kuebler, Tobias Ortmaier, and Joachim H. Nagel. German Patent, DE 10 2005 045 480 A1, Verfahren zum Aufspüren und Lokalisieren von im Inneren eines Materials oder Gewebes vorhandenen, besonderen Strukturen, chartered April 5th 2007.

[224] R. Bousseljot and D. Kreiseler. Auswertung von EKG mit Hilfe der Mustererkennung. *Herzschrittmachertherapie und Elektrophysiologie*, 9(4):270–278, December 1998. DOI: 10.1007/s003990050038.

[225] O.A. Lindahl, S. Omata, and K.-A. Ängquist. A tactile sensor for detection of physical properties of human skin in vivo. *Journal of Medical Engineering & Technology*, 22(4):147–153, July/August 1998. DOI: 10.3109/03091909809032532.

[226] Sadao Omata and Yoshikazu Terunuma. Development of new type tactile sensor for detecting hardness and/or software of an object like the human hand. In *Digest of Technical Papers to the International Conference on Solid-State Sensors and Actuators*, pages 868–871, San Francisco, CA, USA, June 1991. DOI: 10.1109/SENSOR.1991.149023.

[227] Toshiya Ohtsuka, Akira Furuse, Tadasu Kohno, Jun Nakajima, Kuniyoshi Yagyu, and Sadao Omata. Application of a new tactile sensor to thoracoscopic surgery: Experimental and clinical study. *The Annals of Thoracic Surgery*, 60(3):610–614, September 1995. DOI: 10.1016/0003-4975(95)00483-2.

[228] Yoshinobu Murayama, Christos E. Constantinou, and Sadao Omata. Development of tactile mapping system for the stiffness characterization of tissue

slice using novel tactile sensing technology. *Sensors and Actuators A: Physical*, 120(2):543–549, May 2005. DOI: 10.1016/j.sna.2004.12.027.

[229] Yvon Boudreault, Steven Boudreault, and Fernand Jalbert. United States Patent, US 005 186 714 A, Multifunctional Surgical Instrument, chartered February 16th 1993.

[230] Gunter Farin, Klaus Fischer, and Dieter Muller. United States Patent, US 005 776 092 A, Multifunctional Surgical Instrument, chartered July 7th 1998.

[231] Stephen C. Anderson and Christopher A. Julian. United States Patent, US 006 783 524 B2, Robotic Surgical Tool with Ultrasound Cauterizing and Cutting Instrument, chartered August 31st 2004.

[232] Mary I. Frecker, Jeremy Schadler, Randy S. Haluck, Kristin Culkar, and Ryan Dziedzic. Laparoscopic multifunctional instruments: Design and testing of initial prototypes. *Journal of the Society of Laparoendoscopic Surgeons*, 9(1):105–112, January-March 2005.

[233] Mary I. Frecker, Katherine M. Powell, and Randy Haluck. Design of a multifunctional compliant instrument for minimally invasive surgery. *Journal of Biomechanical Engineering, Transactions of the ASME*, 127(6):990–993, November 2005. DOI: 10.1115/1.2056560.

[234] Mary I. Frecker, Randy S. Haluck, Ryan P. Dziedzic, and Jeremy R. Schadler. United States Patent, US 7 208 005 B2, Multifunctional Tool and Method for Minimally Invasive Surgery, chartered April 24th 2007.

[235] Tarek Ahmed Nabil Abou El Kheir. United States Patent, US 2008/0287926 A1, Multi-Purpose Minimally Invasive Instrument that Uses a Micro Entry Port, chartered November 20th 2008.

[236] Petra Badke-Schaub, Gesine Hofinger, and Kristina Lauche. *Human Factors – Psychologie sicheren Handelns in Risikobranchen*, chapter Human Factors, pages 3–18. Springer Verlag, Berlin, Heidelberg, 1st edition, June 2008. DOI: 10.1007/978-3-540-72321-9_1.

[237] Grigore C. Burdea. *Force and Touch Feedback for Virtual Reality*. John Wiley & Sons, Inc., July 1996.

[238] Richard Bartle. *Designing Virtual Worlds*. New Riders Games, 1st edition, July 2003.

[239] Georg Färber (speaker). *Finanzierungsantrag 1999-2001 zum Sonderforschungsbereich 1731 "Wirklichkeitsnahe Telepräsenz und Teleaktion"*. Technische Universität München, Munich, Germany, June 1998.

[240] International Organization for Standardization (ISO). ISO 8373:1994, Manipulating Industrial Robots – Vocabulary. ISO Standards, Beuth Verlag, Berlin, 1994.

[241] Paul Bach y Rita and Stephen W. Kercel. Sensory substitution and the human-machine interface. *Trends in Cognitive Sciences*, 7(12):541–546, December 2003. DOI: 10.1016/j.tics.2003.10.013.

[242] Willibald Pschyrembel. *Pschyrembel Klinisches Wörterbuch*. DeGruyter Verlag, Berlin, New York, 257th edition, 1994.

[243] Sajeesh Kumar and Jacques Marescaux, editors. *Telesurgery*. Springer Verlag, Berlin, Heidelberg, Berlin, 2008.